

MSc Dissertation

Formula Student V-Twin Race Engine Lubrication System

**Oxford Brookes University
Student No.: 06069218**

MSc in Racing Engine Design

**Oxford Brookes University
School of Technology
September 2007**

**Project Supervisor: Geoff Goddard, John
Durodola**

ABSTRACT

The aim of this report is to optimize the oil system of a 600cc 75deg. V-Twin Engine currently being designed for a Formula SAE (FSAE)/Formula Student (FS) Race Car. Dry sump and wet sump oil systems are compared outlining the advantages of a wet sump system for the V-Twin Engine. The oil system requirements are discussed, such as pressure, temperature, and flow rates. Computational fluid dynamics is used to study oil flow through the engine. The CFD model shows pressure drops and flow rates throughout the system. Lubricant properties are researched and a SAE 30 lubricant is assigned to the oil system. The three mechanical systems (piston assembly, valvetrain, and bearings) requiring lubrication are discussed in terms of materials, surface finishes, and lubrication regime. A GT-Power model is created to simulate in-cylinder pressures which are then fed into a Crankshaft Balancing Model. Through crankshaft balancing, main bearing loads are determined to be 22,500N. An in depth detailed analysis of journal bearing design is illustrated. The bearing model determines journal bearing eccentricity ratio, max pressure, oil film thickness, coefficient of friction, torque, power loss, lubricant required, safety factor, temperature rise, minimum surface roughness or rms, and flow rate.

ACKNOWLEDGEMENTS

The author would like to thank his Lord and Saviour Jesus Christ. Through Him all things were made possible. Thank you Jesus!

1 Corinthians 2:9 But as it is written:

*“Eye has not seen, nor ear heard,
Nor have entered into the heart of man
The things which God has prepared for those who love Him”*

Psalm 32:8 *I will instruct you and teach you in the way you should go; I will guide you with my eye.*

Thanks to my father and mother Fritz and Otilia Van-Zwol. Without them none of this MSc in Racing Engine Design would have been possible. You both have guided me and raised me up in a righteous way. You are now seeing the glory of what you have created.

Thanks to my family members who all supported me along the way: Stephanie, Roelfina, Onno, Tjisje, and Lucy Van-Zwol.

Thanks to my girlfriend Michelle Molano who has encouraged and motivated me.

Thanks to my friends and family. Special thanks to Mr. Weldon Montgomery for giving me words of wisdom i.e. Isaiah 54:17 *“No weapon formed against you shall prosper, And every tongue which rises against you in judgment you shall condemn”*. Furthermore, **when you God it you get it.**

Thanks to Geoff Goddard, Stephen Samuel and John Durodola who have given me tremendous amounts of support and guidance. They have increased my knowledge, given me a better understanding of internal combustion engines, and have created in me an excellent mechanical engineering foundation. Last but not least, thanks to Oxford Brookes University and Staff for all their help.

CONTENTS

ABSTRACT	2
ACKNOWLEDGEMENTS	3
CONTENTS	4
LIST OF FIGURES.....	6
LIST OF TABLES.....	9
1 INTRODUCTION	10
1.1 V-TWIN ENGINE SPECIFICATIONS	11
2 BACKGROUND OF LUBRICATION SYSTEMS & PUMPS	12
2.1 LUBRICATION SYSTEM.....	12
2.2 WET SUMP OIL SYSTEM	14
2.3 DRY SUMP OIL SYSTEM.....	14
2.4 PUMP TYPES	16
2.4.1 Positive Displacement & Dynamic Pumps.....	16
2.4.2 Motorsport Industry Oil Pumps	18
3 BACKGROUND OF LUBRICANTS & BEARINGS	20
3.1 LUBRICANTS	20
3.1.1 Lubricant Types	20
3.1.2 Lubricant Additives.....	21
3.1.3 Lubricant Parameters Affecting Performance	23
3.2 LUBRICATION THEORIES-BOUNDARY, MIXED FILM, AND FULL FILM	27
3.2.1 Surface Parameters.....	31
3.2.2 Surface Finishes.....	32
3.3 BEARING MATERIAL COMBINATIONS	35
4 V-TWIN OIL SYSTEM & COMPONENTS	37
4.1 V-TWIN DRY SUMP OIL SYSTEM	37
4.2 PRESSURE REQUIREMENTS	38
4.2.1 V-Twin Oil Pressure Requirements.....	40
4.3 FLOW REQUIREMENTS	42
4.3.1 Main Oil Gallery Sizing	42
4.3.2 V-Twin Main Oil Gallery Sizing	44
4.3.3 V-Twin Crankshaft.....	44
4.3.4 V-Twin Cylinder Heads.....	45
4.4 PUMPS FOR THE V-TWIN.....	45
4.4.1 V-Twin Oil Pressure Pump Design.....	46
4.4.2 V-Twin Scavenge Pump Design	51
4.4.3 V-Twin Centrifuge Pump Design	52
4.4.4 V-Twin Pump Stack.....	53
4.5 OIL FILTER	53
4.5.1 V-Twin Oil Filter.....	56
4.6 PRESSURE RELIEF VALVE (PRV).....	56
4.6.1 V-Twin PRV	57
4.7 V-TWIN OIL TANK.....	58
4.8 V-TWIN SWIRL POT	58

4.9 V-TWIN OIL SUMP	59
4.10 CHAPTER 4 SUMMARY	60
5 V-TWIN BEARINGS & LUBRICATION	62
5.1 V-TWIN CRANKSHAFT JOURNAL SURFACE FINISH	63
5.2 JOURNAL BEARING DESIGN (HYDRODYNAMIC)	64
5.2.1 GT-Power model of piston-crank forces	65
5.2.2 Crankshaft balancing via bearing loads	66
5.2.3 Bearing loads discussion from section 5.2.2	73
5.2.4 Crankshaft pin forces on big-end connecting rod bearings	80
5.2.5 Mathematical Bearing Model	82
5.2.6 Bearing Model Results & Discussion	90
6 CFD OF OIL FLOW THROUGH V-TWIN ENGINE	94
6.2 PRESSURE DROPS AND FLOW RATES THROUGH OIL GALLERIES	94
6.2.1 Recommendations to improve CFD Model of oil flow through engine	98
7 V-TWIN PISTON ASSEMBLY LUBRICATION.....	101
8 V-TWIN VALVE TRAIN LUBRICATION.....	103
9 CONCLUSION.....	105
REFERENCES	107
APPENDIX 1 KINSLER FUEL INJECTION, INC. OIL FILTERS	109
APPENDIX 2 OIL & SCAVENGE PUMP CALCULATIONS	110
APPENDIX 3 MATHEMATICAL BEARING MODEL CALCULATIONS.....	118
APPENDIX 4 FILES ON ACCOMPANYING CD	128
4.1 MICROSOFT EXCEL SPREADSHEET ON OIL SYSTEM PRESSURE & FLOW REQUIREMENTS	128
4.2 MICROSOFT EXCEL SPREADSHEET ON CRANKSHAFT BALANCING	128
4.3 MATHCAD FILE ON OIL PRESSURE & SCAVENGE PUMP DESIGN.....	128
4.4 MATHCAD FILE ON MATHEMATICAL JOURNAL BEARING MODEL	128
4.5 PDF FILE OF MSc DISSERTATION	128
APPENDIX 5 MAIN BEARINGS & BIG END CON-ROD BEARINGS.....	129
5.1 MAIN BEARINGS	130
5.2 BIG END CONNECTING ROD BEARINGS	131

LIST OF FIGURES

Figure 1 Oil flow illustration (SI engine) [Encyclopedia Britannica 2007]	13
Figure 2 Wet Sump Oil System [Moroso 2007].....	14
Figure 3 Dry Sump System [Moroso 2007].....	15
Figure 4 Positive Displacement Pumps [White 2003]	17
Figure 5 Dynamic & PDP Performance Curve [White 2003]	18
Figure 6 Dynamic Viscosity as a function of Temperature for multi-grade engine oils [Pulkrabek 2004].....	25
Figure 7 Effect of Shear Rate on Viscosity [Lansdown 1982]	26
Figure 8 Variation of viscosity with shear rate for an SAE10W-50 lubricant [Taylor 2002]	27
Figure 9 Engine lubrication regimes on the Stribeck Diagram [Stone 1999].....	29
Figure 10 Friction due to asperity contact [Pulkrabek 2004]	29
Figure 11 Full-film lubrication (a) boundary lubrication. (b) full-film lubrication [Pulkrabek 2004].....	30
Figure 12 Surface Finishes & Min. Oil Film Thickness [Booser <i>et al</i> 2001]	31
Figure 13 Common Surface Amplitude Characterizations [Booser <i>et al</i> 2001]	32
Figure 14 Surface coating thickness vs. temperature for various methods [Balzers Ltd. 2007]	34
Figure 15 V-Twin Dry Sump Oil System Schematic	37
Figure 16 Flow Chart for Determining Oil System Pressure.....	39
Figure 17 Crankshaft Drillings	40
Figure 18 Flow Chart for Determining Oil Flow Requirements.....	43
Figure 19 Oil Pump Capacities	50
Figure 20 Oil Pressure Pump	50
Figure 21 Oil Scavenge Pump	52
Figure 22 Centrifuge Pump.....	53
Figure 23 Oil Pump Stack.....	53
Figure 24 Postion of oil filter in system [Hillier 1999]	54

Figure 25 Cartridge type filter (by-pass) [Hillier 1999]	55
Figure 26 Full-flow oil filter [Hillier 1999]	56
Figure 27 Ball-type pressure relief valve [Hillier 1991]	57
Figure 28 Oil Reservoir with baffles	58
Figure 29 Swirl Pot	59
Figure 30 Dry sump	59
Figure 31 Engine friction breakdown-2.0L European engine at idle, medium load (2500rpm), and high load (7500rpm) [Taylor 2002]	62
Figure 32 Engine friction breakdown-3.0L Formula 1 engine @18000rpm [Taylor 2002]	62
Figure 33 GT-Power engine model.....	65
Figure 34 Equivalent connecting rod masses.....	67
Figure 35 Rotating masses for crankshaft balance	68
Figure 36 Equivalent reciprocating masses for balancing	69
Figure 37 Piston Velocities @12,000rpm for calculated data and GT-Power data.....	70
Figure 38 Piston accelerations @12,000rpm	71
Figure 39 GT-Power and real data in-cylinder pressures	72
Figure 40 Primary inertia forces @12,000rpm	74
Figure 41 Secondary inertia forces @ 12,000rpm	74
Figure 42 Total inertia forces-primaries + secondary's @12,000 rpm.....	75
Figure 43 Gas forces @12,000rpm	76
Figure 44 Gas & inertia forces @ idle, mid range, red line.....	76
Figure 45 Even fire-combined loads.....	77
Figure 46 Oddfire-combined loads	77
Figure 47 35% Overbalance @ 12,000rpm (10% greater load on upper half of bearing) 78	
Figure 48 35% overbalance @ 10,000rpm (33% less load on upper half of bearing).....	78
Figure 49 3% underbalance @ 12,000rpm	79
Figure 50 GT-Power main bearing loads @12,000 rpm.....	80
Figure 51 Rotating mass assembly for crankpin forces	81
Figure 52 Eccentricity ratio vs. Ocvirk Number [Norton 2000].....	85
Figure 53 Non-parallel plate theory [Norton 2000]	85

Figure 54 Journal bearing pressure distribution [Norton 2000].....	86
Figure 55 Angles θ_{\max} and ϕ as a function of Ocvirk Number [Norton 2000]	87
Figure 56 Pressure ratios and torque ratios as a function of Ockvirk Number [Norton 2000]	88
Figure 57 Chart for determining oil viscosity [Norton 2000].....	92
Figure 58 Catia Model of Oil System Pipe Network.....	95
Figure 59 Model 1-Velocity vectors of oil flow through engine (3mm orifices)	96
Figure 60 Pressure vectors of oil flow through the engine (3mm orifices)	97
Figure 61 Fluent model of journal bearing [Fluent 2007]	99
Figure 62 Velocity vectors of oil flow through engine (1.25mm orifices).....	99
Figure 63 Cylinder wall surface honing [Hoag 2006]	102

LIST OF TABLES

Table 1 V-Twin Engine Specifications.....	11
Table 2 PDP and Dynamic Pump Types and Components.....	16
Table 3 Engine Oil Additives	22
Table 4 Engine Oil Properties ($T = 298K$, $P = 1bar$) [Ferguson 2001]	24
Table 5 Bearing Materials [Stone 1999]	36
Table 6 Centrifugal Head on Crankshaft Bearings	41
Table 7 Summation of cross-sectional areas for flow requirements.....	44
Table 8 Crankshaft Journal Surface Finishes.....	63
Table 9 Bearing Model Results 1 @ 12,000rpm	90
Table 10 Bearing model results 2 @12,000rpm	92
Table 11 Fluent Model 1 Flow Rates.....	97
Table 12 Fluent Model 2 Flow Rates.....	100
Table 13 V-Twin Piston Assembly Materials.....	102
Table 14 Valvetrain Materials	104
Table 15 Shell Helix Ultra Oil Properties.....	110

1 INTRODUCTION

This dissertation develops an optimized lubrication system for a 600cc V-Twin Engine currently being designed for a Formula SAE (a.k.a. Formula Student) Race Car. The V-Twin engine has some components already designed for the lubrication system however these components need to be optimized. Furthermore, several engineers have worked on a number of system components and it is therefore critical that an analysis of the whole system is carried out to ensure system credibility. The optimized system will increase reliability, reduce wear, and maximize available power output.

Chapter 1 covers the V-Twin engine specifications and which variables affect lubrication performance. Chapter 2 covers the basic functions of an oil system, the advantages and disadvantages of dry sump and wet sump systems, and background on pumps. Chapter 3 gives background information on lubricant properties and bearing properties. Lubricant viscosity behavior with temperature, shear rate, and pressure is discussed. Lubricant additives are discussed. Bearing materials and surface finishes are discussed. Chapter 4 discusses the V-Twin dry sump oil system, determines oil system pressure and flow rates, and discusses oil system components such as pumps, location of pump suctions, filters, pressure relief valves, dry sump design, oil tank design, and swirl pots. Chapter 5 performs crankshaft balancing to determine main bearing forces. A mathematical model for journal bearings is created to determine bearing eccentricity ratio, max pressure, oil film thickness, coefficient of friction, torque, power loss, lubricant required, safety factor, temperature rise, minimum surface roughness or rms, and flow rate. Chapter 6 shows a CFD model of the oil flow through the engine. The purpose of the model is to ensure that oil starvation does not occur in any of the bearings, all common bearing feeds will have equal pressure and flow rates, it checks the oil gallery sizing which is performed in chapter 3, and it checks the flow rates to the main bearings calculated in chapter 5. Chapter 7 discusses lubrication requirements for the piston assembly. Chapter 8 discusses valvetrain lubrication in terms of material choice, surface finish, and lubrication operating zone i.e., boundary, mixed, or full-film lubrication. The dissertation concludes with chapter 9 summarizing the work.

There are several factors which can limit the oil system optimization. These factors include engine packaging, machining limits, cost, time, manufacturing, and production. During a visit to Grainger & Worrell, a casting & light machining facility, it was indicated that the current oil system entrance into the block should not have extreme bends as this would not allow for final machining in the end for cleaning. Cleaning is necessary to remove all loose bits in the oil galleries otherwise this could cause bearing failure.

1.1 V-Twin Engine Specifications

The V-Twin engine specifications are listed in table 1. The specifications are listed to give an overview of the V-Twin engine being discussed. Of the specifications listed, the following parameters will affect lubrication performance: engine speed, fuel type, displacement, and cylinder bank angle. The engine speed affects the crankshaft centrifugal head leading to higher oil system pressures. The fuel type affects the scavenge pump capacity. An alcohol fuelled system requires 7-10 times oil pump capacity, whereas a gasoline fuelled system requires scavenge pump capacity to be 3-5 times oil pump capacity [Goddard 2007]. The more displacement an engine has the more oil needed in the system. The bank angle affects the overall loads on the main bearings.

Swept volume	600cc
# of cylinders	2
Cylinder bank angle	75 deg.
Max engine speed	12500 rpm
Bore	92mm
Stroke	45.5mm
Conrod	103mm
Inlet valve angle	11deg.
Inlet port angle	45deg.
Exhaust valve angle	12deg.
Exhaust port angle	72deg.
Port fuel injection	Yes
Intake restrictor	19mm
Fuel Type (alcohol)	E-85

Table 1 V-Twin Engine Specifications

2 BACKGROUND OF LUBRICATION SYSTEMS & PUMPS

2.1 Lubrication System

The lubrication system is designed to provide clean oil at the right temperature, pressure, and flow rate to all engine components requiring lubrication. The oil is sucked out of the sump into the pump which then feeds the oil through a filter. Clean oil exits the filter at high pressure and supplies the main oil gallery located centrally in the engine block. The first to be fed from the main gallery is the crankshaft. The crankshaft has oil feed lines pre-drilled internally which provide paths to feed the main bearings and the big end bearings of the connecting rods. Oil which leaks from the journal bearings is flung by the rotating crankshaft to provide lubrication for the small end bearings of the connecting rod, the piston gudgeon pins, and piston rings. The oil flung off the crankshaft is not enough and squirt jets are normally added to provide extra lubrication. Next, feed lines from the main gallery are directed through the cylinder head to supply the camshaft bearings. Excess oil is flung by the rotating camshaft to lubricate any valvetrain components. Also, a feed is plumbed from the cylinder head feeds to supply oil to the timing chain or gears on the camshaft drive. The excess oil from all the components is drained through oil galleries back into the sump. A depiction of the oil flow through a general gasoline engine can be seen in figure 1.

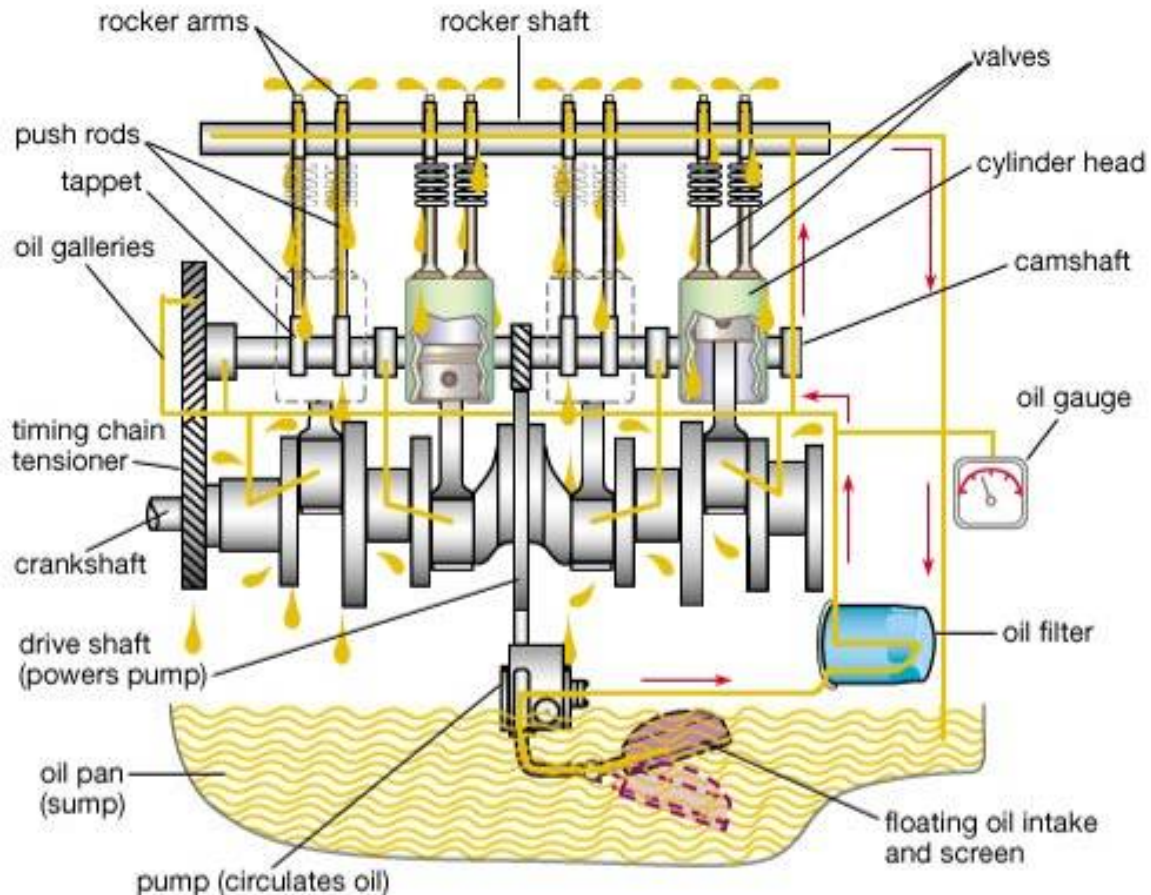


Figure 1 Oil flow illustration (SI engine) [Encyclopedia Britannica 2007]

The two main types of oil systems for motorcycles and automobiles are dry sump and wet sump. The main differences are that wet sump systems contain an oil pan directly underneath the engine with an internal oil pump and dry sump systems contain an oil reservoir located externally along with an external oil pump. Wet sump systems are standard on most road cars as they are cheap, relatively simple, and good for packaging. They are good for low engine speeds and low cornering forces. Dry sump systems are standard for race vehicles as they are more flexible with packaging, offer lower center of gravity of the engine, are suitable for high engine speeds, and are suitable for higher cornering and accelerating/decelerating forces.

At higher engine speeds the oil is subject to harsher treatment as it experiences pressures up to 14000bar in the oil film and then thrown at 300mph into the sump as it

exits the big end bearings [Goddard 2007]. This harsh treatment causes the oil to be aerated which then limits its lubricating performance. With the use of dry sump system components the air churned into the oil can be removed. This is a benefit offered, which the wet sump system can not.

2.2 Wet Sump Oil System

The wet sump system contains an oil reservoir/oil pan directly underneath the engine. The oil pump lies within this reservoir and sucks oil from a tube and supplies it to the rest of the engine. The oil pan has to be big enough to carry 4 to 7 liters of oil which is typical for standard road cars. An illustration of a wet sump system can be seen in figure 2.

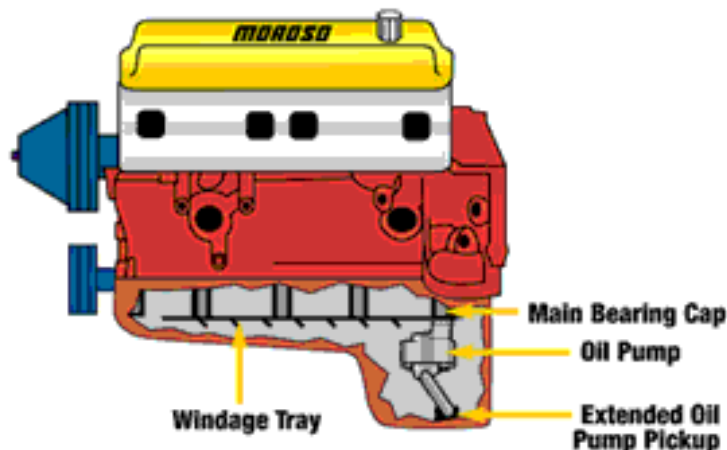


Figure 2 Wet Sump Oil System [Moroso 2007]

2.3 Dry Sump Oil System

A dry sump system contains an external oil tank and external oil pump. An illustration of this system is shown in figure 3. By having an external oil tank the engine can have a flat bottom allowing it to be placed lower, lowering the overall centre of gravity of the vehicle. A lower centre of gravity is advantageous in race cars as it allows for reduced chassis roll, and hence, higher cornering forces can be achieved. The next benefit is increased horsepower because of less aerodynamic drag in the crankcase. Less

aerodynamic drag is achieved because the scavenge pump sucks from the crankcase creating a depression. In this depression all of the rotating parts experience less drag. The depression is normally 0.5bar below atmosphere in high displacement engines such as in Indy cars and 0.25bar for F1 engines with smaller displacement [Goddard 2007]. The depression is controlled with an orifice placed in a high point in one of the valve covers. In a standard car the engine speed range is normally up to 7000rpm, whereas for a race car it can go up to 20,000 rpm. With such high engine speeds a wet sump system would not be adequate as the crankshaft would lose power dipping into the oil at speeds of 300mph. Furthermore, these high speeds would cause high impact forces and stresses which the crankshaft can not cope with.

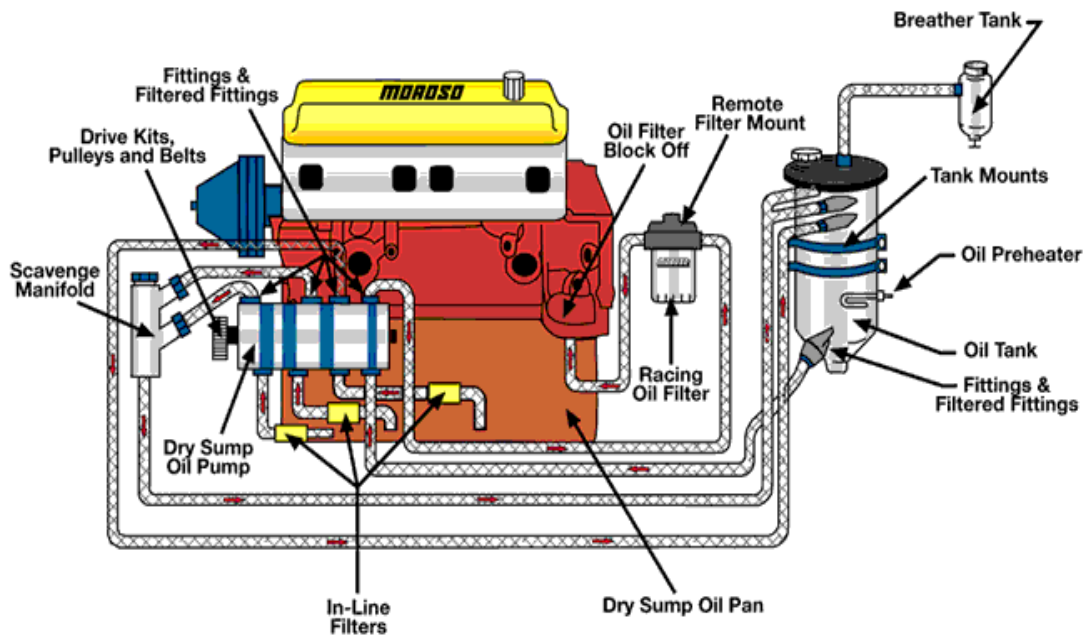


Figure 3 Dry Sump System [Moroso 2007]

2.4 Pump Types

2.4.1 Positive Displacement & Dynamic Pumps

Pumps are classified into two main categories; positive displacement and dynamic or momentum-change pumps. Positive displacement pumps (PDPs) work by forcing the fluid along by a constant volume change process. A gap opens and the fluid enters. The gap then closes and squeezes the fluid out. All PDPs deliver a pulsating or periodic flow as the cavity (gap) volume opens, traps, and squeezes the fluid [White 2003]. PDPs are advantageous because they can pump any fluid regardless of its viscosity. Dynamic pumps work by adding momentum to the fluid by fast moving parts (blades or vanes). The fluid increases momentum while moving through open passages and then enters into a diffuser section where it exchanges its high velocity into high pressure. Dynamic pumps are able to provide higher flow rates than PDPs at a more steady discharge (less pulsating flow), but ineffective at transferring high viscous fluids. Dynamic pumps normally need priming and if the fluid is filled with air then the pump can not suck up the fluid. A good design will place the pump inlet below the fluid so that it has a positive head. The PDP is not as sensitive to air in the liquid and is self priming. It is a good pump for pumping oil as it is not highly affected by the high viscosity of the oil. A summary of the different types of dynamic and positive displacement pumps is shown in table 2 and an illustration of the pumps is shown in figure 4.

Pump Category	Type	Components
Positive Displacement	Reciprocating	Piston or plunger, diaphragm
Positive Displacement	Rotary	Sliding vane, flexible tube or lining, screw, peristaltic (wave contraction)
Positive Displacement	Multiple rotors	Gear, lobe, screw, circumferential piston
Dynamic	Rotary	Centrifugal or radial exit flow, axial flow, mixed flow (radial + axial)
Dynamic	Special designs	Jet pump or ejector, electromagnetic, fluid actuated (gas lift or hydraulic ram)

Table 2 PDP and Dynamic Pump Types and Components

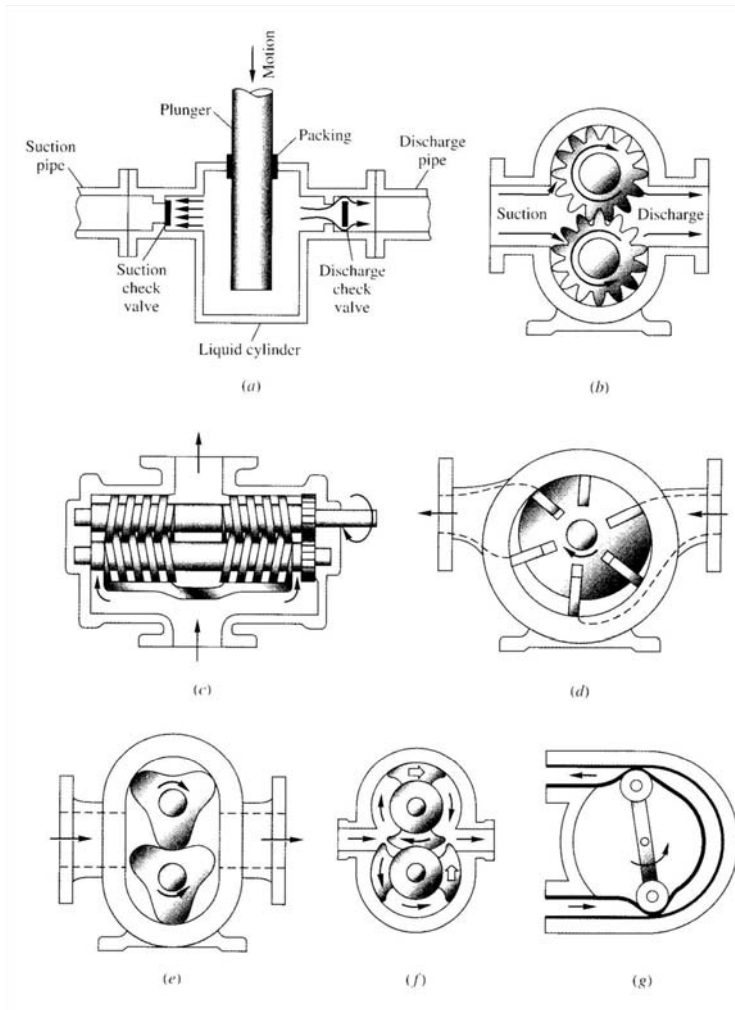


Figure 4 Positive Displacement Pumps [White 2003]

The pumps illustrated in figure 4 are classified as follows: (a) reciprocating piston or plunger; (b) external gear pump; (c) double screw pump; (d) sliding vane; (e) three-lobe pump; (f) double circumferential piston; (g) flexible tube squeegee.

The relative performance of change in pressure (P) versus flow rate (Q) for PDP and dynamic pumps at constant pump speed is shown in figure 5. The PDP generates almost a constant flow rate and unlimited pressure rise with little effect from viscosity changes. The dynamic pump performance degrades with viscosity effects. At zero discharge (shut off conditions) the ΔP is at maximum and as the flow rate increases ΔP goes to zero. The PDP is a better option for an oil pump as viscosity changes have little effect on pump performance, flow rate is nearly constant, and pressure rise is

unlimited. Furthermore, pressure can be controlled with a pressure relief valve and flow rate will change with engine speed.

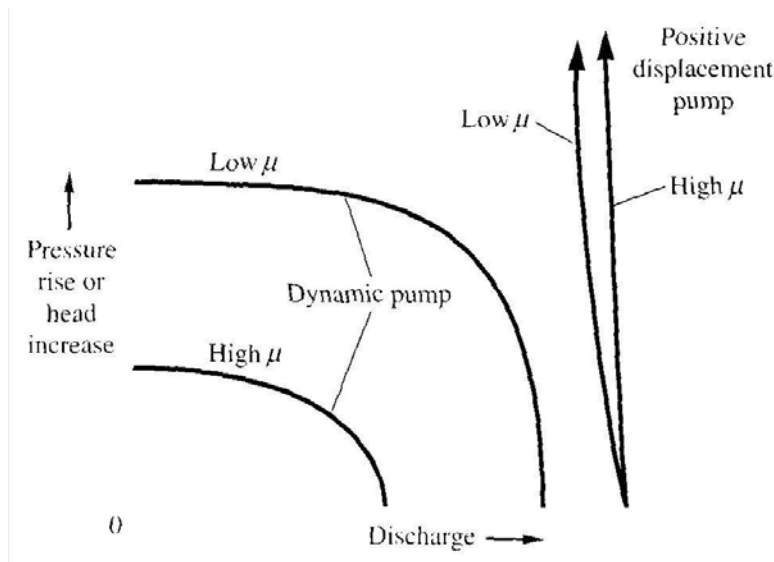


Figure 5 Dynamic & PDP Performance Curve [White 2003]

2.4.2 Motorsport Industry Oil Pumps

For the motorsport industry the following oil pumps are most common:

1. Spur gear pumps
 - a. These pumps offer a small diameter highly effective solution as the filling and delivery can take place through long slots along the whole length of the gear set ensuring excellent volumetric efficiency at all pump speeds [Goddard 2007]. The gear diameter is normally no greater than its width. The number of teeth controls the pulsed flow effect to a minimum. These pumps need to be mounted at the lowest point possible relative to the sump to minimize suction head requirements. The pump is normally driven by a light 5mm pitch chain or gear set off of the crankshaft or cams.
2. Small internal external gear types
 - a. These normally consist of a 4 tooth inner gear rotating inside a 5 tooth outer gear. These were typified by the Hobourne Eaton rotors used

throughout the automotive industry in the 1950's to 1980's [Goddard 2007]. Filling problems arise because of only being able to fill through limited areas on each end. Also, cavitation problems arise at high speeds, therefore, the pump speed is reduced to about half the crankshaft speed. The pressure pulses of these pumps can be quite high. The pulses can become large enough to set the pressure relief valve to go into resonance wearing out its seat and if the filter is too close the pulses could cause the filter to break up [Goddard 2007].

3. Small internal external gear types with multiple teeth
 - a. These were typified by SHW manufacturing. These pumps attempt to improve on the hydraulic losses with multiple teeth designs and improved gear tooth forms. The mistake is normally made by increasing the gear tooth diameter to an extent where the pump then suffers because more torque is needed to achieve the same flow [Goddard 2007].
4. Large diameter multiple toothed internal external gear sets
 - a. These pumps can be run at high speeds, are compact (very flat), and keep pulsed flow effects down to a minimum. The diameter of these rotors can be up to 10times their thickness. The downside is that because of the increased diameter the pump actually turns into a small dynamometer sucking up valuable power. An example is that one of these pumps fitted on the Jaguar V12 absorbed 27bhp at 7000rpm [Goddard 2007]!
5. Vane pumps and swash plate piston pumps
 - a. Very good for high pressure. Flow rate can be precisely controlled independently of engine speeds due to the variable stroke provided by the swash plate. Very expensive and more commonly used in gas turbines.
 - b. The vane pumps are not commonly used as they do not provide a simple cost effective solution.

3 BACKGROUND OF LUBRICANTS & BEARINGS

3.1 Lubricants

Lubricants are dilute polymer solutions, typically consisting of 80% base oil and 20% additives [Taylor 2002]. By choosing the correct lubricant, engine friction can be minimized at the same time increasing power and reducing engine wear. Three important characteristics are needed in a lubricating fluid: [Pulkrabek 2004]

1. It must adhere to the solid surfaces.
2. It must resist being squeezed out from between the surfaces, even under the extreme forces experienced in an engine between some components.
3. It should not require excessive force to shear adjacent liquid layers. The property that determines this is called viscosity.

3.1.1 Lubricant Types

There are two main types of oils used in automotive engines. These are mineral oils and synthetic oils. Mineral oils are most common in yesterday's engines, however, today synthetic oils are becoming more common because they can offer much better performance.

Mineral oils are raffinates (the portion of a liquid that remains after other components have been dissolved by a solvent) which come from petroleum. The issue is that no two batches of oil created are alike because of the infinite possibilities of the raffinates molecular structure arrangements, even though they have the same number of C and H atoms [Basshuysen *et al* 2004]. Also, raffinates are made from crude oils which come from all over the world (notably Middle East and North Sea) which also contributes

to non uniformity within the oils. For high performance applications, raffinates can not offer the performance or consistency of synthetic oils.

Synthetic oils are based on PAO (PolyAlphaOlefin), PIB (PolyIsoButane), PPG (PolyPropylene Glycols), and PEG (PolyEthylene Glycols) hydrocarbon bases. These hydrocarbons are created from ethane (ethylene) after cracking, which is a form of raw gasoline. PAO, PAO plus esters, or PAO plus hydrocrack oils are most commonly used in modern engines. The other synthetic base liquids (PIB, PPG, PEG) are used for hydraulic and industrial gear oils. Synthetic hydrocarbons have a modified molecular structure which allows them to have better fuel economy, wear protection, lifetime, and oil consumption than mineral oils. The one disadvantage of synthetic oils is they can cost 50 to 400% more than mineral oils [Basshuysen *et al* 2004].

PAO based oils have long chain molecules ($-\text{CH}_2\text{-COO-CH}_2-$) which give a very desirable effect to lubricants and that is being dipolar and therefore attracted to metal surfaces [RaceTech 2007]. The problem is that oils have a range of additives in them to reduce wear, inhibit oxidation, clean, and other functions. Some of these additives are also dipolar, and therefore, are in competition with the PAO lubricant for a place against the metal surface. It is essential that an oil be matched to a system for optimal performance.

The long chain molecules carry another advantage and that is under extreme pressure applications. For example, a high impact force applied to the journal bearings during combustion would normally cause the oil film to be splattered out, but because of the long chain molecules the oil is less likely to break apart within the bearing [Goddard 2007]. In other words, as the oil gets squished out, new oil gets pulled in by the chain effect.

3.1.2 Lubricant Additives

Additives are introduced into the base oils (mineral or synthetic) to add properties that do not normally exist in the base oils, remove properties, and reinforce properties. Additives

help to clean the engine components, add corrosion protection, extend oil life, suppress foaming, reduce oil consumption, and increase lubrication performance. Typical additives are summarized in table 3.

Additive	Function	How it Works	Ingredients
Viscosity Modifiers	To improve viscosity at high temperatures. To help with oil evaporation loss.	Long chain polymers which at high temperature extend into the oil to control its viscosity. At low temperatures their solubility is decreased and their long chains curl into themselves having less effect on the surrounding oil [RaceTech 2007].	Polymethacrylate Polyalkylstyrenes Olefin copolymer(OCP) Star polymers PIB Styrene ester polymers
Detergents	To help remove floating particles or debris from the oil and components. To prevent sludge formation.	During combustion, oil-insoluble residues form in solid or liquid state and can form sludge. This is prevented with detergent and dispersant additives. Polar attraction is also used to promote this effect.	Metal sulfonates Metal phenolates Metal salicylates
Anti-wear Additives	To help improve boundary layer lubrication.	A class of compounds known as zinc dialkyldithiophosphates. These molecules attach to the surface by polar attraction.	Zinc alkyl dithiophosphate Molybdenum compounds Organic phosphate Organic sulfur and sulfur phosphorous compounds
Friction Modifiers	To help reduce friction in boundary layer lubrication.	Not suitable in wet clutch motorcycle applications as molybdenum compounds will cause slippage.	Mild EP additives Fatty acids Fatty acid derivatives Organic amines
Extreme Pressure Additives	To help the lubricant survive under high forces seen in the gear train.	Common in motorcycle applications where the same lubricant is used for the transmission and engine.	Zinc alkyl dithiophosphate Molybdenum compounds Organic phosphate Organic sulfur and sulfur phosphorous compounds
Anti-Oxidants	To help with oil ageing. Important for oil change intervals.	At high temperatures engine oils tend to “age” since oxygen bonds to the hydrocarbon molecules yielding acids, and resinous or asphalt-like components can form [Basshuysen et al 2004]. The oil is continuously mixed with air as it flows off, drips off, sprayed off, or flung off. This mixing causes the oil to become thicker and less effective.	Zinc dialkyldithiophosphates Alkylphenols Diphenyl amines Metal salicylates
Corrosion Inhibitors	To protect components against corrosion.	When an engine is turned off, humidity can condense to water inside the engine. Water is a reaction product of fuel. One liter of fuel can produce one liter of water [Basshuysen et al 2004]. Oil can only absorb a limited amount of water and therefore corrosion inhibitors are needed.	Metal sulfonates Organic amines Succinic acid half-esters Phosphorous amines, amides

Table 3 Engine Oil Additives

An issue with additives is that an added property might improve one area of engine operation, but negatively affect another. An additive which helps boundary lubrication in the valvetrain might affect the hydrodynamic lubrication in the bearings by increasing its oil film thickness. For example, anti-wear additives for improving boundary lubrication are dipolar, making them metal surface attractive, if this polar attraction is too great then the fresh incoming oil to the main bearings will be added on top of this layer, increasing the oil film thickness. An increased oil film thickness can cause higher frictional forces and more power losses. A too small oil film thickness can cause surface to surface contact where bearing failure is sure to occur. However, oil chemists can tailor the oil for specific engines and adjust the polarity of additives to suit engine requirements.

3.1.3 Lubricant Parameters Affecting Performance

Three key parameters affect oil viscosity: temperature, pressure, and shear rate. When the viscosity of a lubricant changes the work required to shear the fluid changes, which affects system losses. System performance can be maximized if these variables are considered in the design process.

The main property of oil is its viscosity. Viscosity is a measure of how easily two fluid layers shear apart. Viscosity is expressed as absolute viscosity (η) or kinematic viscosity (ν). The equation relating both is:

$$\eta = \nu \rho \quad (3.1)$$

where ρ is the mass density of the oil. Absolute viscosity is needed for determining lubricant pressures and flows within bearings as it is density dependent, which is temperature dependent.

The viscosity of oil decreases with rising temperature and increases with pressure. The expression for kinematic viscosity as a function of temperature and pressure is

shown in equation 3.2 [Ferguson 2001]. Values of the constants used in eq. 3.2 are given in table 4. With this expression, viscosity changes due to pressure and temperature can be determined. This is very useful in journal bearing design as high pressures and temperatures occur.

$$\nu = C_1 \exp \left[\frac{C_2}{T - C_3} + \frac{P}{C_4} \right] \quad (3.2)$$

Where ν is the kinematic viscosity of oil, C_1, C_2, C_3, C_4 are constants from table 4, T is temperature, and P is pressure.

SAE grade	ρ (kg/m ³)	c_p (kJ/kg K)	ν (m ² /s)	C_1 (m ² /s)	C_2 (K)	C_3 (K)	C_4 (bar)
5W	860	1.99	48.2×10^{-6}	6.44×10^{-4}	900	162	433
10W	877	1.96	86.9×10^{-6}	4.53×10^{-4}	1066	157	296
15W	879	1.95	102×10^{-6}	7.49×10^{-4}	902	173	181
20W	886	1.94	259×10^{-6}	2.63×10^{-4}	1361	150	105
20	880	1.95	129×10^{-6}	5.67×10^{-4}	1028	165	153
30	886	1.94	259×10^{-6}	4.70×10^{-4}	1361	140	105
40	891	1.92	361×10^{-6}	2.17×10^{-4}	1396	151	91.7
50	899	1.91	639×10^{-6}	2.24×10^{-4}	1518	150	75.2

Source: Cameron, 1981.

Table 4 Engine Oil Properties (T = 298K, P = 1bar) [Ferguson 2001]

The Cross equation (eq. 3.3) is useful for determining viscosity due to shear rate effects.

$$\eta = \eta_\infty + \frac{\eta_0 - \eta_\infty}{1 + \frac{\gamma}{\gamma_c}} \quad (3.3)$$

Where η is the viscosity (mPa.s) at shear rate γ (1/s). η_0 is the viscosity at zero shear rate and η_∞ is the viscosity at infinitely high shear rate. γ_c is the shear rate which lies half-way between η_0 and η_∞ . This formula is particularly important in all lubricants because lubricants are designed to readily shear themselves apart. In a high speed bearing, the shear rate is quite high, which causes the temperature to rise. At some point a threshold is met and a 20W-50 oil which is higher in viscosity is now the same as a 5W

-30 oil. This is because as the temperature rises so high due to high shear, the lubricant viscosity is brought down. By looking at figure 6 the reader can see that with high temperatures, all lubricant viscosities become essentially the same.

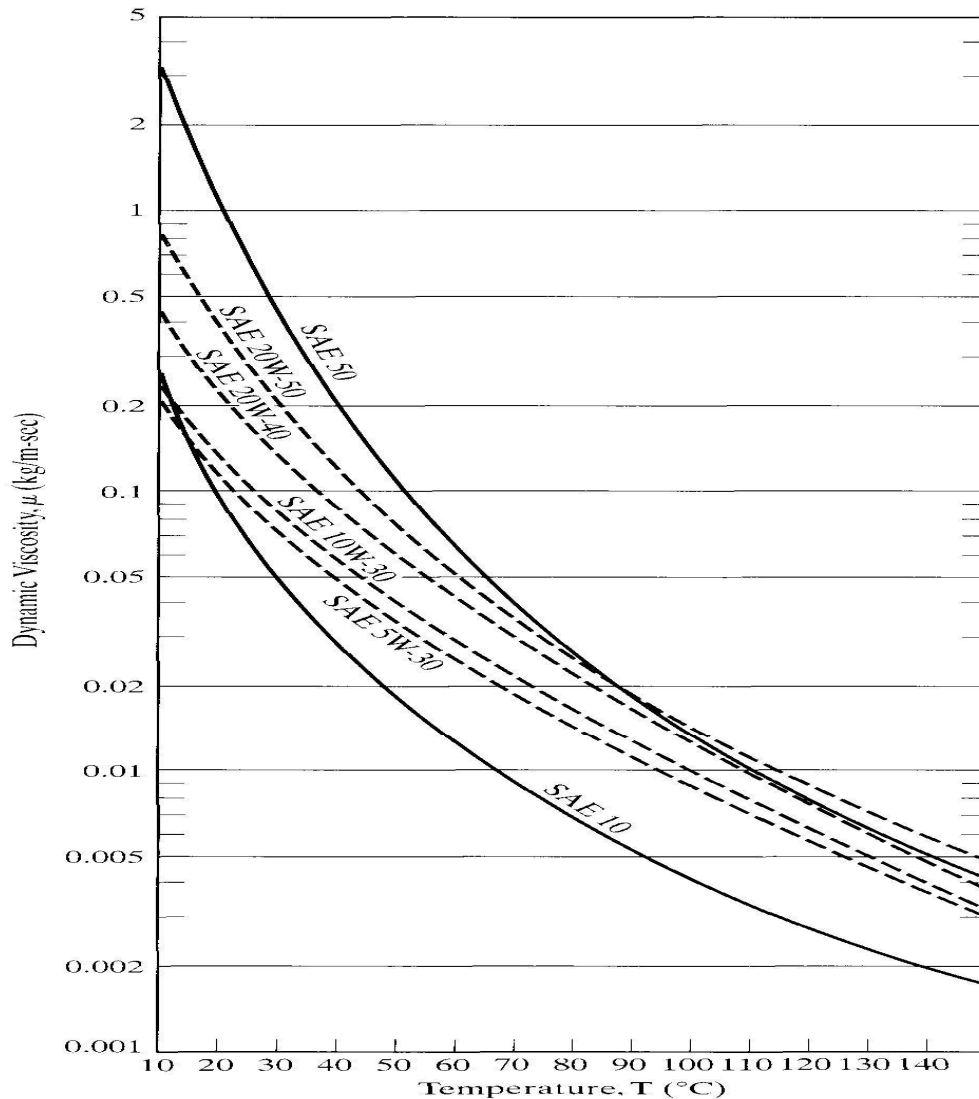


Figure 6 Dynamic Viscosity as a function of Temperature for multi-grade engine oils [Pulkrabek 2004]

Shear rate effects are more important in multi-grade oils (SAE 5W-30, 10W-40) than solid grade oils because large viscosity changes can occur. Lansdown [Lansdown 1982] states

“If a multigrade oil is to have a viscosity at -18C equivalent to an SAE 20W oil, then the base oil must have a lower viscosity, since the viscosity will be increased

by the polymer. When the oil is then sheared rapidly in a high speed bearing, it will behave as if its viscosity is the same as that of the base oil. In other words, in a fast bearing at 100C the 20W/50 oil will be behaving, not like an SAE 50 oil, but like an SAE 10W or SAE 15W oil”.

This effect will most likely not cause any problems in an automobile engine as many tests have been made to accommodate it. It is important to realize the shear effect though, because a 5W-30 oil and a 5W-40 oil will have different viscosities at cold temperatures, but as the shear rate increases the temperatures, the resulting viscosities of both oils can be essentially the same. Normally, in a high performance engine, higher viscosity oils are used because of the resulting low viscosities which occur at race temperatures and speeds. Figure 7 shows the effects of shear rate on SAE 30 and SAE 20W/50 oils. It shows that at high shear rates the multi-grade oil reduces to almost 50% of its starting viscosity.

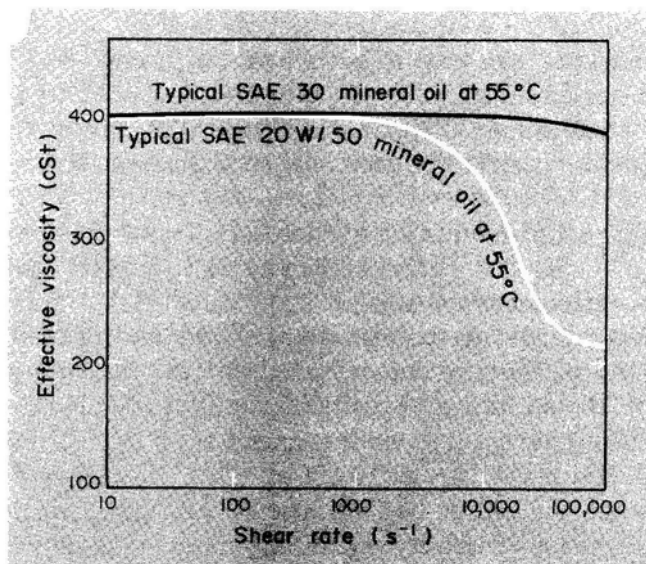


Figure 7 Effect of Shear Rate on Viscosity [Lansdown 1982]

Figure 8 shows how an SAE10W-50 oil varies with temperature and shear rate. As the temperature increases the oil viscosity decreases. As the shear rate increases the oil viscosity decreases, but does not have as much effect as the temperature.

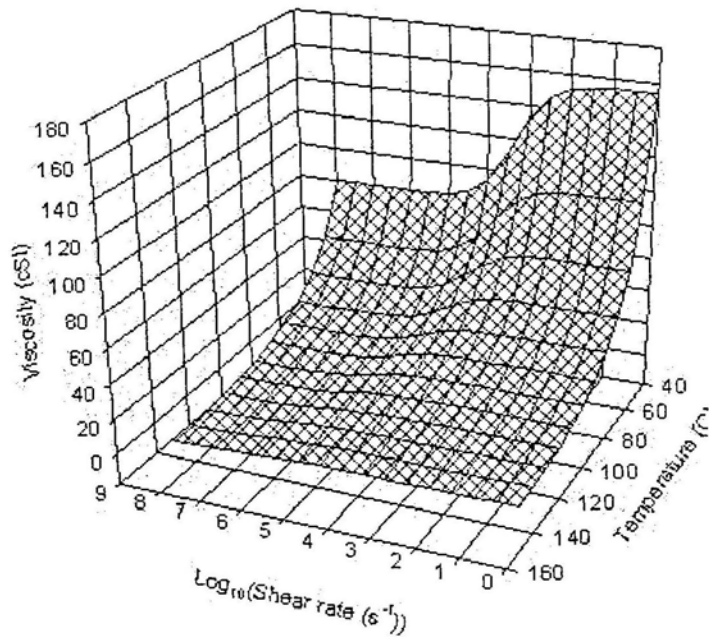


Figure 8 Variation of viscosity with shear rate for an SAE10W-50 lubricant [Taylor 2002]

3.2 Lubrication Theories-Boundary, mixed film, and full film

This section discusses the lubrication zones: boundary, mixed, and full film. It also discusses minimum oil film thickness needed to eliminate asperity contact. The objective is to operate in full film lubrication which is hydrodynamic lubrication; virtually no wear occurs in this region.

The challenge with an engine though is that the piston assembly, bearings, and valve train each operate in a different regime of lubrication. The piston assembly operates in mixed lubrication, the bearings operate in full film lubrication, and the valve train operates in boundary lubrication. Thus, each lubrication regime will require different metallurgical material combinations, different surface finishes, and different lubricant additives. As discussed in section 3.1.2, additives are used to improve lubrication properties depending on the type of lubrication conditions i.e. boundary, mixed film, or full film. This poses an issue because if an additive is introduced to

improve boundary lubrication it could affect hydrodynamic lubrication because both are different types of lubricating systems. Engine oil needs to be developed well enough to suit all three lubrication zones.

Although, it would be an interesting concept if a 'tri-lubricating system' were to be introduced for an engine. This system could have tailored oil for each of the three systems: bearings, piston assembly, and valve train. Of course there would be extra parts, but these parts would be reduced to 1/3 rd of their original size; keeping weight to approximately the same as one main pump and roughly the same power loss. A little extra weight and power loss of say 6hp instead of 3hp is frowned upon, but consider a main crankshaft bearing which consumes 10hp at 10,000rpm, this perhaps could be reduced to half the hp with a oil designed specifically for it. Adding up all the bearing hp savings would already outweigh the losses from having a few extra pumps and parts. And, valve train and piston assembly hp savings could be 10-15% of overall engine power. This is just an idea which needs to be investigated further.

The Stribeck Diagram (shown in figure 9) is referred to for determining which regime of lubrication a component is operating in. The Stribeck diagram is a plot of the Sommerfeld Number vs. the Coefficient of friction. The Sommerfeld Number is useful because it takes into account viscosity, pressure, and velocity; all of which affect the oil film thickness which determines the amount of friction occurring. The goal when designing components for lubrication is to design them to operate in the 'thin film' region of the Stribeck Diagram. In the 'thin film' region, the least friction occurs which leads to reduced wear and reduced power losses.

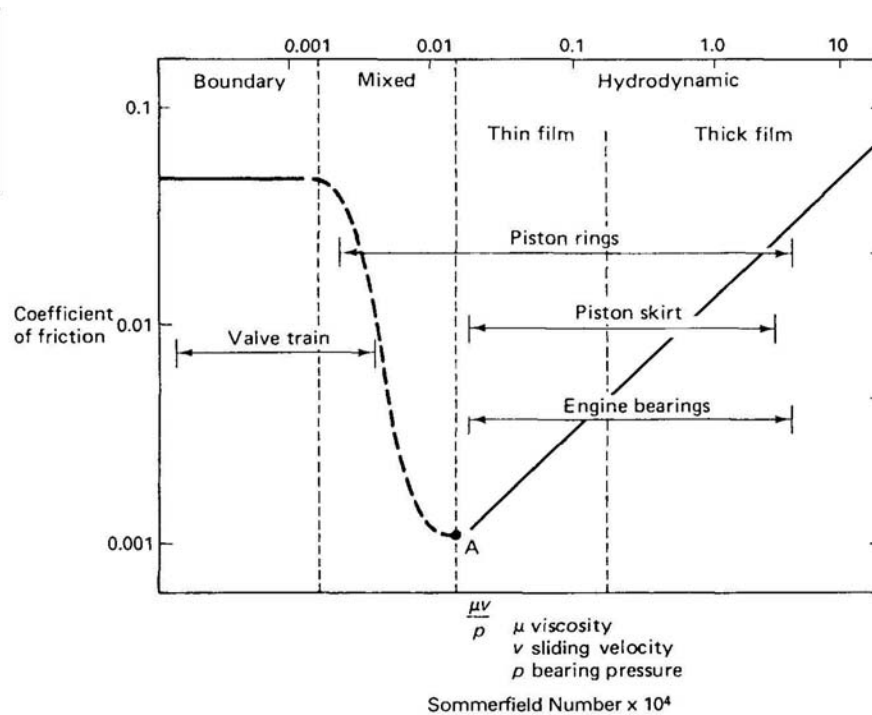


Figure 9 Engine lubrication regimes on the Stribeck Diagram [Stone 1999]

When thin film lubrication is not achieved higher friction values occur. Friction is the contact of asperities between two surfaces rubbing on one another or shearing the peaks off one another. Figure 10 shows the contact between two surfaces is at the asperity tips. Asperities are microscopic peaks and valleys on a material's surface.

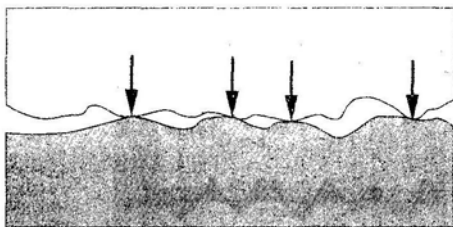


Figure 10 Friction due to asperity contact [Pulkrabek 2004]

Figure 11 shows that when an lubricating oil with correct film thickness is introduced, the two surfaces are hydraulically floated apart so that no asperity contact occurs. This is full film or hydrodynamic lubrication. Hence, no lubrication is boundary lubrication where the asperities are in contact as shown in figure 10 or 11 (a). Finally, the zone between boundary and full-film lubrication is mixed-film lubrication.

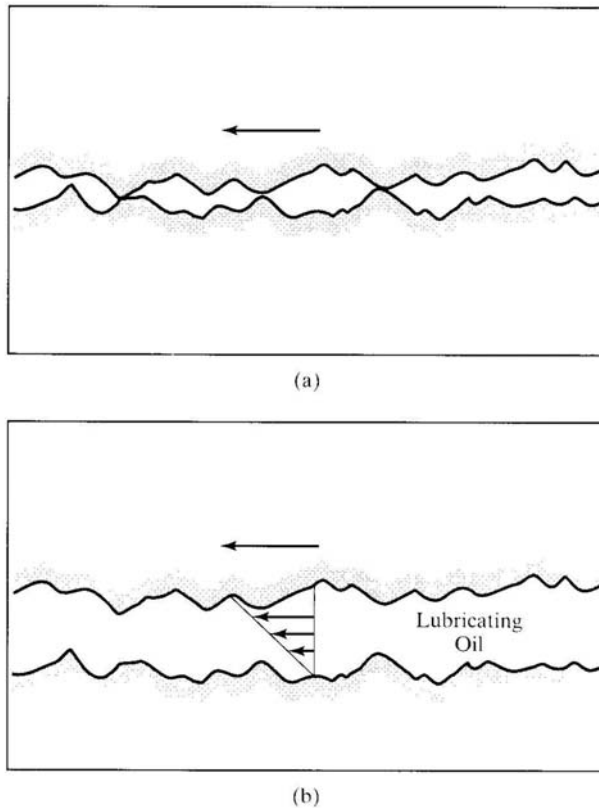


Figure 11 Full-film lubrication (a) boundary lubrication. (b) full-film lubrication [Pulkrabek 2004]

Asperities or surface roughness values can be controlled to an extent. Surface finishes can range from 0.1 micro meter for mirror like finishes to 3.2 micro meters for a standard machined finish. Figure 12 is an excellent chart to refer to for standard finishes, but it also suggests a minimum oil film thickness range for a variety of surface finishes. Automotive and aircraft engine bearings with very finely finished surfaces can have min oil film thicknesses from 2.5 to 5 microns (0.0001 to 0.0002in.) [Booser *et al* 2001]. This minimum oil film thickness will be useful in chapter 6 for journal bearing design because the film thickness for the main bearings is calculated and will be compared to these typical values.

Surface Finish ^a (Centerline Avg. R_a)		Description of Surface	Examples of Manufacturing Methods	Allowable Minimum Film Thickness	
μm	$\mu\text{in.}$			μm	$\mu\text{in.}$
0.1–0.2	4–8	Mirror-like surface without toolmarks	Grind, lap, superfinish	2.5	100
0.2–0.4	8–16	Smooth surface without scratches, close tolerances	Grind and lap	6.2	250
0.4–0.8	16–32	Smooth surface, close tolerances	Grind and lap	12.5	500
0.8–1.6	32–63	Accurate bearing surface without toolmarks	Grind, precision mill, and fine tuning	25	1000
1.6–3.2	63–125	Smooth surface without objectionable toolmarks, moderate tolerances	Shape, mill, grind, and turn	50	2000

^aCombined conjunction roughness $R_a = \left(R_{a, \text{shaft}}^2 + R_{a, \text{bearing}}^2 \right)^{0.5}$ (see Chapter 3)
Source: ESDU (1967), Hamrock (1994).

Figure 12 Surface Finishes & Min. Oil Film Thickness [Booser *et al* 2001]

3.2.1 Surface Parameters

Surface roughness is most commonly classified by R_a , average roughness, and less commonly by R_q , root-mean-square roughness. R_a gives the average deviation of the high's and low's of a profile from the arithmetic mean elevation line. R_q is the root mean square of the individual deviations from the arithmetic mean line. R_q values are more sensitive to occasional high's and low's in a profile which makes it more ideal to use for fine surface finishes of honed surfaces. There is also peak-to-valley height values R_z and R_y which measure the average extremes of the high's and low's within the sampling length. Figure 13 shows the commonly used surface amplitude characterizations, where L is the sampling length normally set to be five times the longest wavelength of profile fluctuations, p 's are peaks, and v 's are valleys.

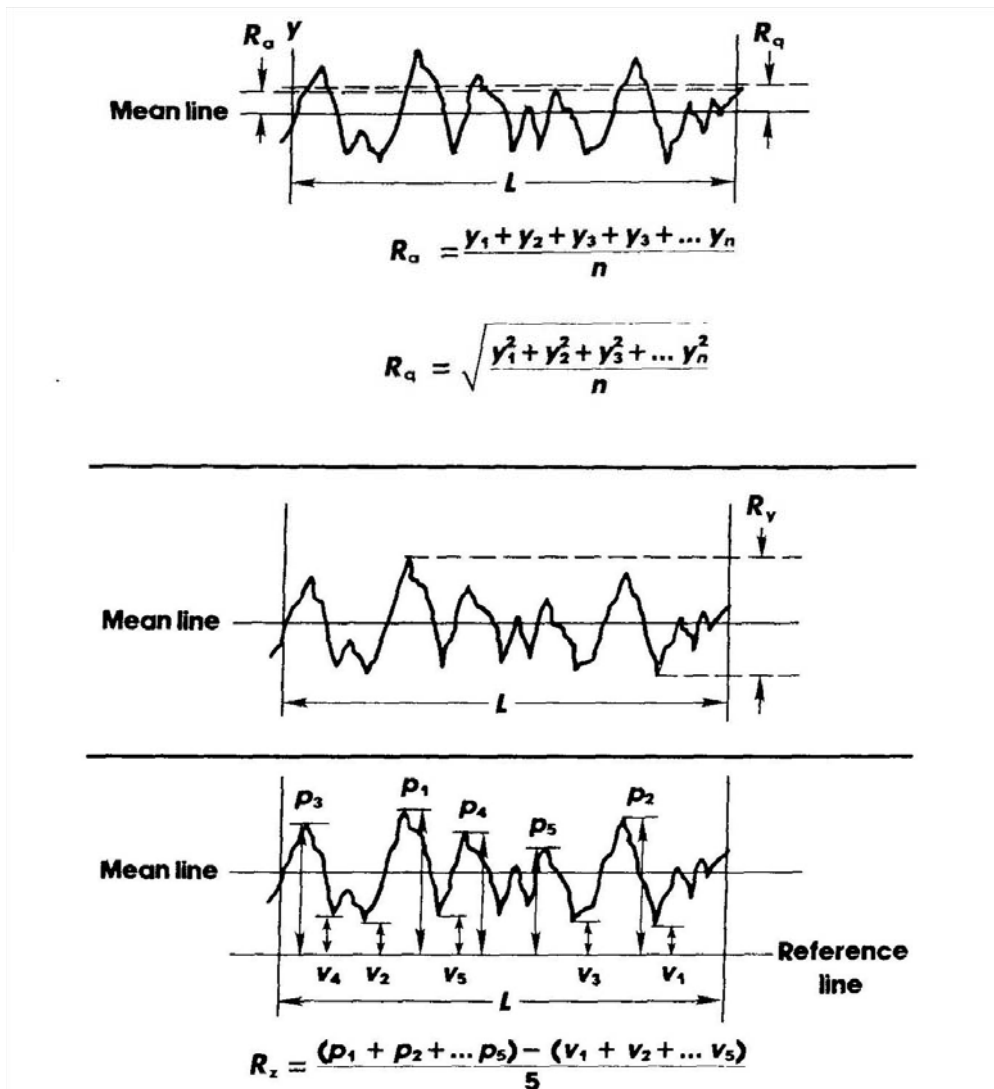


Figure 13 Common Surface Amplitude Characterizations [Booser *et al* 2001]

3.2.2 Surface Finishes

There are many types of surface treatments available to improve surface finishes. The ones of main interest are Plasma Electrolytic Oxidation (PEO) of Keronite ceramic performed by Keronite Ltd., Cryogenic Processing performed by Controlled Thermal Processing Inc., and Physical Vapour Deposition (PVD) or Plasma Assisted Chemical Vapour Deposition (PACVD) performed by Oerlikon Balzers Ltd..

Through PEO processing an aluminium piston crown surface can be transformed into a hard durable layer of Keronite ceramic. This offers protection against erosion and thermal cracking. It acts as a thermal barrier reducing piston temperatures. It does not peel or crack because of atomic bonding, unlike conventional ceramic processes which are sprayed on. Furthermore, Keronite is 100 times more thermally resistant than uncoated aluminium (thermal conductivity = 1.6W/mK). Hardness is in the range of 2000HV with a Ra roughness < 1 micron. In the top ring groove there is 7 times less system wear than with conventional hard anodized surfaces [Keronite Ltd. 2007]. It reduces wear and friction in the cylinder liners and provides a surface Ra of 0.1-0.2 (with polishing). For oil retention, the Keronite porosity can be controlled.

Cryogenic processing brings parts down to temperatures below 120K (-244F, -153C). It is different from cold treatment processing which uses temperatures around 178K (-140F, -96C). This process makes changes to a metal's crystal structure by converting retained austenite into martensite and promotes the precipitation of very fine carbides [Controlled Thermal Processing Inc. 2007]. The best heat treating processes leave about 10-20% austenite. Therefore, internal stresses still result because austenite is about 4% smaller in size than martensite making a mis-match. Through cryogenic processing the austenite is converted to martensite creating a metal with less internal stresses and more uniform hardness. In some cases, the standard deviation hardness has been reduced by 33% [Controlled Thermal Processing Inc. 2007]. This process can be done on all parts, however, parts could grow slightly as the austenite is transformed into martensite. For piston rings this process has been known to reduce ring flutter due to the modified wear and vibrational characteristics of the metal [Controlled Thermal Processing Inc. 2007]. By treating the cylinder block, pistons, and rings less size and shape effects occur in the metals during use [Controlled Thermal Processing Inc. 2007]. Furthermore, this process promotes adhesion and improves wear when combined with Nikasil coatings on the liners.

Physical Vapour Deposition (PVD) or Plasma Assisted Chemical Vapour Deposition (PACVD) are advanced processes which can produce coatings in the range of

1-8 microns thick and within low temperatures not affecting the crystal structure. Figure 14 compares different surface treatment methods and clearly shows why PVD or PACVD processes are best.

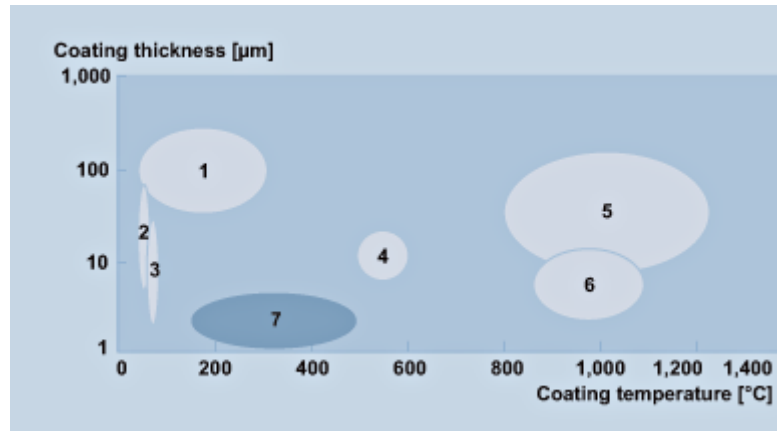


Figure 14 Surface coating thickness vs. temperature for various methods [Balzers Ltd. 2007]

Where 1 Plasma spraying; 2 Electrolytic and chemical deposition; 3 Phosphating; 4 Nitriding (white layer); 5 Boronising; 6 CVD; 7 PVD, PACVD

These processes lead to BALINIT® DLC (diamond like carbon) coatings which provide excellent protection against abrasion, tribo-oxidation and adhesion (scuffing). This coating copes with high speeds, extreme wear, and even running dry [Balzers Ltd. 2007]. This coating is great for pistons, cylinders, and valves which can operate in near dry conditions. In some instances, a lubricating fluid is there only to remove heat and these parts can actually run dry. Alternative and better known coatings to Balanit DLC are Nikasil and Zylan coatings.

Nikasil coatings are comprised of a nickel and silicon carbide matrix which is electrolytically deposited on cylinder walls to a thickness of about 0.07mm [bmwworld 2007]. For cast iron it provides superior cooling which cast iron does not, a harder surface, and is more oleophilic (attracts oil). For aluminum it offers improved lubrication, reduced friction, and superior wear characteristics. The only negative thing to worry about is fuels with high sulphur content; this can dissolve the Nikasil coating.

3.3 Bearing Material Combinations

This section will discuss why bearings are made up of hard and soft materials. As stated in section 3.2, friction is the contact of asperities between two surfaces. If full-film lubrication is present then no asperity contact occurs, however, when asperity contact does occur, shearing of the peaks can take place. For this reason, two different types of materials are used, one hard and one soft, so that the softer material will readily shear when the asperity contact occurs. Furthermore, in hydrodynamic bearings when abrasive particles are in the lubricating oil, these particles will embed into the softer material and therefore not score the bearing.

Asperity contact is much higher in new engines as all the surface finishes are newly finished. With high asperity contact surface stresses are much higher because of less contact area. It is for this reason a new engine must be ‘runned-in or broken-in’ before it can be operated at normal conditions. As the surfaces wear against each other the asperity peaks are sheared off creating bigger contact areas, thus reducing the stresses. Furthermore, all the cut-off asperity peaks are now micro metallic particles in the oil. These particles can cause abrasive wear and quickly wear out parts. For this reason, a new engine will need an oil change more frequently in its beginning stages of operation.

Bearing materials should have good compressive and fatigue strength and; the material should be soft, with a low modulus of elasticity and a low melting point. The soft material allows abrasive particles to be embedded into the bearing while no damage occurs to the hardened journal. The low modulus of elasticity allows the bearing to take shape of the journal for better fits. The low melting point reduces the risk of seizure that could happen during boundary lubrication which occurs at start up. The reader might ask “how is this perfect bearing accomplished since no soft materials exist which have good compressive and fatigue properties?”. The answer is a bi-metal or tri-metal bearing. Strength and fatigue life is gained by a steel backing. The conformability and embedability is gained by a soft phase material which is either cast or sintered onto the steel backing. The overlay (third layer) is 14-33 micro meters thick and helps to improve

corrosion, friction, wear, and seizure. This layer is applied by electroplating or by sputtering the overlay onto the bearing. Thicker overlays provide greater conformability and embed-ability while thinner overlays promote higher load carrying capacity [Stone 1999]. The bearings are classified as ‘thin-wall’ bearings where the steel backing is roughly 1.5mm thick and the soft material is roughly 0.4mm thick.

For racing or high load applications copper based bearings are used. These bearings are mostly lead bronzes, in which the lead is dispersed in a bronze matrix and then cast or sintered onto the steel backing [Stone 1999]. For standard road car or medium duty applications aluminium bimetal bearings are common. These bearings consist of tin or tin and silicon in an aluminium matrix. Common bearing metal materials are listed in table 5.

Designation and nominal composition		Comments
Lead-bronzes		
<i>Vandervell VP1</i>		
Lead	17%	Used in high loading applications such as little-end bearings, and the highest loaded big-ends
Tin	5%	
Copper to	100%	
<i>Vandervell VP2 (SAE 49)</i>		
Lead	23%	Used in connecting-rod and main bearings
Tin	1.5%	
Copper to	100%	
<i>Vandervell VP10</i>		
Lead	10%	Very widely used in high loading applications such as little-end bearings
Tin	10%	
Copper to	100%	
Aluminium-based		
<i>Glacier AS1241</i>		
Tin	12%	Used in big-end and main bearings especially with cast iron journals
Silicon	4%	
Copper	1%	
Aluminium to	100%	
<i>Glacier AS15 (SAE 783)</i>		
Tin	20%	Used in big-end and main bearings with a medium loading, and camshaft bearings
Copper	1%	
Aluminium to	100%	
Whitemetals		
<i>Glacier GM130 (SAE 12)</i>		
Antimony	7.5%	Camshaft bearings, and low-loaded main bearings
Copper	3%	
Tin to	100%	
<i>Glacier GM155 (SAE 13)</i>		
Antimony	10%	Camshaft bearings, and low-loaded main bearings
Tin	6%	
Lead to	100%	

Table 5 Bearing Materials [Stone 1999]

4 V-TWIN OIL SYSTEM & COMPONENTS

4.1 V-Twin Dry Sump Oil System

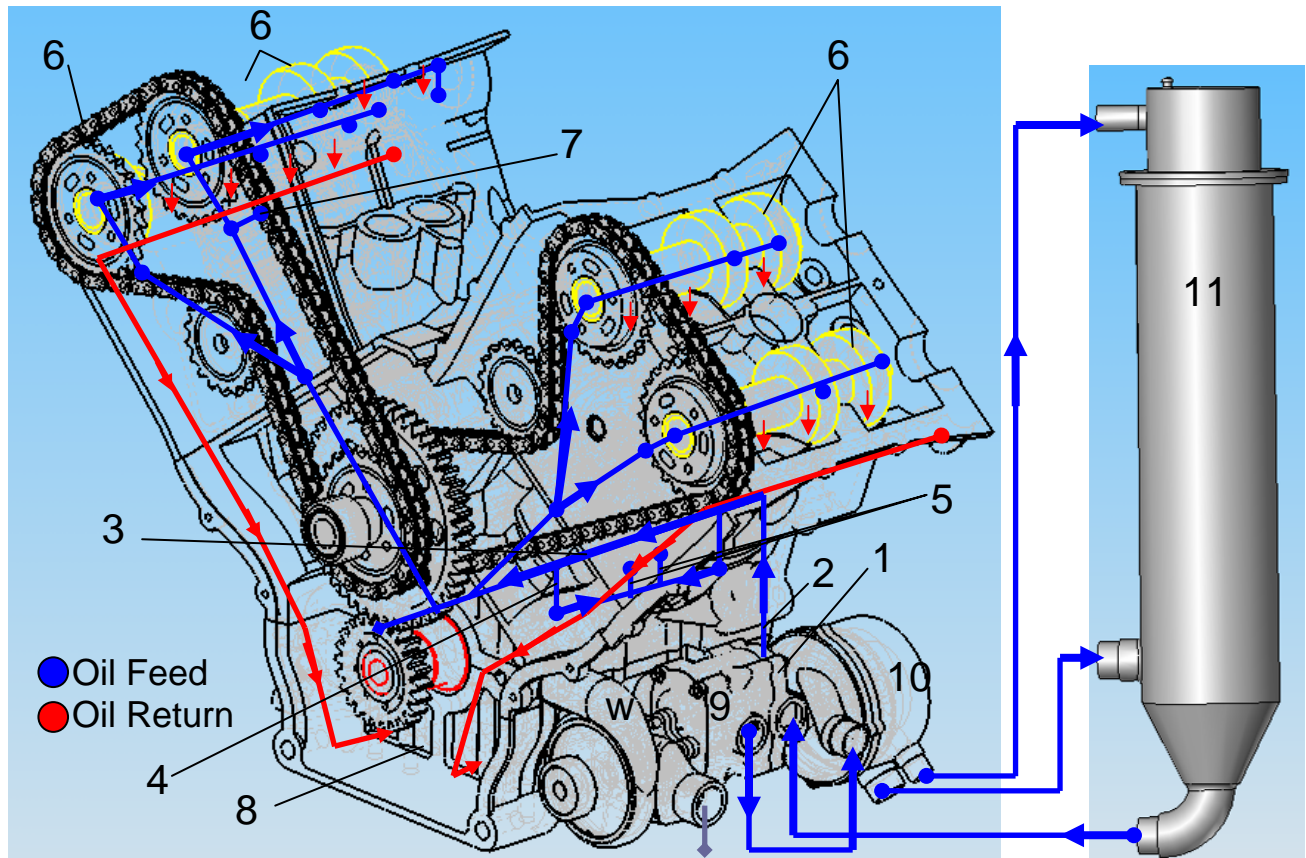


Figure 15 V-Twin Dry Sump Oil System Schematic

The V-Twin dry sump oil system is shown in figure 15. The numerals represent the main stages of the oil as it goes through the engine. 1 Oil pump; 2 Oil filter; 3 Main oil gallery; 4 Oil feeds to main bearings; 5 Oil feeds to big end bearings of connecting rod; 6 Camshafts and valvetrain; 7 Squirt jet for timing chain; 8 Oil sump; 9 Scavenge pump; 10 Centrifuge pump; 11 Oil Tank; and (W) Water pump.

The dry sump system was chosen for the V-Twin as it had several advantages over a wet sump system. It offered the following which the wet sump could not:

- A shorter engine, which lowers the center of gravity of the race car.

- An oil system capable of withstanding high cornering forces >1g and acceleration/deceleration forces >1g.
- A system where the oil could be recycled from all the air churned into it from going through the engine.
- Increased horsepower as it reduces the windage losses of the rotating crankshaft.

Note: Dry sump seals will need to be installed in reverse order as the dry sump is in depression. Depression will be controlled by an orifice sizing in the valve covers. Depression = 0.25 bar less than atmospheric pressure.

4.2 Pressure Requirements

The pressure of an oil system must be able to resist the centrifugal head produced by the rotating crankshaft. However, if there are any hydraulics in the system such as ones for variable valve timing then the pressure due to this will have to be added. If no hydraulics are present then the pressure of the oil pump can be determined from the centrifugal head equations 4.1 and 4.2.

$$H_c = \frac{\rho \times a \times \omega^2}{2} \times (r_2^2 - r_1^2) \quad (4.1)$$

$$P_c = \frac{\rho \times \omega^2}{2} \times (r_2^2 - r_1^2) \quad (4.2)$$

Where H_c is the centrifugal head of the oil in the crankshaft, P_c is the pressure of the oil in the crankshaft, ρ is the density of oil, 'a' is the cross-sectional area of the oil feed, ω is the angular velocity of the crankshaft, r_1 is the inner radius of the crankshaft oil feed, and r_2 is the outer radius of the crankshaft oil feed. The oil pump pressure must be selected so that it is greater than the sum of the centrifugal head pressure; pressure created by the mass of oil normal to the main bearings which is rotating inside the crankshaft. A safety margin of 1bar is usually added to the pressure. This will be the minimum pressure at which the pressure relief valve will be set to open. The system pressure overcomes the centrifugal head pressure in order to force the oil flow into the crankshaft drillings. Once oil is in the crankshaft, the centrifugal head now works with the oil to supply positive pressure on the big end bearings of the connecting rod.

The camshaft bearings only need about 1bar of pressure to perform [Goddard 2007]. A pressure dropper such as an orifice can be placed in the cylinder head to block interface to drop the cylinder head oil gallery supply pressure to the camshafts. Alternatively, labyrinth type pressure droppers are used to keep flow rates high but drop the pressure. A labyrinth type pressure dropper could be a tube with machined female threads. All other component pressure requirements can be adjusted with pressure relief valves or orifices since none of them will require more pressure than the main bearings.

A flow chart for determining oil system pressure requirements is shown in figure 16.

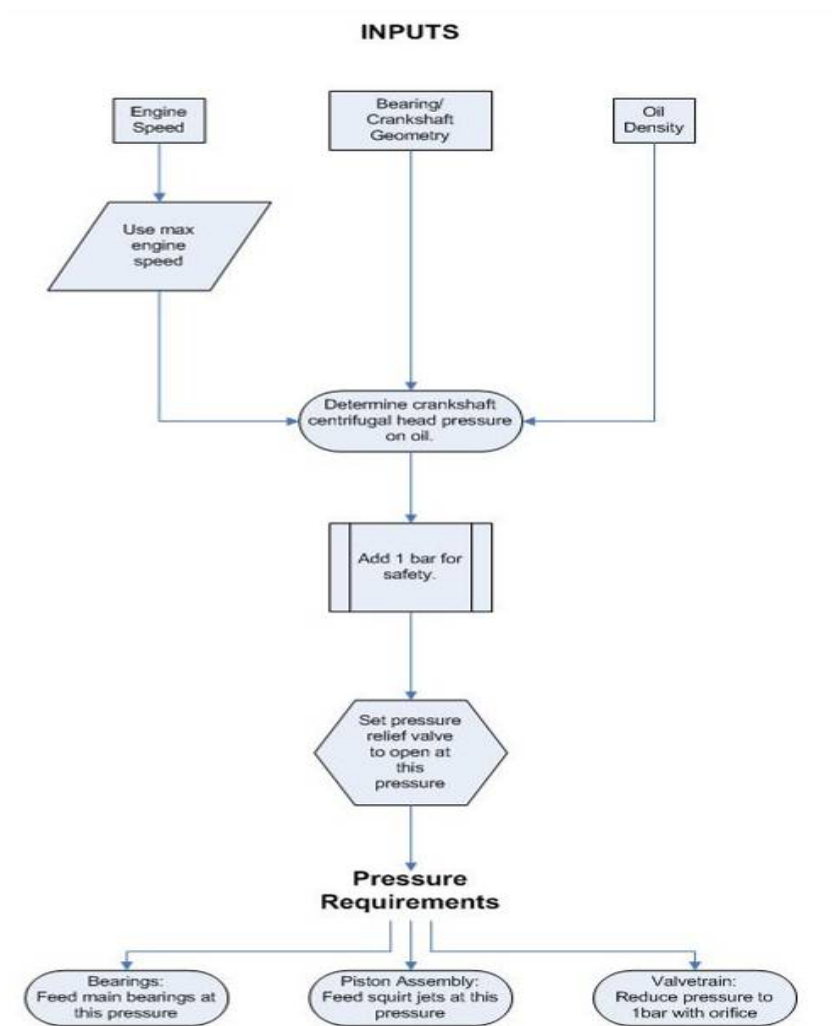


Figure 16 Flow Chart for Determining Oil System Pressure

4.2.1 V-Twin Oil Pressure Requirements

Drawings of the V-Twin crankshaft are shown in figure 17. The drillings for the oil subject to centrifugal head, as well as, the oil feed paths can be seen. Also, r_1 and r_2 used in equation 4.2 to calculate the centrifugal head pressure are shown.

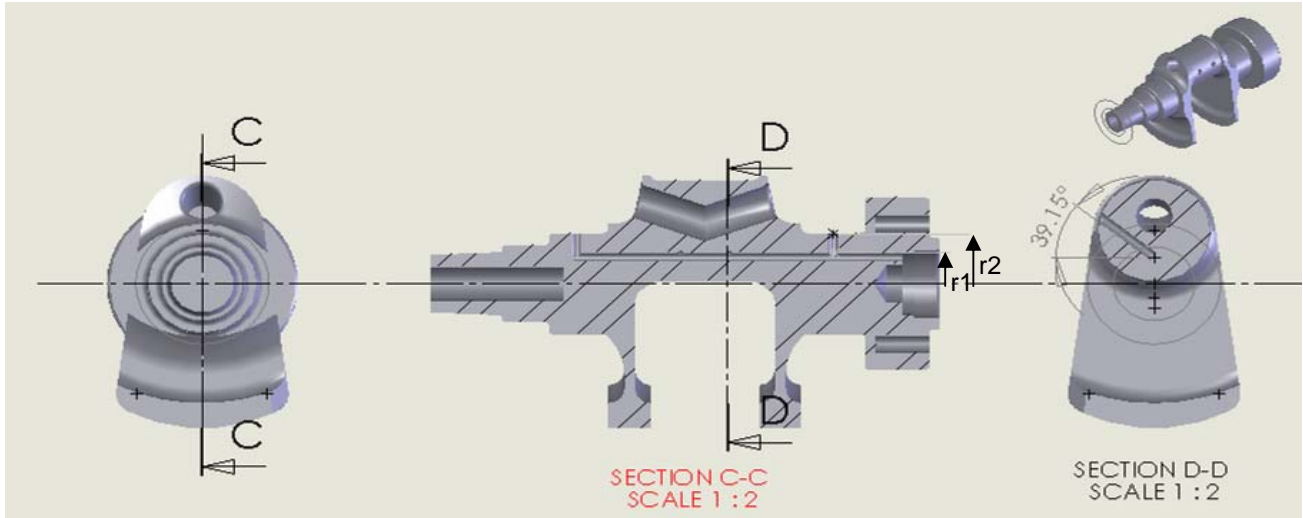


Figure 17 Crankshaft Drillings

Table 6 summarizes the pressures found for the V-Twin using equation 4.2. The pressure calculated for the main bearings (pump must overcome this pressure) was 3.0 bar. Therefore, with a 1bar safety margin added, the pump pressure needed = $3.0 + 1 = 4.0$ bar. To see how this pressure related to other engines a comparison was made to an F1 V10, a Cosworth DFV, and an IRL Engine. Of the three engines, speed affected the pressure the most. This is because in equation 4.2 the speed term is squared. The main variables affecting the pressure were rpm and bearing radius.

Engine Type	Main Bearing Diameter (mm)	Engine Speed (rpm)	Oil Pressure Required
IRL Engine	62.7	10500	2.8
Cosworth DFV	60.3	12000	3.5
F1 V10	42.0	19000	5.6
V-Twin	49.2	12500	3
V-Twin non-offset gallery	49.2	12500	4.6

Table 6 Centrifugal Head on Crankshaft Bearings

The location of the drillings in the crankshaft also affected the centrifugal head pressure. For example, if the oil gallery inside the crankshaft was on the centerline of the crankshaft, then the oil pressure would be much higher. The pressure was calculated for a non-offset oil gallery and is shown in table 6 as 4.6 bar, which is 1.6bar higher than the current setup. Many standard crankshafts employ the non-offset method and therefore have much higher pressures. Higher pressures require larger pumps which use more hp and add undesirable weight to the vehicle affecting overall performance.

The centrifugal head for the big end bearings of the connecting rods was calculated using equation 4.3.

$$P_{be} = \frac{\rho \times \omega^2}{2} \times (r_2^2 - r_1^2) \times \sin(\theta) \quad (4.3)$$

Where P_{be} is the centrifugal pressure on the big end connecting rod bearings and θ is the angle of the oil drilling in the crankshaft. Refer to figure 17 to see θ . θ is necessary because the oil drillings are not normal to the axis of rotation but at an angle of 39.15 degrees. This angle was necessary to clear the hollow section of the crankshaft which was removed to save weight. The big end bearings had a positive pressure of 7 bar. This implies that 7bar of pressure is supplied to the big end bearings of the con-rods just from rotation of the crankshaft.

4.3 Flow Requirements

4.3.1 Main Oil Gallery Sizing

As the number of cylinders in an engine increases the chances of oil starvation in the furthest main bearings from the oil supply becomes a common problem. This happens because of an improper mass balance in the system. The cross-sectional areas of all the feeds must be less than the main gallery cross-sectional area to ensure the main gallery can supply all of the feeds.

Oil flow velocity should be kept to under 3m/s to minimize internal pipe erosion. Furthermore, by keeping the velocity low this will help to separate any air in solution in the oil [Goddard 2007]. Flows of 3m/s are adequate for suction and flows of 10m/s are adequate for oil delivery e.g. from the oil scavenge pump to the oil reservoir [Goddard 2007].

Main gallery sizes are based on summing the cross-sectional areas of the holes feeding the main bearings plus the cylinder head feeds and any other feeds such as squirt jets for pistons, valvetrains, timing chain/gears, etc... This sum is to ensure that the orifices in the system are the bearing feeds/leaks and not the gallery itself. The main gallery cross-sectional area should be at least 25% larger than this total to ensure that a common operating pressure can reach all points in the system [Goddard 2007]. 25% larger is added as a safety factor so there is some reserve in the event of an oil leak or so. Equations 4.4 and 4.5 are the general equations which can be used for any engine for determining the main gallery size.

$$A_{gallery} = 1.25 \times \sum A_{oil_feeds} \quad (4.4)$$

$$\therefore d_{gallery} = \sqrt{1.25 \times \sum A_{oil_feeds} \times \frac{4}{\pi}} \quad (4.5)$$

Where $A_{gallery}$ is the cross-sectional area of the oil gallery supplying all of the feeds, $\sum A_{oil_feeds}$ are the cross-sectional area summations of all the feeds being supplied from the main gallery, and $d_{gallery}$ is the main oil gallery diameter needed.

A flow chart for determining oil flow requirements is shown in figure 18.

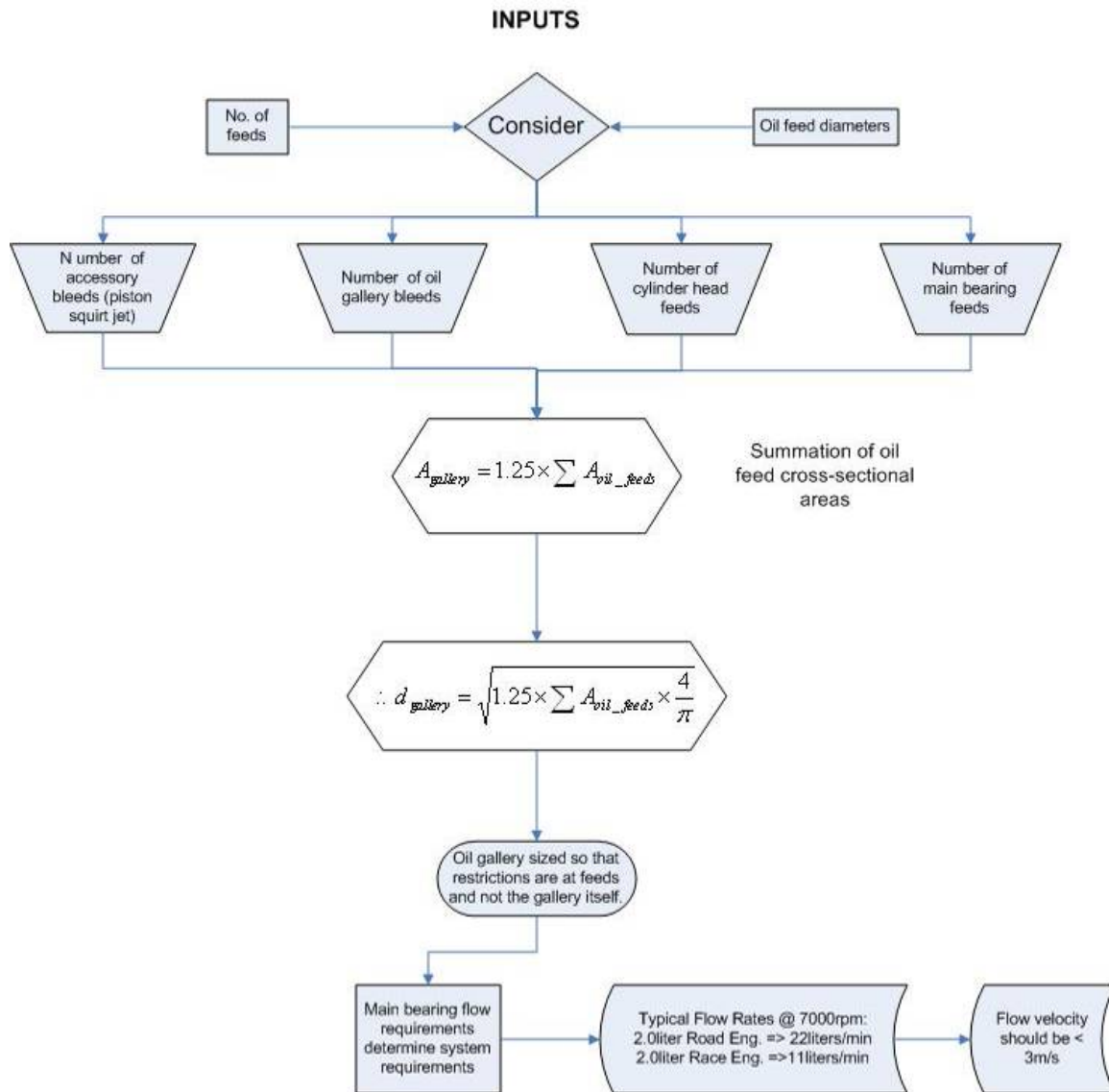


Figure 18 Flow Chart for Determining Oil Flow Requirements

4.3.2 V-Twin Main Oil Gallery Sizing

Equation 4.6 is a summation of the total cross-sectional areas for the V-Twin Engine which is to be used in eq. 4.5.

$$\sum A_{oil_feeds} = 2A_{cylinder_head} + 2A_{main_bearing} + A_{main_gallery_bleed} + 2A_{piston_squirt_jet} \quad (4.6)$$

Table 7 shows the V-Twin Engine results from equations 4.5 and 4.6. The table lists the main oil gallery size along with all of the feeds being supplied by the main gallery. The sizes determined ensure all feeds are supplied with a balanced flow rate. The diameter for the main gallery was calculated to be 12.4mm which is about twice the original design diameter of 6mm. The cylinder head feed diameters were changed from 2mm to 6mm as the length to diameter ratio for drilling is impractical.

Component	Quantity	Current Diameter	Needed Diameter
Main oil gallery	1	6.0	12.4
Oil feed from pump	1	6.0	12.4
Oil feed to main bearings	2	3.5	3.5
Oil feed to cylinder heads	2	2.0	6.0
Oil air bleed	1	0.7	0.7
Piston squirt jet	2	0.7	0.7

Table 7 Summation of cross-sectional areas for flow requirements

4.3.3 V-Twin Crankshaft

The crankshaft gallery requirements were calculated with equations 4.4 and 4.5. The same approach used for the main gallery sizing was used, but with an extra consideration of bearing clearances. The bearing feed sizes needed to be greater than the bearing clearance sizes because the oil needs to come in as fast as it is leaking out through the clearances. It is therefore important to size the feeds accordingly so they are not the restrictions, but the bearing clearances are.

4.3.4 V-Twin Cylinder Heads

The cylinder oil gallery sizes need not be as large as the main gallery or crankshaft sizes because the pressure is much lower but, the gallery sizes can be no smaller than 6mm in diameter due to machining tolerances. The gallery diameters were calculated using equations 4.4 and 4.5 to be 2.9mm, however they can not be machined to this size. Diameters of 6mm will be used with an orifice to get the right pressure and flow requirements.

4.4 Pumps for the V-Twin

For integration and packaging purposes the oil pressure, scavenge, and centrifuge pumps will be one pump stack all driven at the same speed. In addition, a water pump is fitted to the pump stack making a total of four pumps. The pump stack integration helps to reduce weight, lower the 'CoG', reduce brackets, and provides compactness. Normally, all of these pumps are spread around the engine on a standard road car making it necessary for more belts and gears to drive them, which results in more engine power losses.

Pump efficiency is what is important for the design of the V-Twin Engine if maximum horsepower is to be achieved. The goal is to make the pump efficiency, (η) , as high as possible over a wide range of flow, Q . Total pump efficiency is dependent upon volumetric efficiency, mechanical efficiency, and hydraulic efficiency. The total pump efficiency is $\eta = \eta_v \times \eta_h \times \eta_m$. The volumetric efficiency is

$$\eta_v = \frac{Q}{Q + Q_L} \quad (4.7)$$

where Q_L is the loss of fluid due to leakage within the pump casing clearances (such as in-between gears and rotors). The hydraulic efficiency is

$$\eta_h = 1 - \frac{h_f}{h_s} \quad (4.8)$$

where h_f has three parts: (1) shock loss at the entrance due to unsynchronized inlet flow and pump rotating part, (2) friction losses in the rotating part passages, and (3) circulation loss due to imperfect match at the exit side of the blades. The mechanical efficiency is

$$\eta_m = 1 - \frac{P_f}{bhp} \quad (4.9)$$

where P_f is the power loss due to mechanical friction in the bearings, packing glands, and other contact points [White 2003].

Based on the pumps discussed and pump efficiencies the gear-type pump (shown in figure 4 of ch. 2, pump (b)) was chosen. The reasons are summarized as follows:

- i. High volumetric efficiency because of adequately sized entrance/exit port areas
- ii. Compact and suitable for pump stack
- iii. Cost effective
- iv. Small diameter and less torque needed
- v. Pulsed flow kept low due to good number of teeth and gear tooth design. Pace Products [Pace Products 2007] launched a 6 and 7 tooth gear design in 2003 reducing pulsed flow effects even further.
- vi. Hydraulic and mechanical efficiencies work together therefore clearances can be designed to maximize both of these.
- vii. Good reliability.
- viii. Horsepower requirements very small, <1hp for V-Twin.

4.4.1 V-Twin Oil Pressure Pump Design

This section shows the design process for the V-Twin oil pressure pump. The pump is a positive displacement gear type pump. The reader is referred to appendix 2 for detailed calculations. This section shows the base formulas used and solutions found. The

calculations are based on the formulae from High Performance Gear Design by Alec Stokes. Stoke [Stokes 1970] states "The formulae given have all been used frequently during the work which I have done for the Engine Development Division of Rubery, Owen & Co. Ltd. on Formula 1 racing car engine and transmission gears, which are very highly stressed in order to keep weight down to an absolute minimum".

Stokes found that with improved gear tooth design, oil gear pumps are capable of achieving 87 to 94% efficiencies, which was proven with experimental tests. He also found that by using gears which have no crowning at all and the basic whole depth, 2.157/diametral pitch, (opposed to the British Standard whole depth, 2.25/diametral pitch) pump efficiency can be increased. Reducing the whole depth to the basic gave the following advantages [Stokes 1970]:

1. Increased root strength of gears,
2. Less clearance at root of teeth, thus avoiding turbulence being created in the oil, caused by oil being carried back through the pump in the extra area which is not swept clear.

The Stokes method is shown in part 3 of the equations listed in appendix 2. Equations 4.10-4.12 are for calculating pump flow rates.

$$Q_{nom} = \frac{GearCenters \times addendum \times FaceWidth \times rpm}{44} (gal / min) \quad (4.10)$$

$$Q_{slip} = \frac{GearCenters + FaceWidth}{2} \left(\frac{P}{100 + R} \right)^{\frac{2}{3}} (gal / min) \quad (4.11)$$

$$Q_{act} = Q_{nom} - Q_{slip} \quad (4.12)$$

Where Q_{nom} is the nominal pump flow rate, Q_{slip} is the slippage in the pump flow, and Q_{act} is the actual flow rate out of the pump, P is pump pressure in psi, and R is viscosity in seconds Redwood 1. Slippage always occurs but in order to reduce it the viscosity

could be increased. The negative side effect is that by increasing the viscosity the power needed to drive the pump will increase. Using equations 4.10-4.12 the actual flow rate of the oil pump at 0.4 X 12,500rpm engine speed is 13.0 liters/min.

Equation 4.13 computes the maximum permitted pitch line velocity in the pump gears. If the max pitch line velocity is exceeded, pump efficiency goes down as the onset of cavitation begins. Also, by staying below the max pitch line velocity high contact pressures within the gears are kept within a suitable working range. The oil pump speed was set to 0.4 times engine speed as this kept the pitch line velocity of the gears below the max permitted pitch line velocity. Maximum pitch line velocity permitted was calculated with equation 4.13 to be 1602ft/min while the actual velocity was 1466 ft/min. This shows the pump is within limits. If the pump speed was 0.5 times engine speed this would make the actual velocity 1833ft/min which exceeds the maximum limit.

$$V_{\max} = \frac{40,000}{(R + 100)^{\frac{2}{3}}} (ft / min) \quad (4.13)$$

Equation 4.14 determines the power loss in the pump gears. As the viscosity, R, or the velocity, V, is increased the power losses increase.

$$P_c = \frac{(R + 100)}{100,000} V_{\max}^{\frac{3}{2}} \quad (4.14)$$

Equation 4.15 determines the horsepower required to drive the pump. Using equation 4.15, the power required to drive the pump at 0.4 X 12,500rpm is 0.4hp. The numbers sounds very small, but remember the pump gears only have a diameter of 33.78mm (1.33in) and thickness of 5mm (0.197in), which is very small. This hp value is approximately 67 magnitudes of order less horsepower than the pump used on the Jaguar V12 Engine mentioned in section 2.4.2 on Motorsport Industry Pumps.

$$bhp = \frac{Q_{nom}(P + P_c)}{1430}(hp) \quad (4.15)$$

Equation 4.16 is an alternative to equation 4.12 to determine the pump capacity or flow rate out of the pump. This equation was developed by Stokes because of the optimized gear tooth design he used. His pumps flowed more and it was necessary to develop a new flow rate equation. By increasing pump speed, gear tooth width, or total swept volume of idler gear teeth the pump flow rate can be increased in equation 4.16. With equation 4.16 a flow rate of 15.2 liters/min was equated at 0.4 X 12,500rpm engine speed. This equation yields about 2liters/min more flow rate for the same engine speed than equation 4.12.

$$PumpCapacity = \frac{TotalSweptVolumeOfIdlerGearTeeth \times FaceWidth \times rpm}{277.42} \quad (4.16)$$

Oil pressure and scavenge pump capacities using equation 4.16 were plotted for the entire engine speed range and are shown in figure 19. The pump capacity increases linearly with engine speed. A linearly increasing flow rate is desired because as the engine speed increases the parts require more lubrication. The scavenge pump capacities are shown for both gasoline and E85 fuel systems. The reason for both fuel systems is discussed in the next section 4.4.2 on V-Twin Scavenge Pump Design.

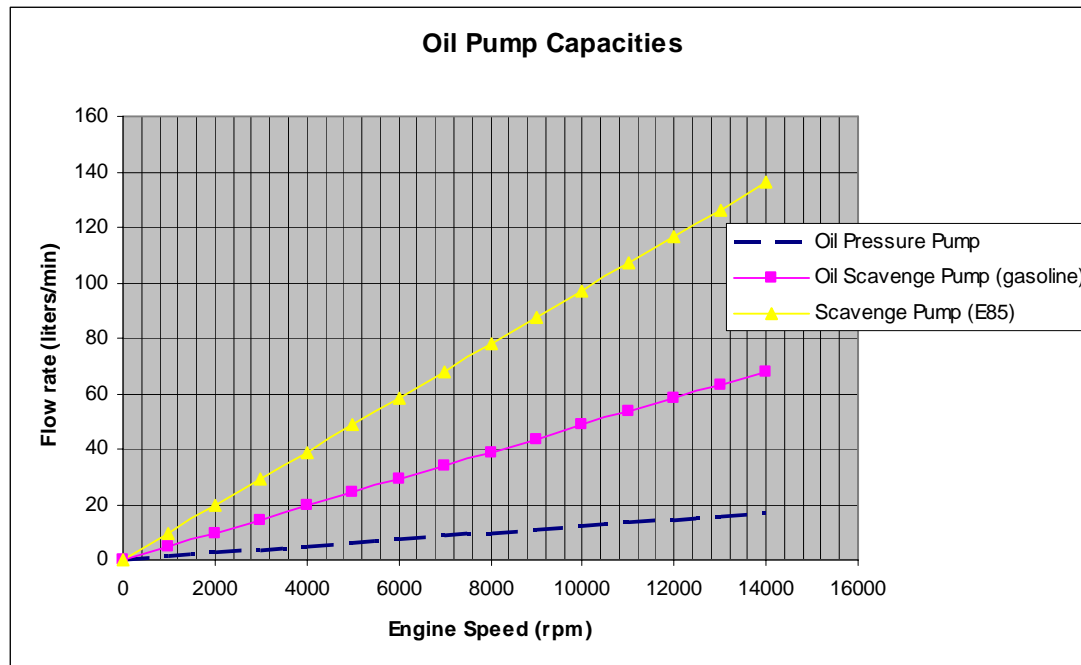


Figure 19 Oil Pump Capacities

A depiction of the oil pressure pump is shown in figure 20. The front cover is removed. The housing is integrated with the scavenge pump. One rotor is driven while the other rotates on its shaft.

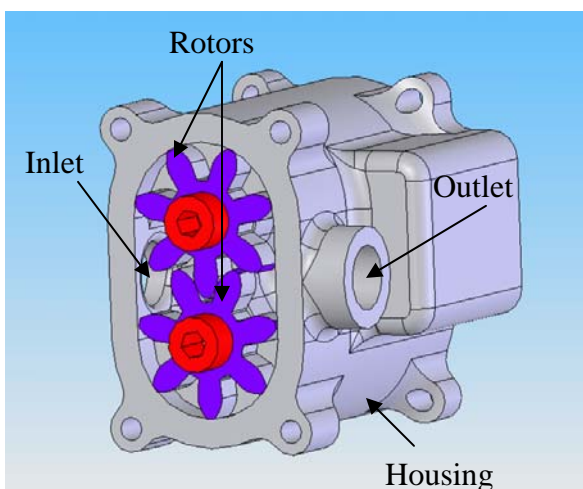


Figure 20 Oil Pressure Pump

4.4.2 V-Twin Scavenge Pump Design

This section discusses the design process for the V-Twin oil scavenge pump. The same gear tooth geometry as the oil pressure pump was used, therefore, simplifying the design process. Equations 4.10-4.16 were used to determine pump capacities. In order to gain pump capacity, the rotors were lengthened while all other geometry of the oil pump was kept the same. The reader is referred to appendix 2 for detailed calculations.

The pump is a positive displacement gear type pump. It is required to pump at 1bar and 7-10 times the capacity of the oil pressure pump [Goddard 2007]. High flow low pressure is needed because at this stage the oil has just gone through its life in the engine, it is mixed with air and it needs to be pumped back into the oil reservoir. The reservoir does not need to be under pressure, but needs to be full of oil at all times.

Scavenge pump capacities range from 3-5 times oil pump capacity for gasoline engines and 7-10times oil pump capacity for alcohol fuelled engines [Goddard 2007]. The fuel system on the V-Twin is E85 i.e. 85% ethanol and 15% gasoline. Scavenge pump capacity was made to be 8 times the oil pressure pump capacity. The reader is referred to figure 19 of section 4.4.1 for a plot of gasoline and alcohol fueled scavenge pump capacities. Pump capacity at 12,000rpm is approximately 115litres/min.

More pump capacity is needed on alcohol fuelled engines because blow by of fuel through the piston rings is greater. As the alcohol blows by the rings and enters the crankcase it goes through a phase change. This causes huge changes in volume making it necessary to increase the scavenge pump capacity [Goddard 2007].

The pump gear diameter is 33.78mm (1.33in) and has a thickness of 40.03mm (1.576in). The thicker gears resulted in total pump power requirement of 2.2hp at max engine speed (12000rpm). This is 1.8hp more than the oil pressure pump, however, the power requirement is still quite small.

A depiction of the scavenge pump is shown in figure 21. The front cover is removed. The outlet feeds straight into the centrifuge pump and the inlet sucks from the oil sump.

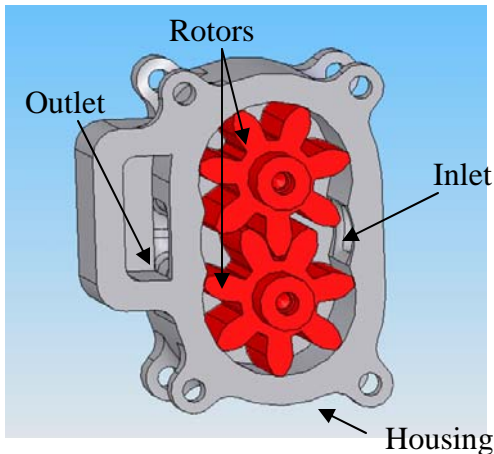


Figure 21 Oil Scavenge Pump

4.4.3 V-Twin Centrifuge Pump Design

The centrifuge pump is needed to separate the air/oil mixture back into oil and air. It does this by pulling thousands of 'g' on the air/oil mix ensuring that total separation of oil and air occurs. After the centrifuge the oil goes straight to the oil reservoir while the air goes to the swirl pot, which will capture any last drops of oil in the air.

Figure 22 shows a depiction of the centrifuge pump with its front cover removed. As the oil/air mixture enters the pump it is centrifuged causing the oil which is higher in density than the air to separate. The oil exits out of the circumferential grooves while the air exits through the radial drillings on the hub.

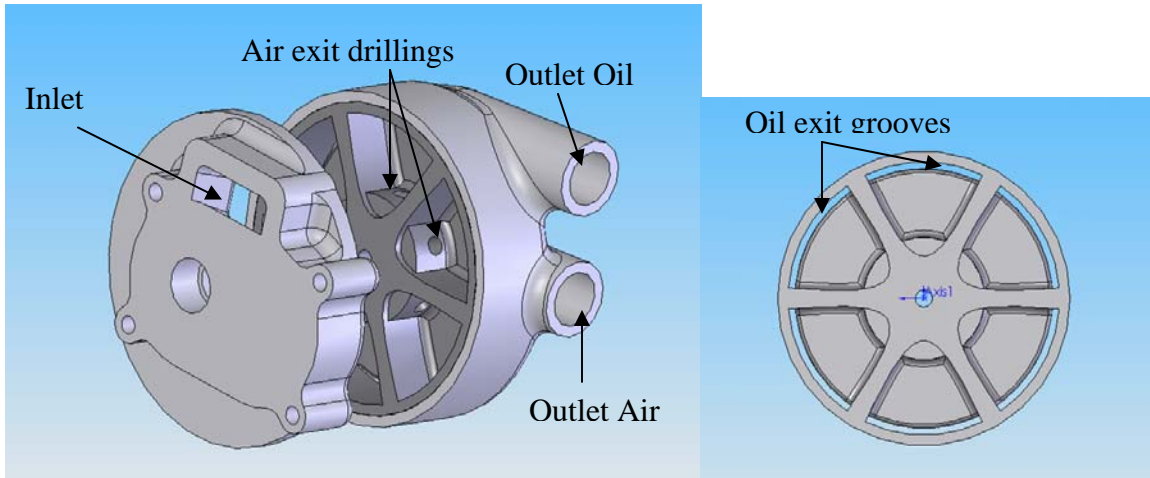


Figure 22 Centrifuge Pump

4.4.4 V-Twin Pump Stack

A depiction of the oil pump stack assembled is shown in figure 23. The water pump is not attached. It attaches on the front where the yellow bearing is shown.

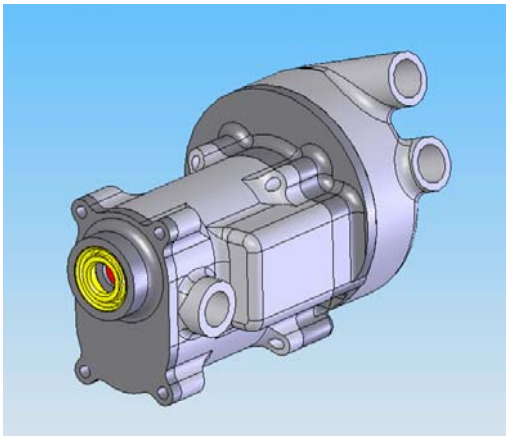


Figure 23 Oil Pump Stack

4.5 Oil Filter

An oil filter is essential in any lubricating system and is typically designed to trap all particles over 25 microns (0.025mm) [Hillier 1991]. It helps to filter out abrasive

particles, air churned oil, and sludge/dirt. It is placed after the oil pump and before the main bearings as shown in figure 24.

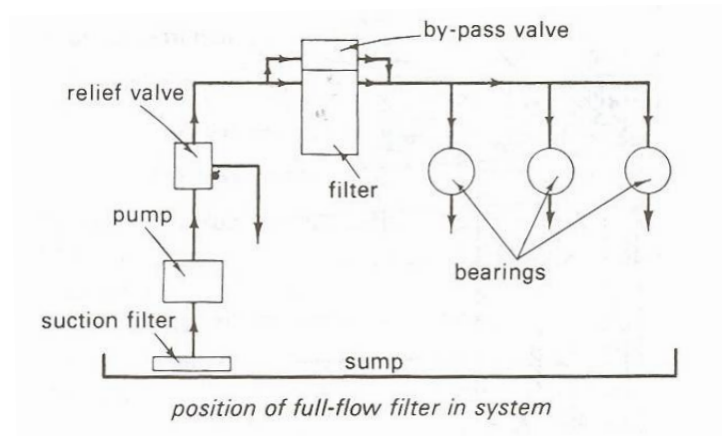


Figure 24 Position of oil filter in system [Hillier 1999]

Oil filters range in sizes, materials, filter area, and design. The size of the filter will be dictated by the amount of surface area needed by the filter element. Materials are normally resin impregnated paper for the filter element and a cylindrical metal canister for the housing. Typically, the more filter area the better. The reason is as follows: the finer the pores of the filter element the better the filtration but also greater restriction to the flow, thus, the larger the surface area of the filter element the less restriction.

Two types of filters are used: full-flow and by-pass. Full-flow allows all the oil to pass through the filter. A by-pass filter has a valve that opens when the pressure drop across the filter exceeds a certain value (e.g. 1bar). The by-pass tends to open on cold conditions as well to ensure the bearings are sufficiently fed. By-pass filters are common on standard road cars because if the user does not pay attention to oil changes, the filter will become blocked. To avoid engine damage from oil starvation a by-pass oil filter has been chosen by car manufacturers as a sort of 'safety'. Figure 25 shows a typical cartridge type by-pass filter with a valve that lifts when the filter becomes blocked. At the oil entrance there are two plastic valves, these are anti-drain back valves which open under slight pressure, but prevent oil draining back to the pump once the engine is shut-

off. These valves ensure there is no oil supply delay at engine start up which would occur if the filter had to be re-filled.

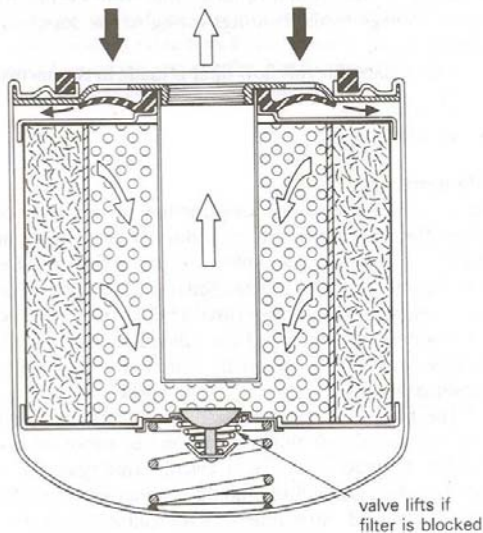


Figure 25 Cartridge type filter (by-pass) [Hillier 1999]

For racing applications, all of the oil needs to be filtered as tolerances are much ‘tighter’. Figure 26 shows a full-flow filter. A by-pass valve is also present, but in the case of racing this will be removed. The by-pass valves are normally triggered on cold starts since the oil is more viscous, but the concern is that dirty oil is fed to the bearings which could easily damage them. Chapter 3 discussed that oil film thicknesses range from 2.5 to 7 microns and if a metallic particle of 25microns enters the bearing this could cause damage. In order to eliminate the by-pass valve two options can be used: 1 preheat the oil to reduce the viscosity; 2 increase the filter element surface area to increase flow and filtration.

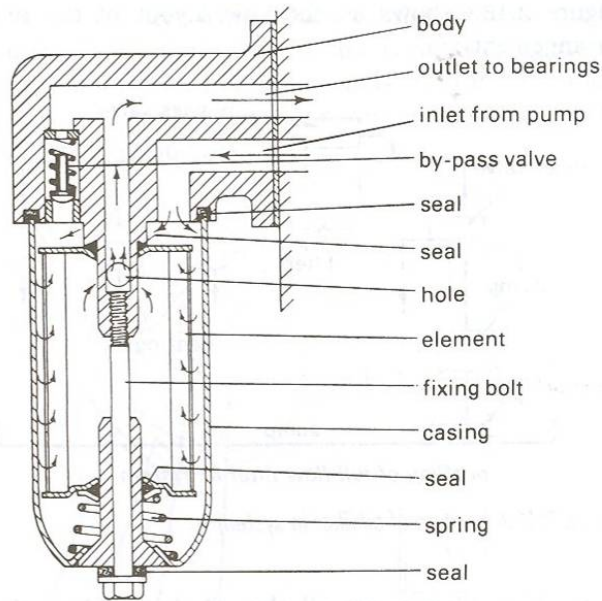


Figure 26 Full-flow oil filter [Hillier 1999]

4.5.1 V-Twin Oil Filter

Time did not permit the V-Twin oil filter to be designed. The design would involve purchasing an off-the-shelf oil filter element and then designing a housing to carry it. Kinsler Fuel Injection, Inc. supplies filter elements and housings. In appendix 1, pg. 48 of the Kinsler parts catalog is shown. Part # 8325 is recommended. The part is a 25-micron filter with 73 sq. inches of pleated screen. The filter element area might be too large for the V-Twin application, however, it is hard to justify that at this stage. Some further development work would need to be done.

4.6 Pressure Relief Valve (PRV)

The pressure relief valve (PRV) is an automatic mechanical valve which is set to open at a certain pressure. It is needed because oil pumps are positive displacement pumps, as discussed in section 2.4, which keep raising the pressure while keeping a steady flow rate. The PRV is set to 4bar. This pressure setting was determined by the crankshaft centrifugal head calculations in section 4.2.1.

The common types of PRV's are: ball valve and spring, poppet valve and spring, spool valve and spring. The ball valve is the simplest but manufacturers prefer the poppet valve type [Goddard Notes]. For racing purposes the spool valve is preferred as this damps the pump delivery resonance to produce a much finer control of the oil pressure [Goddard]. A ball valve type PRV is shown in figure 27.

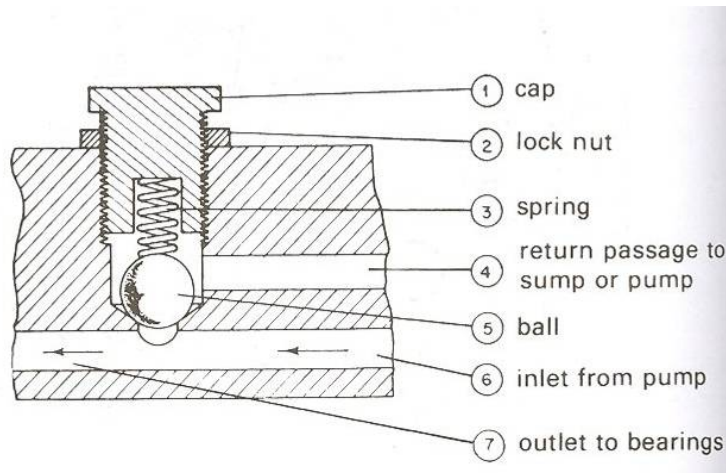


Figure 27 Ball-type pressure relief valve [Hillier 1991]

Although the ball-type PRV is simple it is not easily controlled to accuracy. The reason is once the valve opens, the area is increased on the ball face and therefore changes the resultant pressure. With a spool-type the area is constant and the pressure can be controlled more precisely.

4.6.1 V-Twin PRV

Time did not permit the pressure relief valve to be designed. The design needs to be a spool-type for precise control of the pressure. Spool diameter will be determined from oil hose size. The working pressure desired is 4bar. With the pressure and diameter known the spring constant can be determined. The outlet of the PRV needs to be modified from a constant cross-sectional area to a changing type. This is to allow for the area of the exit to match the pressure acting on the spool and keep a balance in areas. This balance will ensure that at 4bar pressure the PRV is completely open and is flowing at its maximum.

4.7 V-Twin Oil Tank

The V-Twin oil tank is a cylindrical tank capable of holding 2.5 litres of oil. The volume of oil is based on testing performed by Geoff Goddard Engines Ltd. The length to diameter ratio alone provides baffling for cornering and accelerating. Furthermore, two internal conical shaped baffles are used to baffle the oil. Figure 28 shows the oil tank with a cross-sectional view of the internal baffles. The top oil inlet is into the swirl pot which comes from the air outlet of the centrifuge pump. The second oil inlet on the bottom is the main oil inlet from the centrifuge oil outlet.

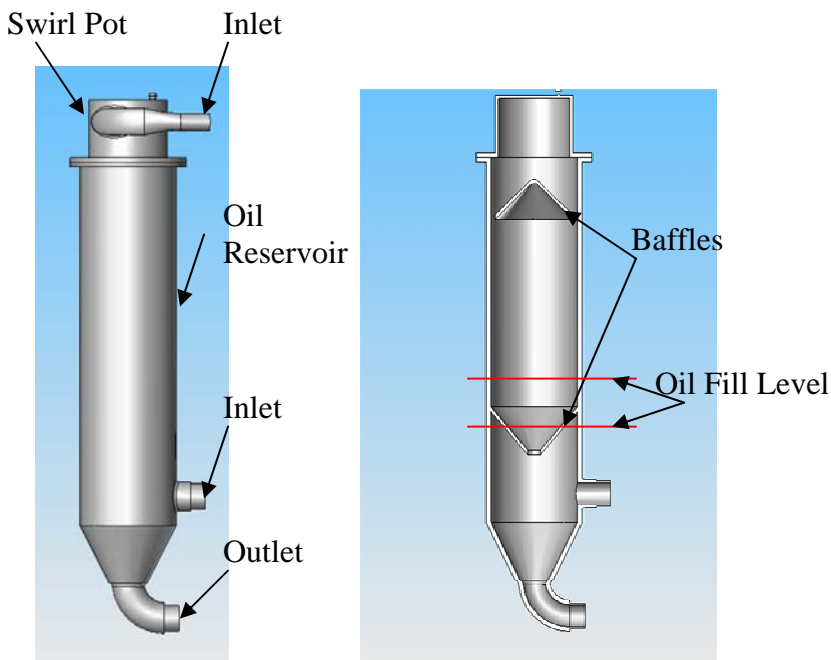


Figure 28 Oil Reservoir with baffles

4.8 V-Twin Swirl Pot

Both a swirl pot and centrifuge pump is used on the V-Twin. At low speeds the centrifuge pump might not be optimal and therefore the addition of a swirl pot will help. As the oil/air mixture enters the swirl pot it is fishtailed to increase volumetric efficiency

and help with oil/air separation. Any excess air bleeds out through the top vent. Figure 29 shows the V-Twin swirl pot. The top vent is too small and is currently unfinished.

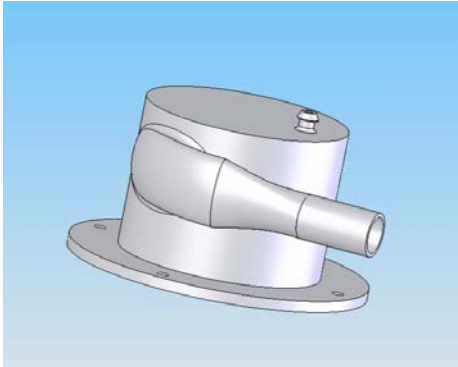


Figure 29 Swirl Pot

4.9 V-Twin Oil Sump

The oil sump is shown in figure 30. The crankshaft rotates counter clockwise forcing excess oil into the holding tank area. Vents are added to the holding tank to not allow for any pressure buildup. If pressure buildup occurred this would not allow the oil to flow properly into the holding tank.

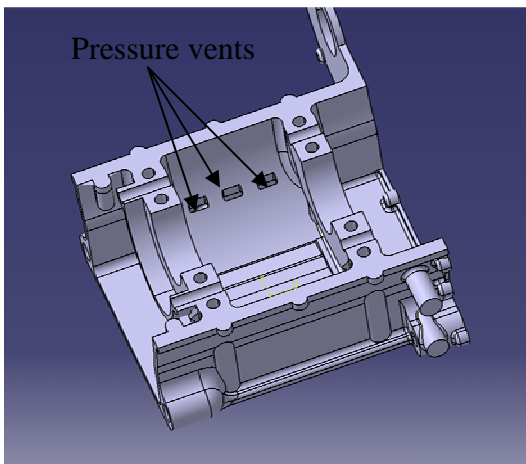
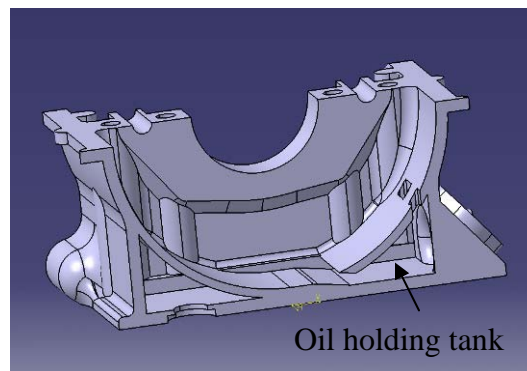


Figure 30 Dry sump



4.10 Chapter 4 Summary

Oil system pressure requirements were determined from the crankshaft centrifugal head. Using equation 4.2 the pressure required was 3bar + 1bar for safety making a total system pressure of 4bar. The flow requirements were based on a balance of area summations. This balance was necessary to ensure no oil starvation occurred and that a common operating pressure could reach all points in the system. The balance was performed by making the cross-sectional area of the main gallery equal to the summation of oil feeds from the main oil gallery. The oil gallery was increased by 25% to add safety into the system in the event of an oil leak or restriction. The main gallery was sized to 12.4mm.

Positive displacement pumps (PDPs) were best for maintaining constant flow rates with oil viscosity changes. The pressure supplied would rise to more than the system requirements and it was necessary to add in a pressure relief valve. Both the oil pressure pump and scavenge pump were twin rotor pumps. The flow rates of the scavenge pump were made 8 times that of the oil pressure pump. An increased capacity was needed because at the end of the engine oil cycle, oil returning to the sump is an air/oil mixture with more volume. Furthermore, the use of E85 fuel demanded a larger capacity scavenge pump because of increased blow-by through the piston rings.

Oil filter design was covered stating the more filter element area the better. Increased area meant less restricted flow at higher filtration ratings. The V-Twin filter was not designed as time did not permit. Attention was made towards Kinsler Fuel Injection, Inc. who provides 25micron oil filters with large filter areas.

The pressure relief valve was not designed for the V-Twin as time did not permit. Awareness was made to a spool type valve for precise control of the oil pressure. The outlet of the PRV also needs to be changing in area from small to large in order to match the area of the pressure acting on the spool valve face. This will ensure max flow rate occurs at the pressure desired.

The oil pressure pump capacities determined in section 4.4 will be used in chapter 6 to compare pump requirements to system requirements. The oil galleries and sizes will be modeled and checked with Fluent CFD software in chapter 6.

5 V-TWIN BEARINGS & LUBRICATION

This chapter discusses lubricants and specific additives which increase lubricant performance. It creates a mathematical model for journal bearings. It also discusses crankshaft balancing which determines the bearing forces used in the bearing model.

The bearing model is a tool for indicating the redline of the V-Twin engine, the SAE viscosity oil needed, minimum crankshaft journal surface roughness needed to eliminate asperity contact, and horsepower lost in the main bearings.

Valve train and piston assembly lubrication will be discussed but not as in detail as the main bearings. The reason for this is because the author is targeting the greatest power losses in the engine which happen at high engine load in the bearings. The highest losses are in the bearings and this can be seen in figure 31 which shows the engine friction breakdown for a European inline 4 2.0litre engine. And, in figure 32 the engine friction breakdown is shown for a 3.0litre V10 Formula 1 engine.

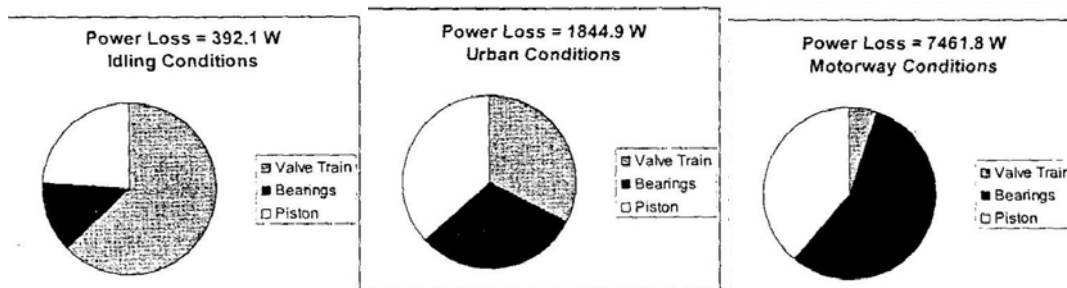


Figure 31 Engine friction breakdown-2.0L European engine at idle, medium load (2500rpm), and high load (7500rpm) [Taylor 2002]

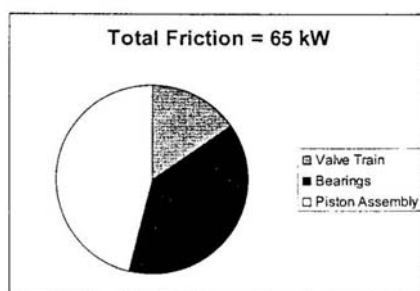


Figure 32 Engine friction breakdown-3.0L Formula 1 engine @18000rpm [Taylor 2002]

Figures 31 and 32 show that the most power losses occur in the bearings at high engine speeds, for this reason, the bearings were chosen to be studied more in depth.

5.1 V-Twin Crankshaft Journal Surface Finish

Data was supplied by Professor Geoff Goddard [Goddard 2007] on crankpin or journal surface roughness (see table 8). From the supplied data it can be seen the average surface roughness, Ra, is 0.0408 micro meters. This is a very smooth surface finish compared to standard mirror finishes of 0.1-0.2 micro meters as was shown back in figure 12. With these kinds of surface finishes, the minimum oil film thickness will be allowed to run thinner before any metal to metal contact occurs. Furthermore, the reliability of the bearings is increased because the safety factor increases which depends on surface finish roughness and oil film thickness.

Taylor Hobson

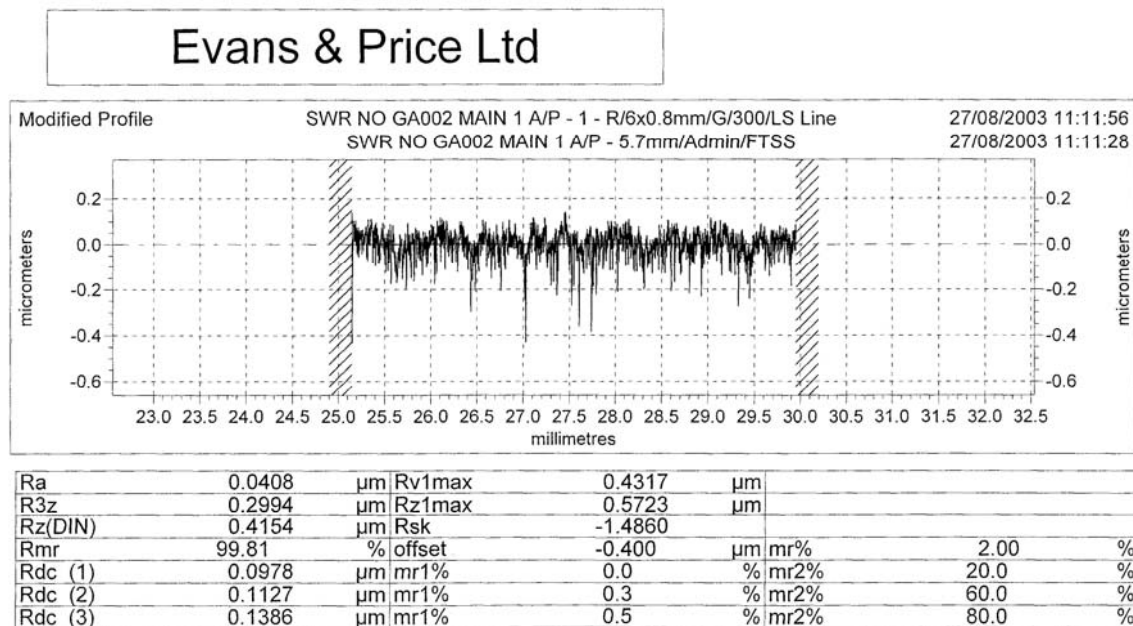


Table 8 Crankshaft Journal Surface Finishes

5.2 Journal Bearing Design (hydrodynamic)

There are numerous bearing theories available for bearing design such as Sommerfield Solution, Ockvirk Solution, Boyd and Raimondi's Method, and many empirically derived ones. The Ockvirk short bearing theory is used as it is the most accurate and straightforward of the bunch; Sommerfield's is good for bearing length/diameter (L/d) above 4, Ockvirk is good for L/d of 0.25-0.75, and Boyd and Raimondi's is just not practical. Furthermore, the Ockvirk Solution was validated experimentally by DuBois and Ockvirk under a research contract for NASA (National Aeronautics and Space Administration), which makes it one of the most commonly used theories [Booser *et al* 2001]. In addition to so many theories available one might ask the question "what makes these bearings successful if there is no exact bearing model available?". The reason bearings are successful is they are self adjusting fluid and thermal control systems [Barwell 1979]. In other words, hydrodynamic bearings are self healing systems.

5.2.1 GT-Power model of piston-crank forces

Virtual engine software GT-Power was used to determine the in-cylinder pressures which were converted to forces on the main bearings. A model of the engine was constructed and takes into account all of the engine specifications of table 1. The model also accounts for custom designed cams, indolene fuel, minimum advance for best torque, and many other variables. The GT-Power engine model is shown in figure 33. With this model the in-cylinder pressures were found. Max pressures were 110bar. The data from GT-Power model will be discussed in the next section on bearing loads from crankshaft balancing.

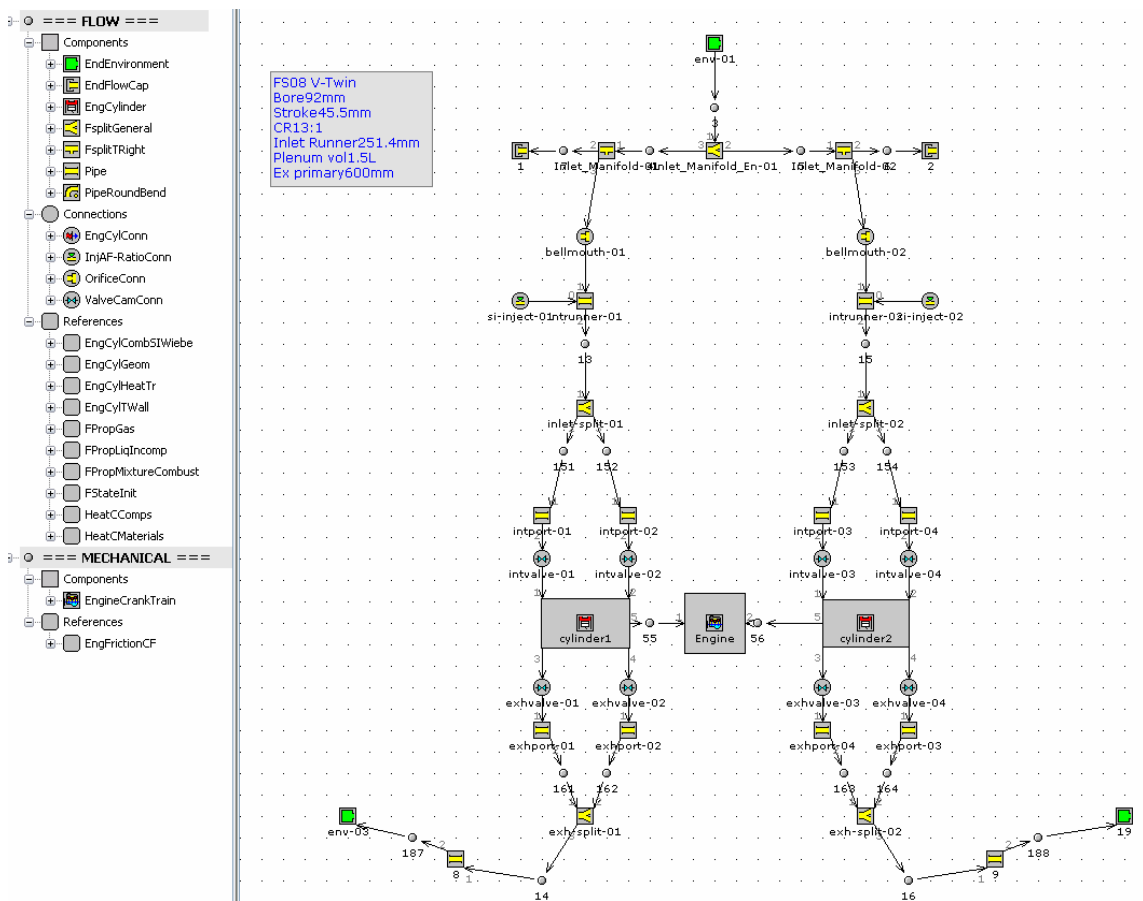


Figure 33 GT-Power engine model

5.2.2 Crankshaft balancing via bearing loads

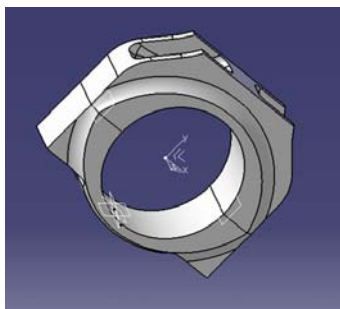
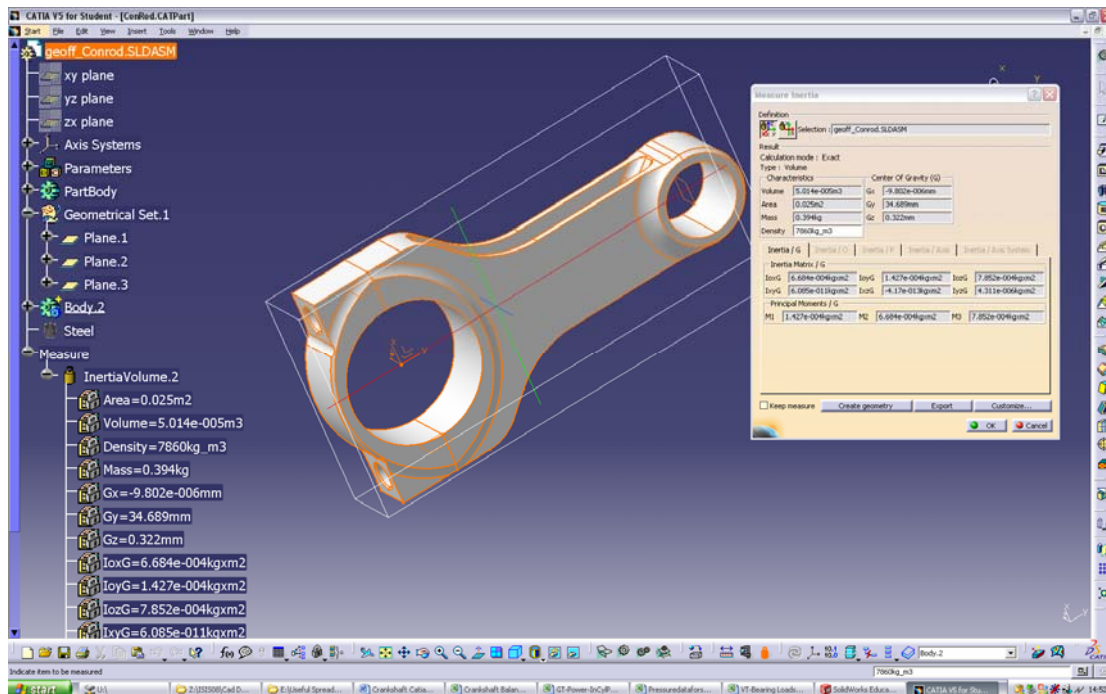
Crankshaft balancing is necessary in order for any engine to run smoothly. If unbalanced, reciprocating and rotating forces can be extremely high. These forces will over exert the crankshaft and quickly fatigue or over stress it to failure. Also, the main bearings receive higher forces which reduce oil film thicknesses. If the oil film thickness reduces too much, metal to metal contact will occur and the bearing will fail. In order to balance the crankshaft there are two things to consider; the rotating mass and the reciprocating mass. The crankshaft rotates while the piston reciprocates, however, the connecting rod rotates and reciprocates. Therefore, the con-rod needs to be split into two parts about its center of mass. The big end is added to the crankshaft and the small end is added to the piston assembly.

Two balancing types exist; dynamic and static. Static consists of balancing the rotating masses. This is done in Catia CAD Software by adding or subtracting weight from the crankshaft balance weights. Dynamic balancing consists of determining the inertia forces due to the equivalent reciprocating masses and then superimposing them onto the gas forces. The steps following will show the entire crank balancing process, which include:

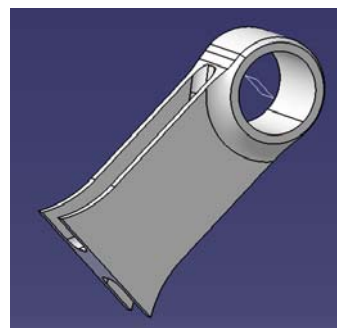
- step 1: determine equivalent masses
- step 2: static balance
- step 3: calculate inertia forces
- step 4: calculate gas forces
- step 5: add inertia and gas forces
- step 6: determine phases between cylinders 1 & 2
- step 7: Dynamic crankshaft overbalancing

Step 1 Determine equivalent masses

1. Use Catia to determine center of mass location on connecting rod as shown in figure 34. If an iges file is imported in, make sure it is a 3Dsolid or converted to a solid in Catia. Catia normally imports *.iges files as surfaces and will give the wrong mass data.
2. Split the con-rod into two masses about its center of mass to make two masses; the big end and small end mass as shown in figure 34.
3. The small end of the con-rod mass can now be added to the piston assembly. This becomes the equivalent reciprocating mass for balancing. This assembly should include piston, gudgeon pin, piston rings, gudgeon pin C-clips and small end bearing.
4. The big end of the con-rod mass can now be added to the crankshaft pin. The rod bolts and big end bearings must also be added. This becomes the equivalent rotating mass for balancing.



Equivalent rotating con-rod end



Equivalent reciprocating con-rod end.

Figure 34 Equivalent connecting rod masses

Step 2 Static Crankshaft Balancing

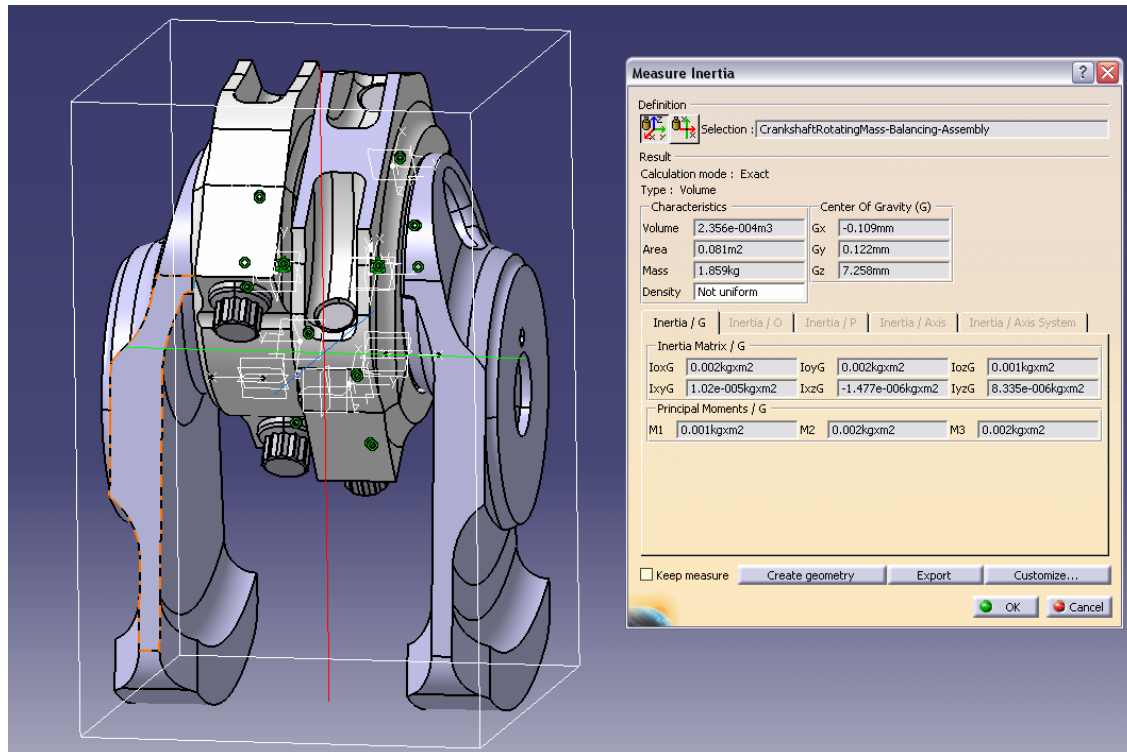


Figure 35 Rotating masses for crankshaft balance

Initial crankshaft rotating balance is 7.258mm off centerline of crankshaft axis.

The following steps are for static balancing:

1. Create two assemblies in Catia, one for the rotating mass (see figure 35) and one for the reciprocating mass (see figure 36) (used in step 3). The equivalent rotating mass assembly must include con-rod bolts, con-rod big end bearings, crankshaft, and equivalent rod end. The reciprocating mass assembly must include piston, piston rings, gudgeon pin, gudgeon pin C-clips, and equivalent reciprocating con-rod end.
2. Catia can be used to find the total mass and location of the center of mass for the rotating balance assembly.
3. Rotating Mass:
 - a. Using Catia, check that center of mass location is approximately 0,0,0 about the crankshaft axis of rotation. It will slightly deviate from 0,0 in the x and y axis' because of the internal radial oil galleries which are perpendicular to the crank axis of rotation.
 - b. If balance is off, material can be added to the crankshaft balancing weights until center of mass location is 0,0,0.
4. This completes the static rotating balance.

Step 3 Determine inertia forces due to equivalent reciprocating mass

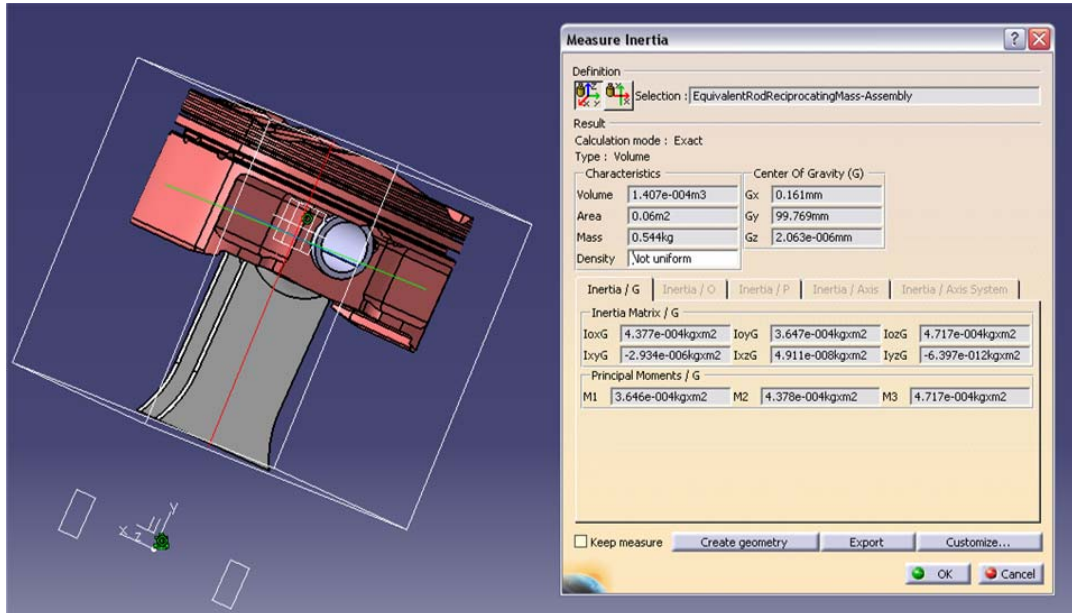


Figure 36 Equivalent reciprocating masses for balancing

To determine the inertia forces the following formulas 5.1-5.4 (taken from [Stone1999]) are needed. Equation 5.1 is used to determine the approximate position of the little end of the connecting rod.

$$x \approx r \left\{ \cos \theta + \frac{l}{r} \left[1 - \frac{1}{2} \left(\frac{r}{l} \right)^2 \times \left(\frac{1}{2} - \frac{1}{2} \cos 2\theta \right) \right] \right\} \quad (5.1)$$

Where x is piston position, r is crankshaft throw, $\cos \theta$ is a primary force term, $\cos 2\theta$ is a secondary force term, and l is connecting rod length. The differential of 'x' gives equation 5.2 which is approximate piston velocity.

$$\dot{x} \approx -r\omega \left(\sin \theta + \frac{1}{2} \frac{r}{l} \sin 2\theta \right) \quad (5.2)$$

Where \dot{x} is the approximate piston velocity and ω is angular velocity $\frac{d\theta}{dt}$. The second differential of 'x' gives equation 5.3.

$$\ddot{x} \approx -r\omega^2 \left(\cos \theta + \frac{r}{l} \cos 2\theta \right) \quad (5.3)$$

Where \ddot{x} which is the approximate piston acceleration. Once the acceleration is known the axial force due to the reciprocating mass can be found with equation 5.4.

$$F_r \approx m_r \omega^2 r \left(\cos \theta + \frac{r}{l} \cos 2\theta \right) \quad (5.4)$$

Where F_r is the axial force due to reciprocating mass and m_r is the equivalent reciprocating mass. All these formulas are input into an Excel spreadsheet and plotted over 720deg of crank angle. With thousands of numbers input and many formulas being used, errors could easily be made. Therefore, checks were performed on various data sets and compared to other engine data to ensure the solutions were logical. Figure 37 shows piston velocities calculated from equation 5.2 compared to values from GT-Power; values are identical. Piston velocities peak around 30m/s which is normal compared to a modern Formula 1 engine which has peak piston speeds of 37-48m/s @ 17,000-18,000 rpm and a European 2.0litre which has peak piston speeds of 32m/s @ 7500rpm [Taylor 2002].

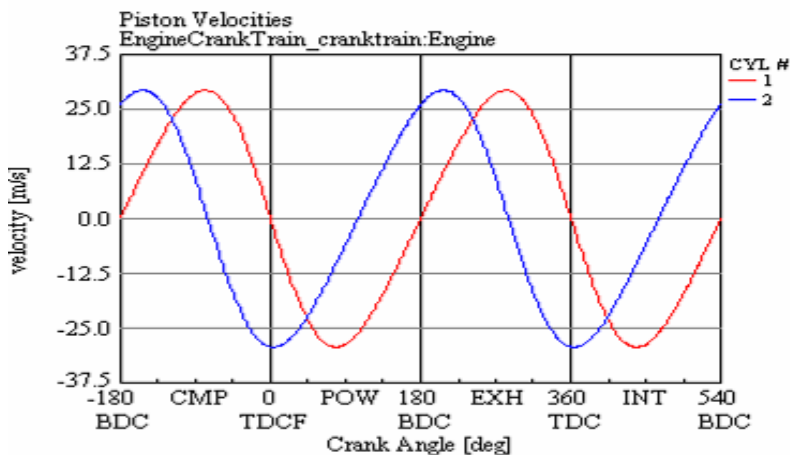
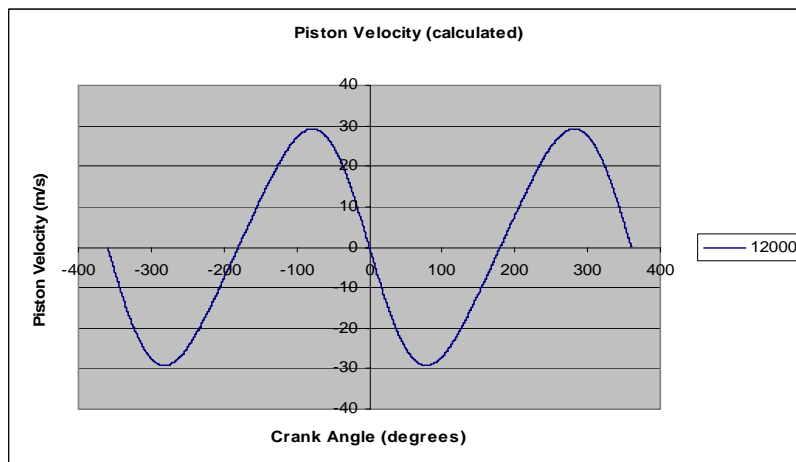


Figure 37 Piston Velocities @12,000rpm for calculated data and GT-Power data

The piston accelerations were also plotted (figure 38) to indicate the extremes the piston goes through. An acceleration of 4,500 g's can be seen!

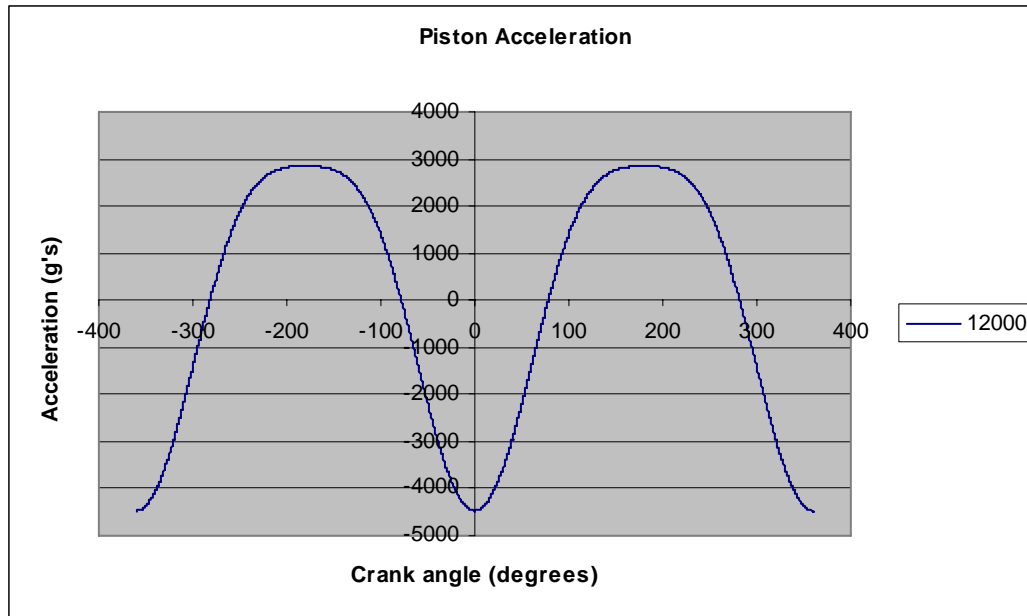


Figure 38 Piston accelerations @12,000rpm

Step 4 Calculate gas forces

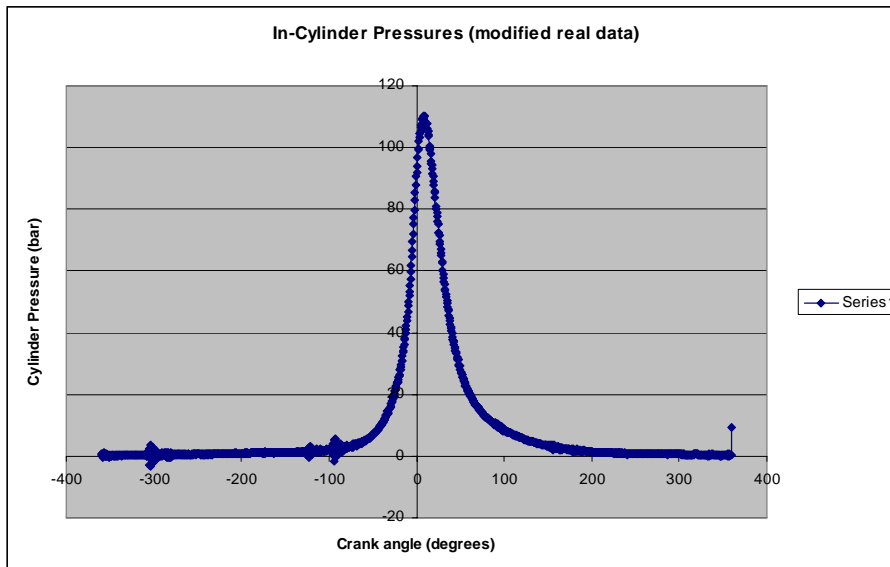
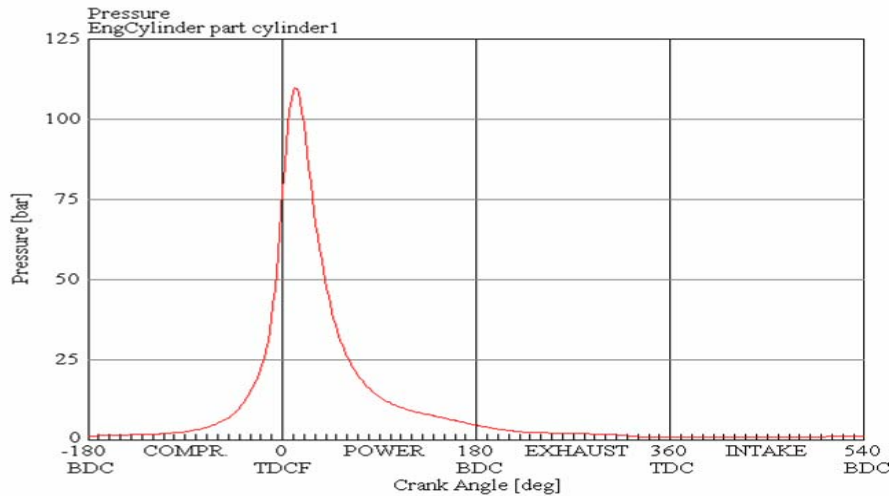


Figure 39 GT-Power and real data in-cylinder pressures

1. In-cylinder pressures are needed. They can be computed from GT-Power or taken from real data. GT-Power tends to not give the full 720 degrees of crank angle data making it difficult to obtain accuracy. Pressure data was supplied by Professor Geoff Goddard [Goddard 2007] and then modified by a correction factor to obtain approximately the same values as GT-Power. The supplied data also provided pressure measurements for every half-degree which GT-Power could not. See figure 39 for a comparison of the modified and real pressure data's.
2. Compute gas forces by multiplying piston bore area times in-cylinder pressures. All this should be done in the same spreadsheet as the inertia forces.

Step 5 Combine inertia and gas forces

1. Basically, add inertia and gas forces calculated in spreadsheets together.

Step 6 Determine phases between cylinders 1 and 2

1. Since the engine is a 75 degree V-twin, cylinder 1 phase can be taken at 75 degree crank angle. This involves 'cut and paste' the total loads calculated in step 5 starting from 75 degree crank angle. 0-75 load values will be pasted on to the tail end of the first pasted loads.
2. For cylinder 2 the phase is taken at $75 + 360$ deg for odd fire or can be taken at 0 deg for even fire. Even fire is simultaneous firing offset by 75 deg. and odd fire is offset by one crank revolution (360deg.).
3. Add the phased forces of cylinders 1 & 2 to get a resultant force. Plot this over a polar diagram in order to see the loads.

Step 7 Dynamic Crankshaft Over Balancing

1. The classical way is to now add 50% of the reciprocating mass to the crankshaft balancing weights. This is to be added to the balancing equations. By adding 25, 15, 7, or 0 percent of the reciprocating mass could result in a better distributed bearing load. Equal load on both sides of the bearing would seem optimized, but remember the top half of the bearing is grooved and therefore should only take about 1/3 of the load.
2. The rotating masses at this point are completely balanced. A percentage of the reciprocating mass is taken and added to the crank balancing weights, thus over balancing it. In practicality, a percentage of mass can not be reduced from the reciprocating assembly because all of the parts are standard, but by adding a percentage to the balance weights it will offset the gas loads. In other words, adding this extra mass will overbalance the crank, but reduce the gas loads on the top half of the bearings.

5.2.3 Bearing loads discussion from section 5.2.2

Equation 5.3 contained a primary term ($\cos \theta$) and a secondary term ($\cos 2\theta$). Therefore, equation 5.4 was split into two parts, one with the primary term and one with the secondary term. Figure 40 shows the primary forces calculated from equation 5.4. Figure 41 shows the secondary forces calculated from equation 5.4. The primary forces are approximately 20,000N due to the reciprocating mass. The secondary forces are much smaller and peak around 4,000N. The primaries are due to the reciprocating masses. The piston accelerates and decelerates in one stroke from BDC to TDC, this

causes a secondary force due to the acceleration vectors changing directions throughout the stroke.

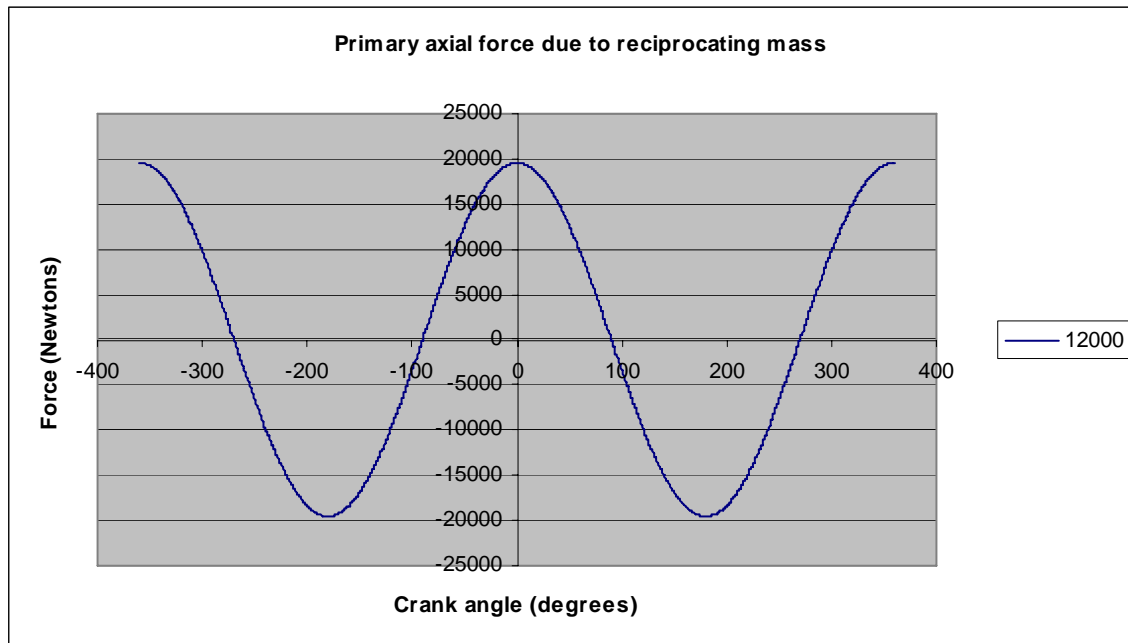


Figure 40 Primary inertia forces @12,000rpm

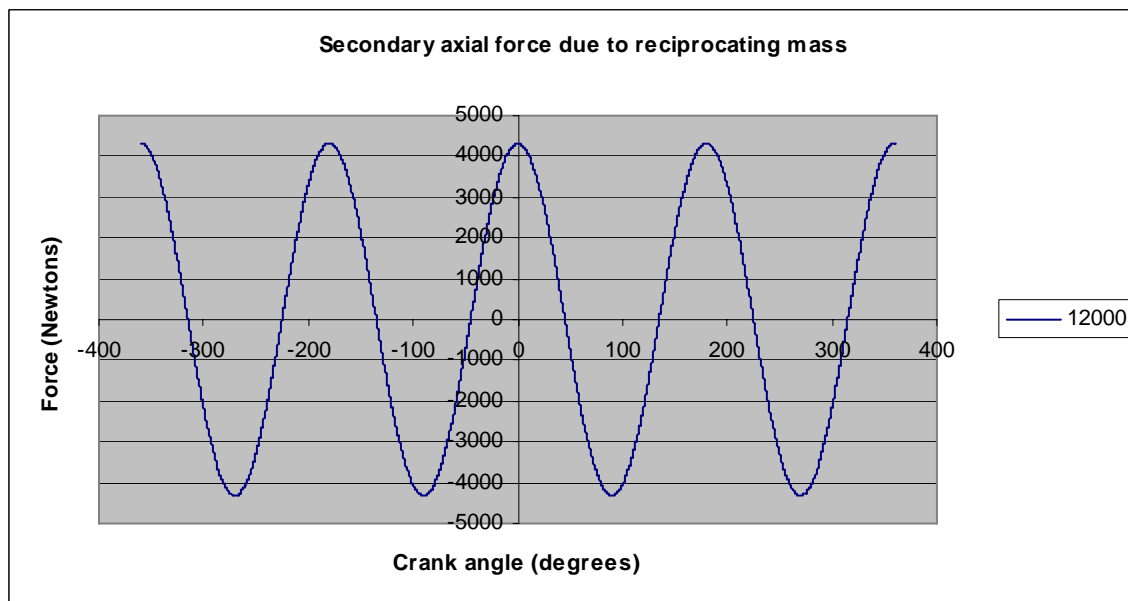


Figure 41 Secondary inertia forces @ 12,000rpm

Sometimes the secondary forces can be very small compared to the primary forces and can be considered negligible. In this case, the secondary forces are about 20% of the

primary forces and therefore will be taken into consideration. By combining the two forces the total inertia force can be found. The total inertia force is shown in figure 42 and peaks around 23,000N.

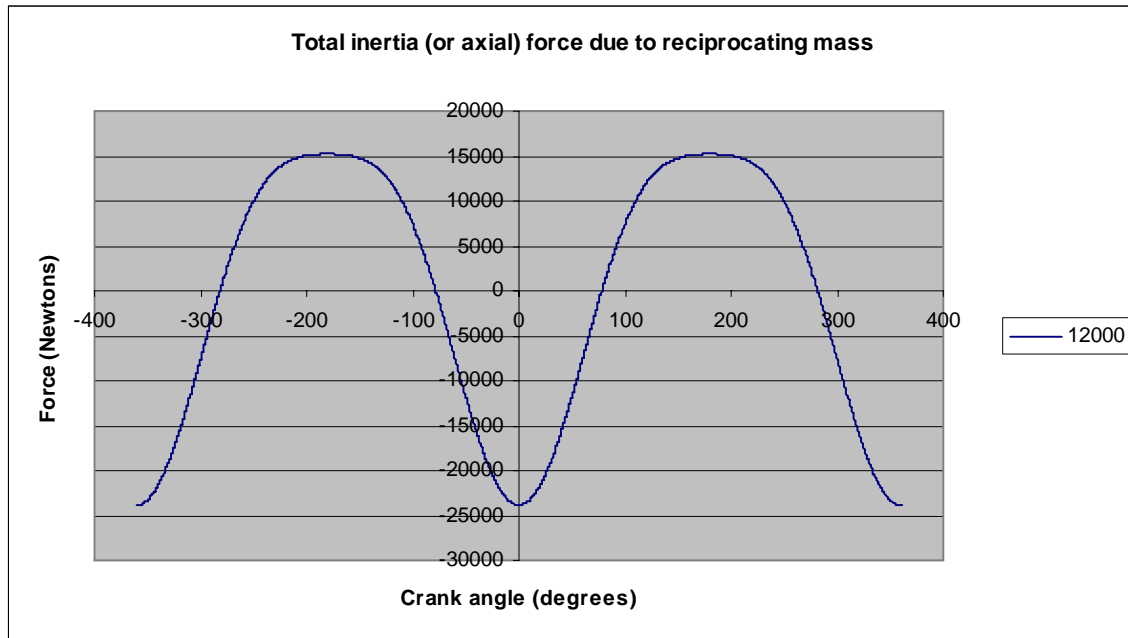


Figure 42 Total inertia forces-primaries + secondary's @12,000 rpm

The total gas forces calculated from the in-cylinder pressures are shown in figure 43. The peak gas forces are approximately 65,000N which is 4.0 times larger than the inertia forces. The other gas forces shown are for idle (3000 rpm) and mid-range (7000rpm) conditions. This graph was useful in visualizing the gas forces but also for seeing the engine timing. The peak pressure is slightly after TDC. This is important because if the peak pressure was at TDC the con-rod would not be bent and the force would transfer straight into the crank.

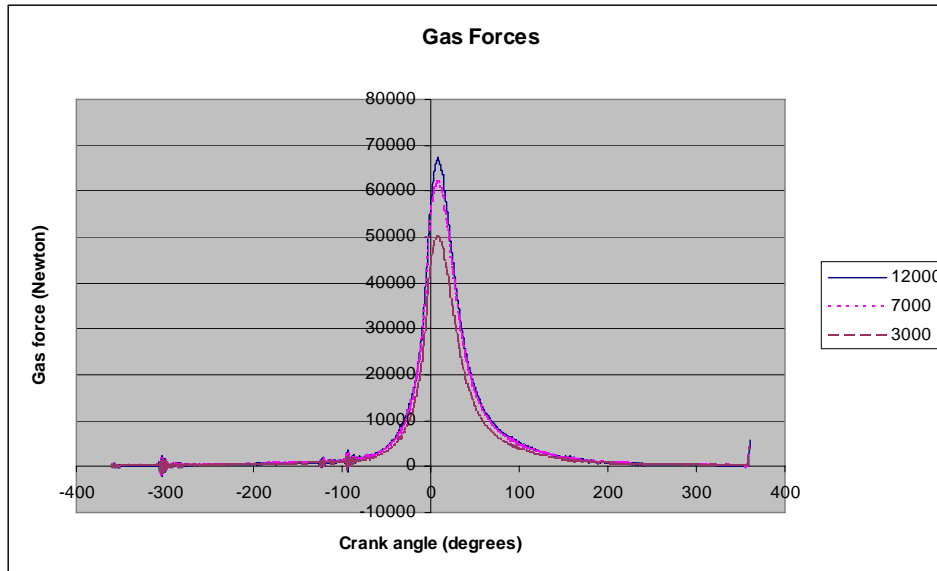


Figure 43 Gas forces @12,000rpm

By combining the gas and inertia forces (see figure 44) the total force is reduced by about 10,000Newtons. Figure 44 shows the gas forces dominate at slow engine speeds, but at 12,000 rpm the inertia forces increase to approximately 25,000N, where as the gas forces are approximately 42,000N. If the engine speed goes above 14,000N the inertia forces exceed the gas forces. Engine speed is very important to consider when balancing the crankshaft and determining bearing loads.

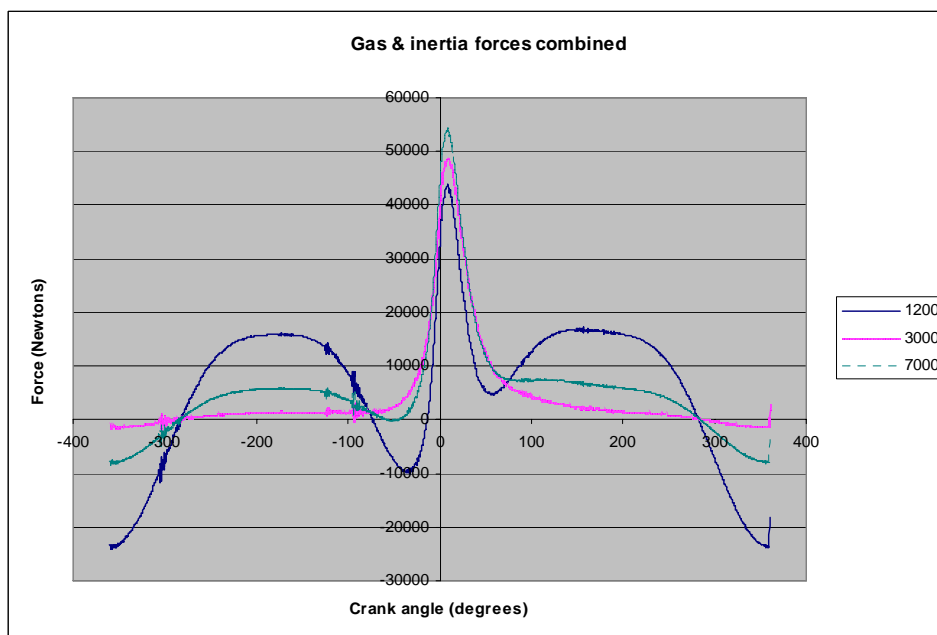


Figure 44 Gas & inertia forces @ idle, mid range, red line

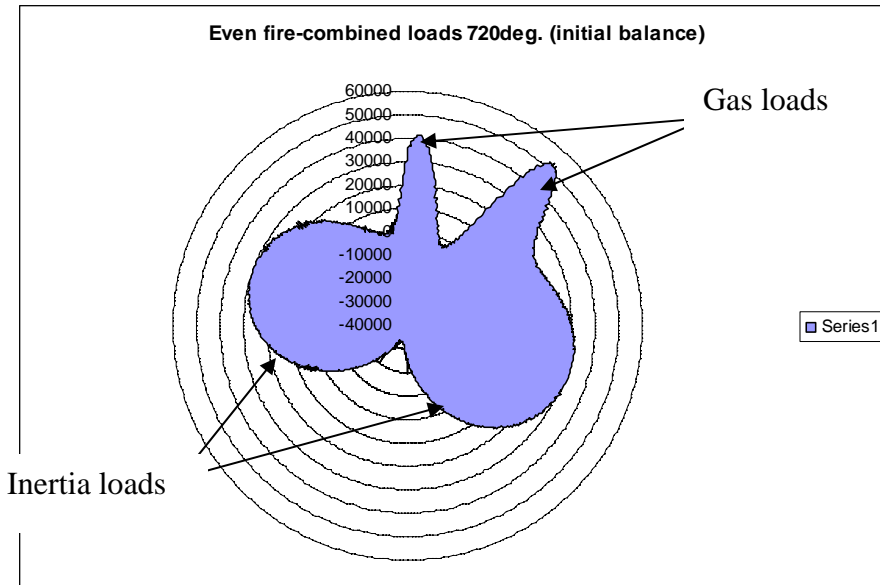


Figure 45 Even fire-combined loads

Figure 45 shows a polar plot of the main bearing loads (NOTE: THIS LOAD WILL BE SHARED BETWEEN TWO BEARINGS) for an even fire. Even fire is cylinder 1 firing and then cylinder 2 firing right after (75deg. later). The peak force is approximately 55,000 Newtons. With an odd fire (see figure 46) the peak force is reduced by 10,000 Newtons to 45,000 Newtons. Odd fire is cylinder 1 firing and then cylinder 2 firing (360 + 75deg.) later. From these plots it is wise to choose an odd-firing order as it reduces peak loads.

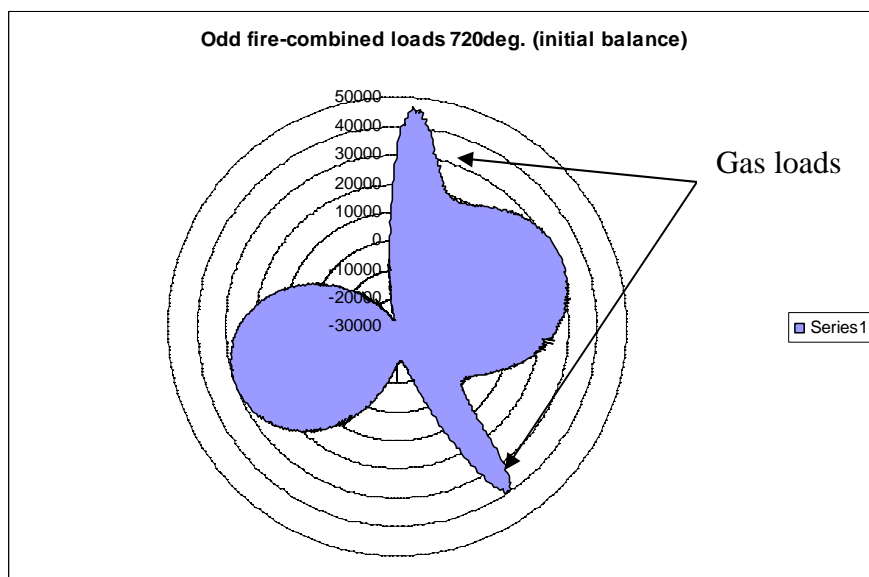


Figure 46 Oddfire-combined loads

When experimenting with different balance loads the original goal was to balance at 10,000rpm where max engine power occurred. It was surmised that if balancing was optimized then power could be maximized. Further investigation led to figures 47&48 which show that bearing loads are sufficient at 10,000rpm with a 35% overbalanced crankshaft, but as the speed increases to 12,000 rpm the upper bearing loads increase. Previously stated was the top half bearing loads need to be approximately 1/3rd of the bottom half because of the top half groove.

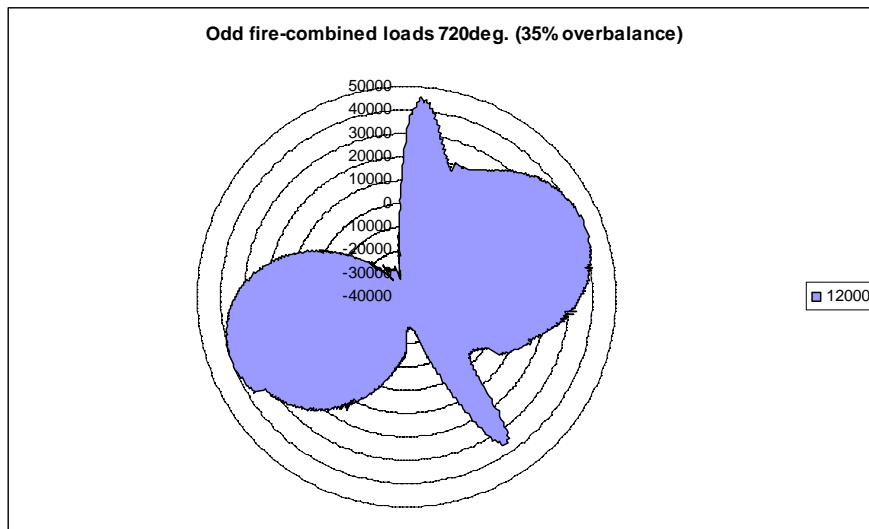


Figure 47 35% Overbalance @ 12,000rpm (10% greater load on upper half of bearing)

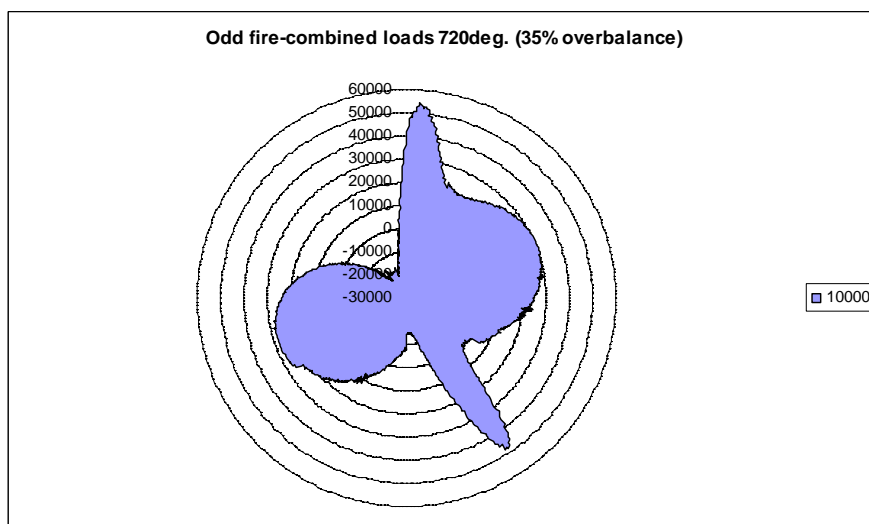


Figure 48 35% overbalance @ 10,000rpm (33% less load on upper half of bearing)

From figure 47&48 investigation a question arose “how is the over rev range (redline) of an engine determined?”. The answer is it limited by three parameters; camshaft design, max bearing loads, and connecting rod bolts. Max bearing loads was chosen for the limiting rev range factor. The crankshaft balancing ended up with a 3% under-balance (see figure 49) which made it so the upper half of the main bearings received 33% less load than the bottom half. The top half of the bearings are receiving a 30,000 Newton load while bottom half are receiving a 45,000 Newton load @12,000rpm. Remember these forces are shared by two bearings making the loads 22,500N and 15,000N. These loads can now be taken to the next section and used in the mathematical bearing model to determine minimum oil film thickness.

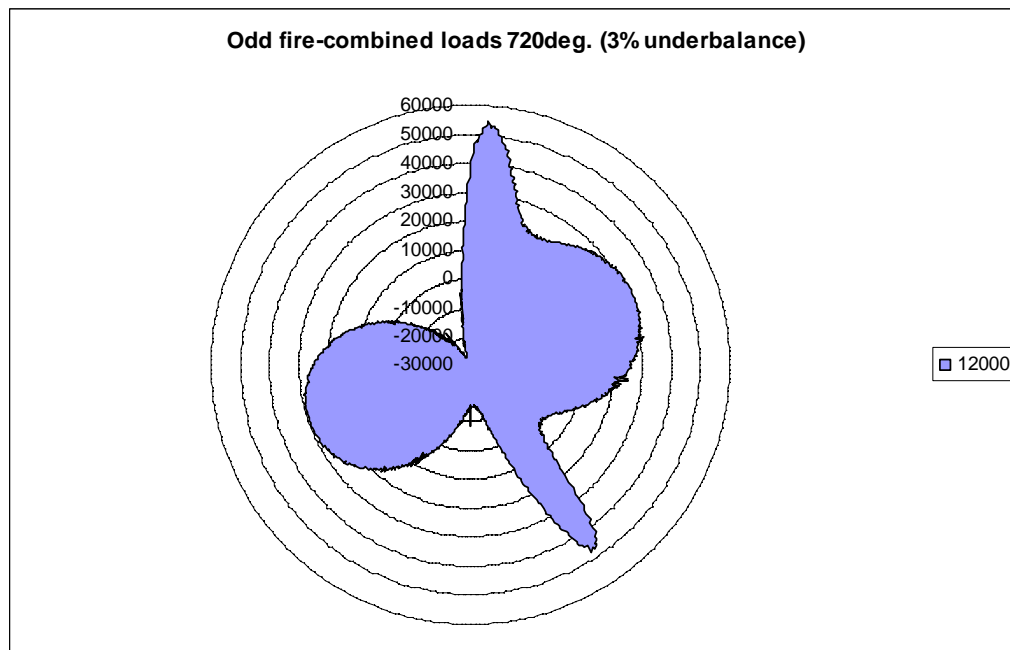


Figure 49 3% underbalance @ 12,000rpm

In order to verify the calculated bearing loads a comparison was made to the main bearing loads from GT-Power. Figure 50 shows the load values computed by GT-Power to be approximately 25,000N, which is a 10% difference. The small difference is attributed to the crank balancing performed.

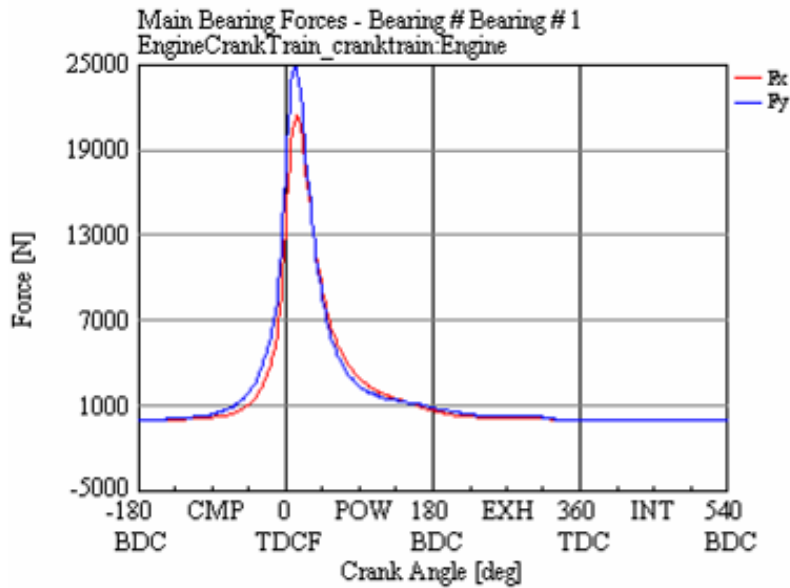


Figure 50 GT-Power main bearing loads @ 12,000 rpm

5.2.4 Crankshaft pin forces on big-end connecting rod bearings

Crankshaft pin forces are calculated with equation 5.5.

$$F = m_r \times r \times \omega^2 \quad (5.5)$$

Where F is the crankshaft pin force, m_r is the equivalent rotating masses (i.e. crankpin, rod bolts, big end of rod rotating mass equivalent, and big end bearings), r is the distance from the crankshaft center of rotation to the rotating mass center, and ω is engine speed. Figure 51 shows the rotating mass assembly; where $m_r = 590$ grams, $r = 21.9$ mm. Using equation 5.5, for an engine speed of 12,000rpm, $F = 20,404$ N. This force shared between two bearings becomes $F = 10,202$ N. This is 55% less force than the main bearing forces of 22,500N.

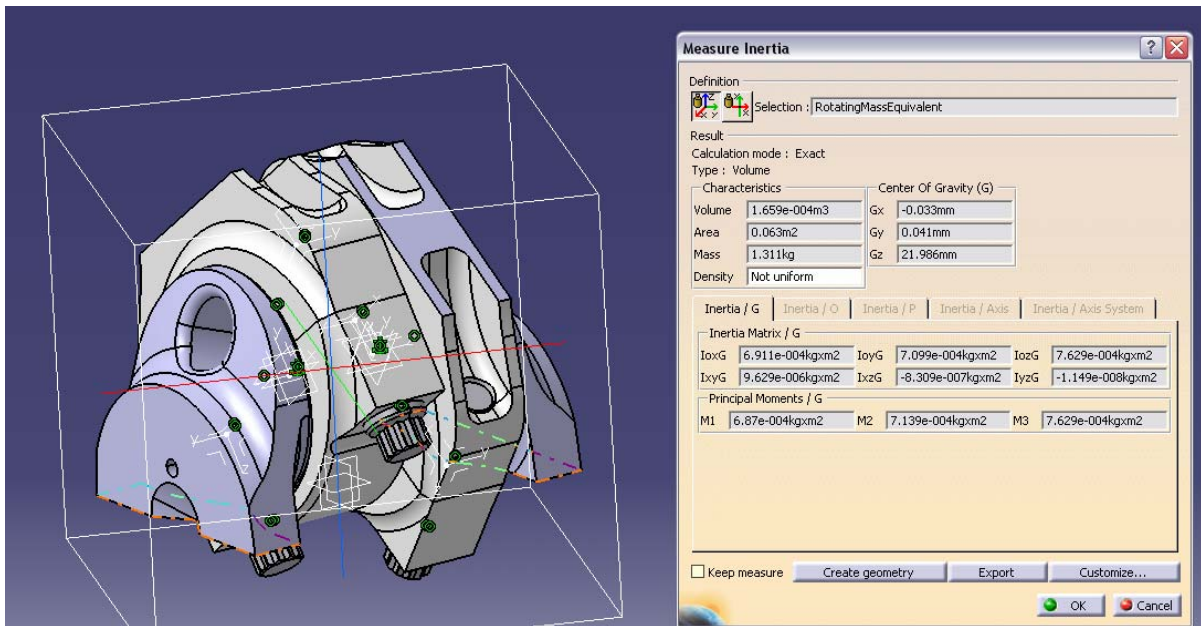


Figure 51 Rotating mass assembly for crankpin forces

5.2.5 Mathematical Bearing Model

This section will show the design process for the main journal bearings. A mathematical bearing model is created based on the Ockvirk Solution or short bearing approximation method. The inputs to the model are bearing geometry, engine speed, and forces from the crankshaft. The outputs of the model are *bearing eccentricity ratio, max pressure and its location, minimum oil film thickness, coefficient of friction, torque, power loss, required lubricant, flow rate, and temperature rise*.

It is to be noted that lubrication theory for surfaces in relative motion is extremely complex mathematically. Solutions to the partial differential equations that govern the behavior are based on simplifying assumptions that yield only approximate solutions [Norton 2000].

Given:	F = 22,500N	Max bearing loads (calculated in section 5.2.3 Crankshaft Balancing)
	Temp = 65C (150F)	Bearing inlet engine oil temperature
	n = 12,000rpm	Engine speed-max (redline zone)
	d = 49.2mm	Main bearing diameter (off the shelf part)
	L = 20mm	Main bearing axial length (off the shelf part)
Assumptions:	CR = 0.0017	Clearance ratio
	O _N = 90	Ockvirk Number is a dimensionless load factor which makes it convenient to compute, compare, and plot various bearing parameters.
	O _N = 90	An upper limit for severe loading, $\varepsilon_x = 0.93$
	O _N = 60	An upper limit for heavy loading, $\varepsilon_x = 0.90$
	O _N = 30	An upper limit for moderate loading, $\varepsilon_x = 0.82$

Nomenclature:

U	Tangential velocity
c_d	Diametral clearance
c_r	Radial clearance
ε_x	Eccentricity ratio
K_ε	Dimensionless parameter
η	Lubricant viscosity
p_{avg}	Average pressure
θ_{max}	Angle at which max pressure occurs
p_{max}	Max pressure
ϕ	Angle which locates the $\theta = 0$ to π axis
T_s	Stationary torque
T_r	Rotating torque
Φ	Power loss
μ	Coefficient of friction
h_{min}	Minimum oil film thickness
ω	Engine speed in rad/sec
r	Bearing radius
ρ	Oil density, 885 kg/m ³
c_p	Oil Specific Heat Capacity, 1670 J/kg*K
J	Mechanical equivalent of heat, 4.15 J/cal
Q	Flow rate
Temp	Temperature rise in bearing. Add to inlet temp. for resultant temperature.

First, tangential velocity is determined from engine speed and bearing diameter using equation 5.6a.

$$U = \frac{d}{2}n \quad (5.6a)$$

Second, diametral and radial clearances are found using equation 5.6b and 5.6c. Clearance ratios depend on the assumed clearance ratio and bearing diameter.

$$c_d = CR \cdot d \quad (5.6b)$$

$$c_r = 0.5c_d \quad (5.6c)$$

Diametral clearance is extremely important. If the clearance is too big then the following factors could happen; reduced load carrying capacity, oil whirl (a vibration that occurs in high speed journal bearings), cavitation erosion (low pressures trailing rotating journal which create suctions strong enough to pull bearing material off), etc... On the other hand, a too little clearance leads to oil flow restriction; this increases the temperature which changes the viscosity which reduces the film thickness. It is essential the right bearing clearance be used.

3rd, the eccentricity ratio is found from equation 5.6d or from figure 52 using the suggested Ockvirk Number and experimental curve. The theoretical curve tends to undershoot the real values. The eccentricity ratio is a proportion of how offset the journal center is from the bearing center. The eccentricity ratio ranges from 0 at no load to 1 at full load where the journal is contacting the bearing.

$$\varepsilon_x = 0.21394 + 0.38517 \cdot \log(O_N) - 0.0008 \cdot (O_N - 60) \quad (5.6d)$$

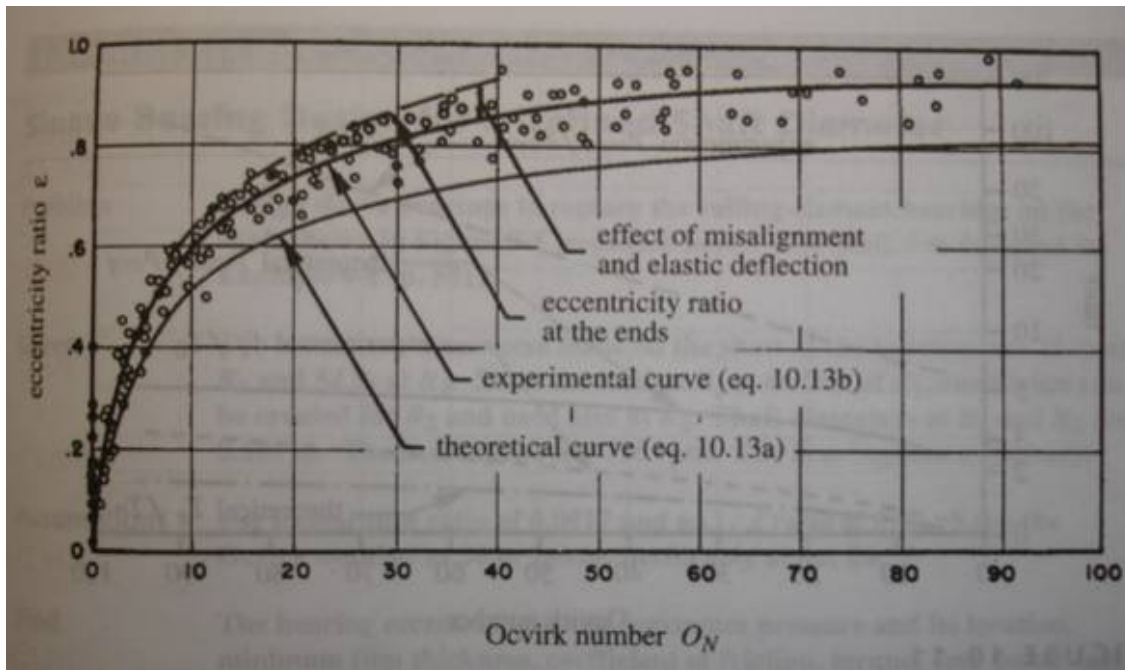


Figure 52 Eccentricity ratio vs. Ocvirk Number [Norton 2000]

Furthermore, without the eccentricity ratio a hydrodynamic bearing can not carry a load. The best way to understand the phenomenon is to consider two non-parallel plates with a oil film in-between them (see figure 53). As one plate is dragged across the other stationary plate, oil will be carried at high velocity into the decreasing gap developing a pressure strong enough to support a transverse load. Figure 54 shows the pressure distribution around the bearing. It can be seen that the high pressure is created opposite to the applied load P , this is all due to the eccentricity ratio.

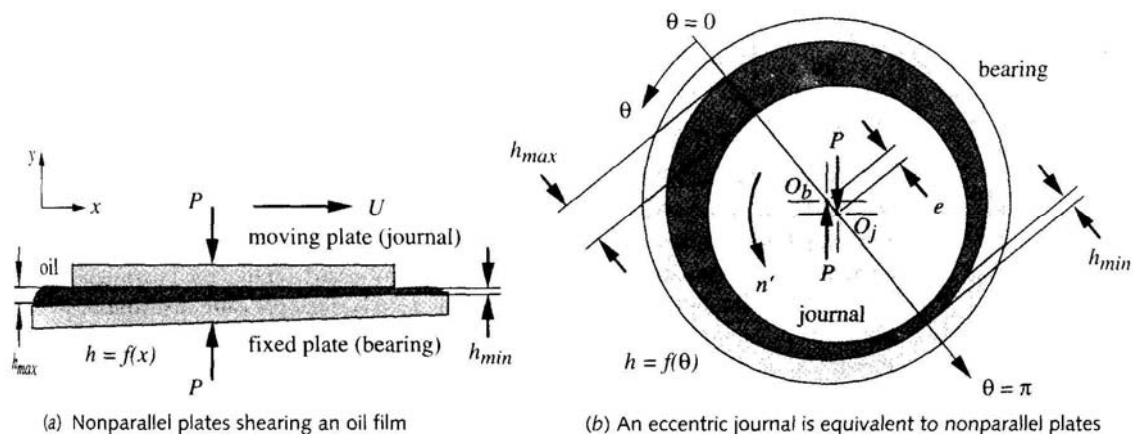


Figure 53 Non-parallel plate theory [Norton 2000]

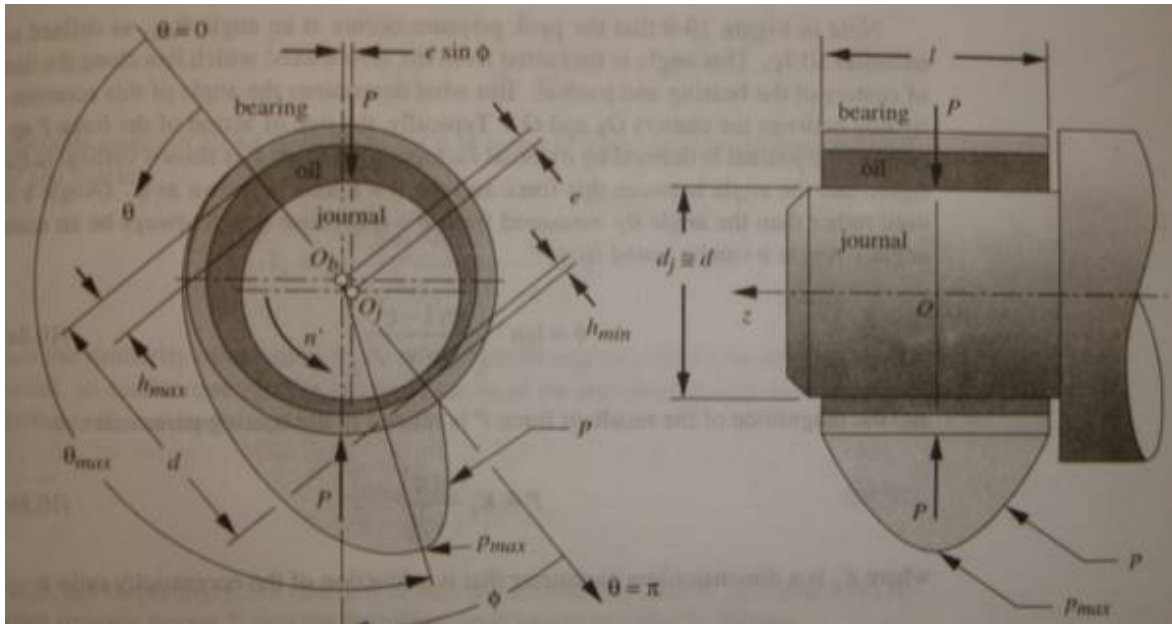


Figure 54 Journal bearing pressure distribution [Norton 2000]

4th, the dimensionless parameter K_ε is found from equation 5.6e.

$$K_\varepsilon = \frac{O_N}{4 \cdot \pi} \quad (5.6e)$$

5th, the viscosity is found from equation 5.6f. Originally, the equation is in terms of force, F , but it is rearranged to compute viscosity since the force is already known.

$$\eta = \frac{F \cdot c_r^2}{K_\varepsilon \cdot U \cdot L^3} \quad (5.6f)$$

6th, the average pressure in the oil film is found from equation 5.6g.

$$p_{avg} = \frac{F}{L \cdot d} \quad (5.6g)$$

7th, the angle θ_{max} at which the max pressure occurs is found using equation 5.6h. The equation uses the eccentricity ratio. Refer to figure 54 for more information. θ_{max} can

also be found from figure 55 by knowing the Ockvirk number. If using the chart, use the experimental curves.

$$\theta_{\max} = a \cos \left(\frac{1 - \sqrt{1 + 24\varepsilon^2}}{4\varepsilon} \right) \quad (5.6h)$$

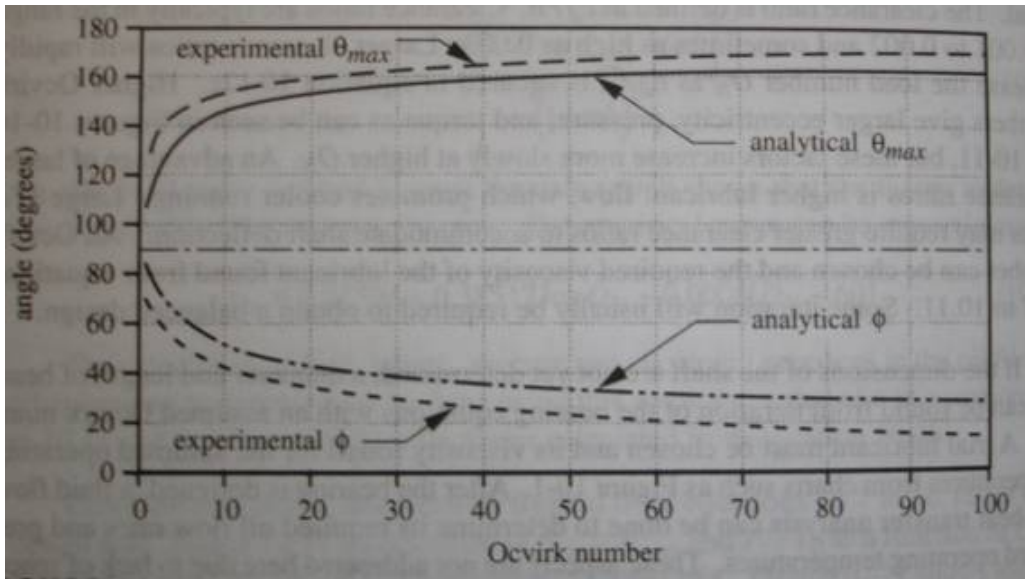


Figure 55 Angles θ_{\max} and ϕ as a function of Ockvirk Number [Norton 2000]

8th, the maximum pressure can be found from equation 5.6i. The values computed can be compared to the pressures ratios of figure 56.

$$P_{\max} = \frac{\eta \cdot U}{0.5 \cdot d \cdot c_r^2} \cdot \left(\frac{L^2}{4} - z^2 \right) \cdot \frac{3 \cdot \varepsilon \cdot \sin(\theta_{\max})}{(1 + \varepsilon \cdot \cos(\theta_{\max}))^3} \quad (5.6i)$$

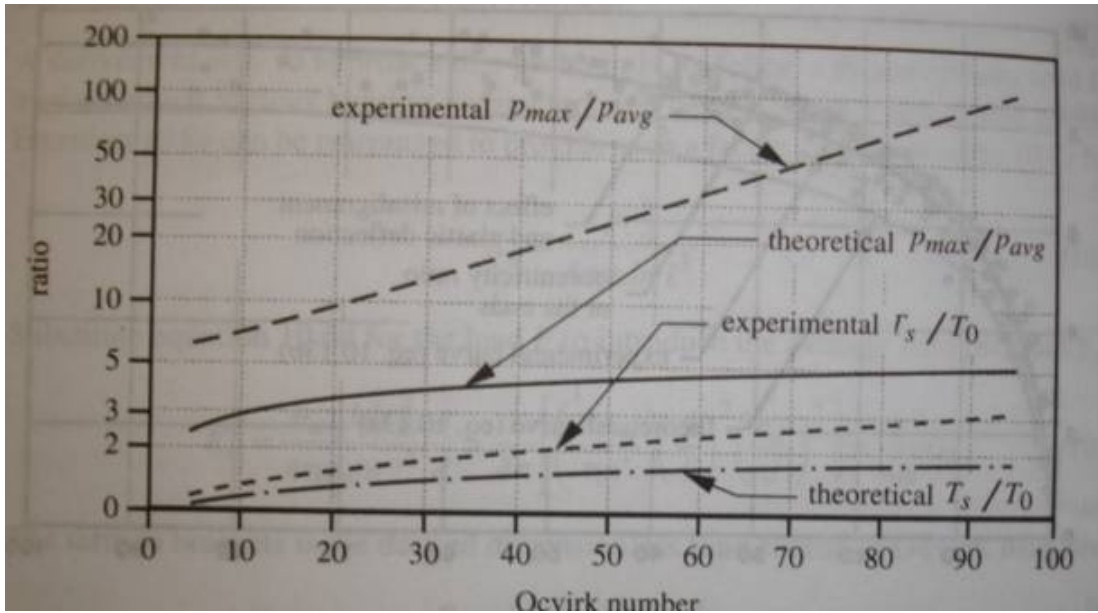


Figure 56 Pressure ratios and torque ratios as a function of Ockvirk Number [Norton 2000]

9th, find angle ϕ from equation 5.6j.

$$\phi = a \tan \left(\frac{\pi \cdot \sqrt{1 - \varepsilon^2}}{4 \cdot \varepsilon} \right) \quad (5.6j)$$

10th, the stationary and rotating torques can be found from equations 5.6k and 5.6l.

$$T_s = \eta \cdot \frac{d^2 \cdot L \cdot U}{c_d} \cdot \frac{\pi}{\sqrt{1 - \varepsilon^2}} \quad (5.6k)$$

$$T_r = T_s + F \cdot c_r \cdot \varepsilon \cdot \sin(\phi) \quad (5.6l)$$

11th, the power loss can be found from equation 5.6m or from equation 5.6n. Equation 5.6n is an empirically derived relationship for bearings provided by [Goddard]. For bearing pumping efficiency use 50% as a best case condition.

$$\Phi = T_r \cdot n \quad (5.6m)$$

$$\Phi_{alt} = 0.00007 \times \text{Bearing Pressure}(psi) \times \text{FlowRate}(gal / \text{min}) \times \text{Bearing Pumping Efficiency} \quad (5.6n)$$

12th, the bearing flow rate is found from equation 5.6o. The flow rate found here can be used in equation 5.6n.

$$Q = \omega \cdot r \cdot L \cdot c_r \cdot \varepsilon \quad (5.6o)$$

13th, the coefficient of friction is found from equation 5.6p.

$$\mu = \frac{2 \cdot T_r}{F \cdot d} \quad (5.6p)$$

14th, the minimum oil film thickness is found from equation 5.6q and the max oil film thickness is found from equation 5.6r.

$$h_{\min} = c_r \cdot (1 - \varepsilon) \quad (5.6q)$$

$$h_{\max} = c_r \cdot (1 + \varepsilon) \quad (5.6r)$$

15th, the specific oil film thickness is found from equation 5.6s.

$$h_c = \frac{4}{3} h_{\min}, \quad \Lambda = \frac{h_c}{\sqrt{R_{q1}^2 + R_{q2}^2}} \quad (5.6s)$$

16th, determine the safety factor from metal to metal contact using equation 5.6t. The max force is found by rearranging equation 5.6f and calculating for an Ockvirk number of 95 (this is considered to be extreme max load). The actual force is the bearing load force.

$$N = \frac{F_{\max}}{F_{actual}} \quad (5.6t)$$

17th, determine the temperature rise in bearing due to oil cooling by using equation 5.6u. The value found here is added to the inlet oil temperature (approximately 65 deg. C).

$$Temp = \frac{\Phi}{J \cdot Q \cdot \rho \cdot c_p} \quad (5.6u)$$

5.2.6 Bearing Model Results & Discussion

$O_N =$	$\varepsilon_x(O_N) =$	$\frac{\eta(O_N)}{\mu\text{reyn}} =$	$\frac{p_{\max}(O_N)}{\text{psi}} =$	$\frac{\Phi(O_N)}{\text{hp}} =$	$\frac{h_{\min}(O_N)}{\mu\text{m}} =$	$T_r(O_N) =$	
10	0.639	29.109	22760	25.3848	15.09	15.1	N·m
15	0.703	19.406	26068	18.4916	12.42	11.0	
20	0.747	14.554	30253	14.9608	10.58	8.9	
25	0.78	11.643	35315	12.8059	9.18	7.6	
30	0.807	9.703	41356	11.3528	8.08	6.7	
35	0.829	8.317	48534	10.3083	7.17	6.1	
40	0.847	7.277	57052	9.5239	6.40	5.7	
45	0.863	6.469	67166	8.9162	5.74	5.3	
50	0.876	5.822	79188	8.4346	5.17	5.0	
55	0.888	5.292	93499	8.0466	4.67	4.8	
60	0.899	4.851	110565	7.7303	4.23	4.6	
65	0.908	4.478	130952	7.4706	3.84	4.4	
70	0.917	4.158	155352	7.2565	3.49	4.3	
75	0.924	3.881	184604	7.0800	3.17	4.2	
80	0.931	3.639	219735	6.9350	2.89	4.1	
85	0.937	3.425	261990	6.8168	2.63	4.0	
90	0.943	3.234	312882	6.7217	2.40	4.0	
95	0.948	3.064	374240	6.6469	2.19	3.9	

Table 9 Bearing Model Results 1 @ 12,000rpm

Referring to table 9, at the chosen Ockvirk number, 90, the eccentricity ratio of 0.943 is quite high. If the eccentricity ratio reaches 1 then metal to metal contact occurs. It is normal for a race engine to run at high eccentricity ratios. In order to make it successful high machining tolerances and surface finishes are required. The viscosity needed is 3.234 micro reyns which is equivalent to a SAE25 grade oil; this was determined using figure 57 and a temperature of 65 deg. C, which is normal engine operating temperature. The max pressures reach 312,882psi which is very high, however, these high pressures are good to counter-act the high gas and inertia forces. The average pressure (not shown

in table 9, see appendix 3) is 3900psi. The power loss from the bearing is 6.7hp. This is quite a lot, but referring back to figures 31&32 it can be seen that the bearings consume most of the power at high speeds.

$$O_N = \left(\frac{p_{avg}}{\eta \cdot n} \right) \cdot \left(\frac{d}{L} \right)^2 \cdot \left(\frac{c_d}{d} \right)^2 \quad (5.10)$$

Equation 5.10 is the Ockvirk number (or load number) equation. In table 9 it was varied from 15 to 95 to show the different effects it has on the bearing parameters. By varying the clearance ratio $\frac{c_d}{d}$, or the bearing diameter to length ratio $\frac{d}{L}$, the load number will rapidly increase as these terms are squared. As the load number increased so did the eccentricity and pressure. On the other hand, as the load number decreased, higher losses, film thicknesses, and lubricant viscosities occurred.

The bearing design needs to be balanced. In order to do so some compromises will need to be made. For example, if extra cooling is desired the clearance ratio could be increased which would increase the flow rate. However, this will require more pumping work and therefore more horsepower losses. Race engines are normally preheated to 50-70C, otherwise there are no clearances at cold temperatures.

Micro
reyns

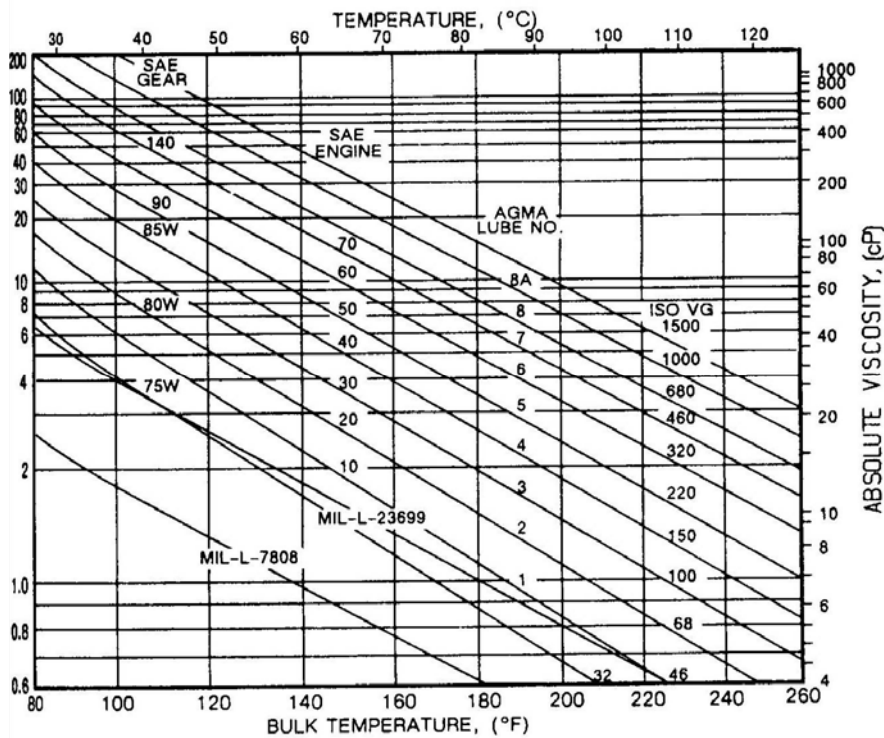


Figure 57 Chart for determining oil viscosity [Norton 2000]

Eccentricity Ratio	0.943
Max Pressure	312,882 psi
Min. Oil Film Thickness	2.40 micro meter
Coeff. of friction	0.0072
Torque	4.0 Nm
Power loss	6.7 hp
Alternate power loss	5.3 hp
Lubricant Required	SAE 25
Safety Factor	1.0
Temperature Rise	20 deg. C
Min. Surface rms required	3.2 micro meter
Flow rate	9.2 Litre/min

Table 10 Bearing model results 2 @12,000rpm

Table 10 presents all the data resulting from the bearing model. Some of this information is repeated in table 9, however some extra variables are presented in table 10 and will be discussed. The alternative power loss equation (5.6n) yielded 5.5hp compared to equation (5.6m) which yielded 6.7hp. 1.5 hp difference is not bad considering all the parameters involved in the bearing model. The coefficient of friction

came out to be 0.0072 which is within range for hydrodynamic lubrication; mixed film lubrication is about 0.05 and full film about 0.001 [Booser 2001]. Torque is 4Nm and is dependent on how high the shear rate is within the oil film. The lubricant required is SAE 25. There is no SAE 25, so the next grade up is SAE 30. The safety factor is 1.0, which is on the limit, but remember that this is at 12,000rpm which is the redline of the engine. Also, by increasing the oil grade to SAE30 this will help to increase the safety factor. In the future, if problems are encountered with the SAE30 grade, a SAE40 grade could be used to possibly fix the problems. A temperature rise of 18 deg. C was found. This implies that with an inlet temperature of 65 deg. C, the resulting temperature would be 83 deg. C which is standard for hot engine oil. The minimum surface finish required to avoid asperity contact is 3.2 microns. As discussed in section 6.1-Surface Parameters, surface finishes achievable are 0.04 microns. This makes 3.2 microns an easy target to meet. Furthermore, by providing a smoother surface finish, this will provide the bearings a safety margin or cushion in the event of overloads. The flow rate is 9.2 litre/min. Back in section 4.4.1-Oil Pressure Pump Design, the oil pump flow rate was found to be approximately 15 litre/min @12,000rpm engine speed. A difference of about 6 litre/min is perfect to add some safety into the system. Furthermore, by giving some leeway to the pump, the pump lifetime will be increased.

6 CFD OF OIL FLOW THROUGH V-TWIN ENGINE

This chapter uses computational fluid dynamics (CFD) to analyze the oil flow through the engine. It is a tool for determining pressure drops due to system losses as well as verifying no restrictions occur before any of the main bearing feeds. It is a check on the area summations performed in section 4.3.2 for determining main oil gallery sizes.

6.2 Pressure drops and flow rates through oil galleries

In order to create the oil pipe network system the actual CAD model was used. All of the solid features were deleted so that only the oil passages remained. Figure 58 shows the engine and pipe network which was subtracted from the full engine model. The oil passages were made into solids. The model was then imported into Gambit 2.2.30 for meshing. A tetrahedral mesh with a volume of 398,444 was used. The mesh and model was then imported to T-Grid 3.6.8 to refine the mesh by checking skewness quality. Skewness quality of 0.6 was used. With a good mesh, the model was imported into Fluent 6.2.16. The inlet gauge pressure was set to 4bar and all outlets were set to 0bar. After 664 iterations the model converged. Figure 59 shows the CFD results from Fluent.

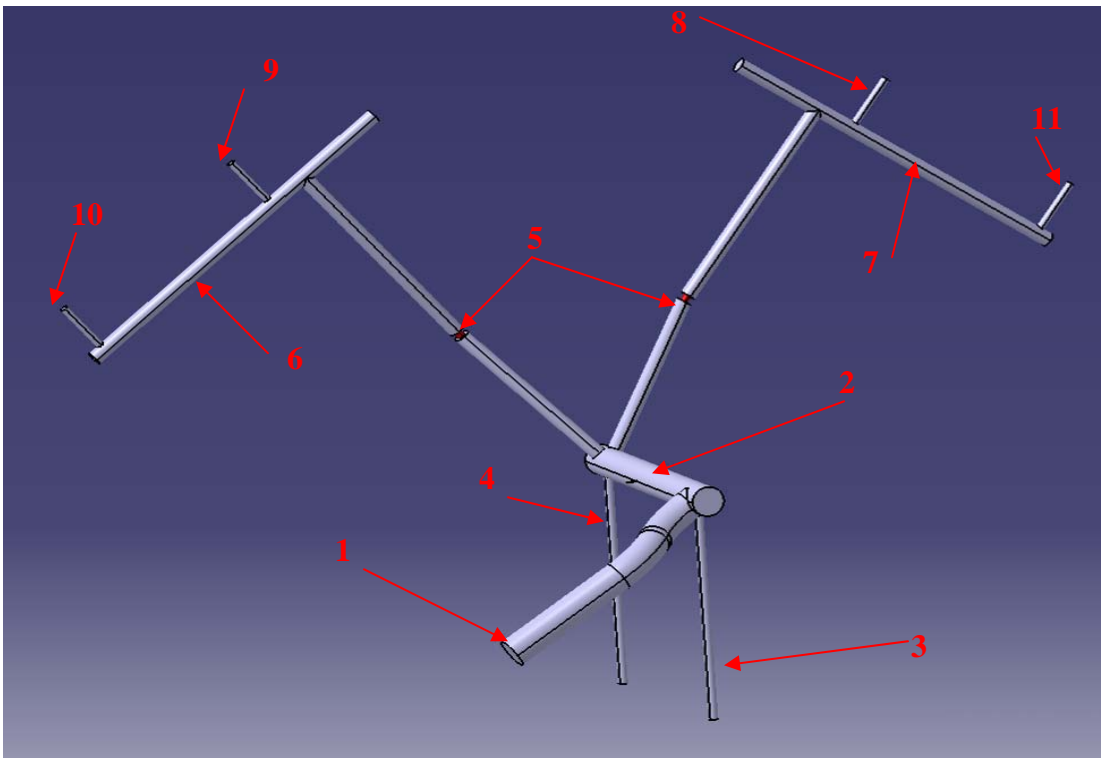
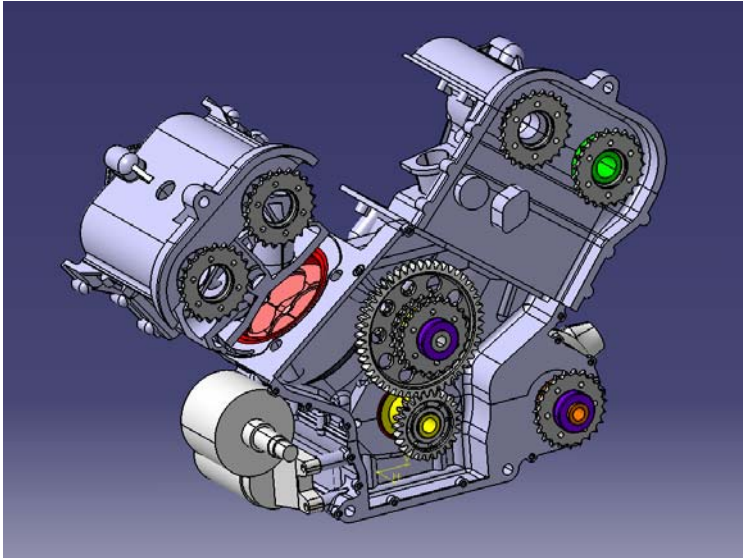


Figure 58 Catia Model of Oil System Pipe Network

The numerals in figure 58 represent: 1 Oil inlet from pump; 2 main oil gallery; 3 main bearing #1; 4 main bearing #2; 5 orifices or pressure droppers; 6 left bank cylinder head oil gallery; 7 right bank cylinder head oil gallery; 8 right bank intake camshaft bearing #1; 9 left bank intake camshaft bearing #1; 10 left bank exhaust camshaft bearing #1; 11 right bank exhaust camshaft bearing #1.

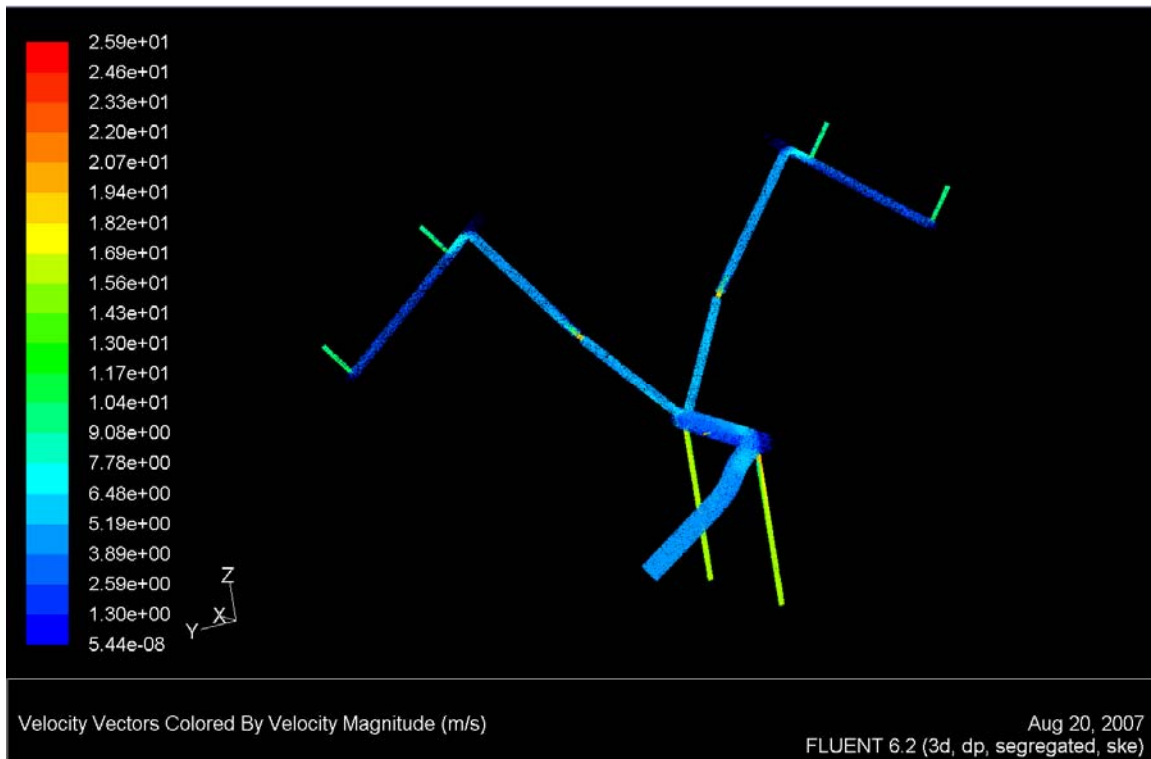


Figure 59 Model 1-Velocity vectors of oil flow through engine (3mm orifices)

Figure 59 shows the velocity comes in at around 2-3m/s for the main oil gallery which is 12.4mm in diameter. The velocity increases to 13-15m/s in the main bearing feeds due to a diameter change to 3mm. At the block to head interface there is a 3mm orifice to drop the pressure into the cylinder heads. In the cylinder head galleries (6mm diameter) the flow velocity is around 1-3m/s. This is similar to the main gallery flow velocity because the pressure has changed. The flow velocity into intake cam bearing 1 is between 9-14m/s.

A summary of the results from figure 59 is shown in table 11 in terms of flow rates. The flow rates in the main gallery are 14.5-21.7 liter/min which closely match the capacity of the oil pressure pump which is around 15liter/min. The system performance almost matches the pump performance indicating a good system. The main bearing flow rates are 5.5-6.4 liter/min which is under the requirements. From section 6.2.6 the main bearings need about 9liter/min flow rate. This suggests the Fluent model was modeled with incorrect boundary conditions or the pressure inlet needs to be greater to overcome the system losses.

Component	Diameter (mm)	Velocity (m/s)	Flow rate (liter/min)
Main oil gallery	12.4	2-3	14.5-21.7
Main bearings	3	13-15	5.5-6.4
Cyl. Head gallery	6	1-3	1.7-5.1
#1 Cam bearings	3	9-14	3.8-5.9

Table 11 Fluent Model 1 Flow Rates

Figure 60 shows the pressure inlet is 4bar (supplied by pump) and is constant throughout the main gallery. The pressure drops to 0.2-1.8 bar in the main bearing feeds. The pressure drops to between 1-1.5bar in the cylinder head galleries right after the orifices. Pressure feeding the intake cam bearing 1 is around 0.25-0.5bar. The pressure is low and is adequate to feed the bearing because the cam bearing has no pressure on its bottom half of the bearing where it is being fed with oil. There is no pressure on the bottom half because the tappet is pushing on the cam lobe which pushes the cam into the top half of the bearing shell.

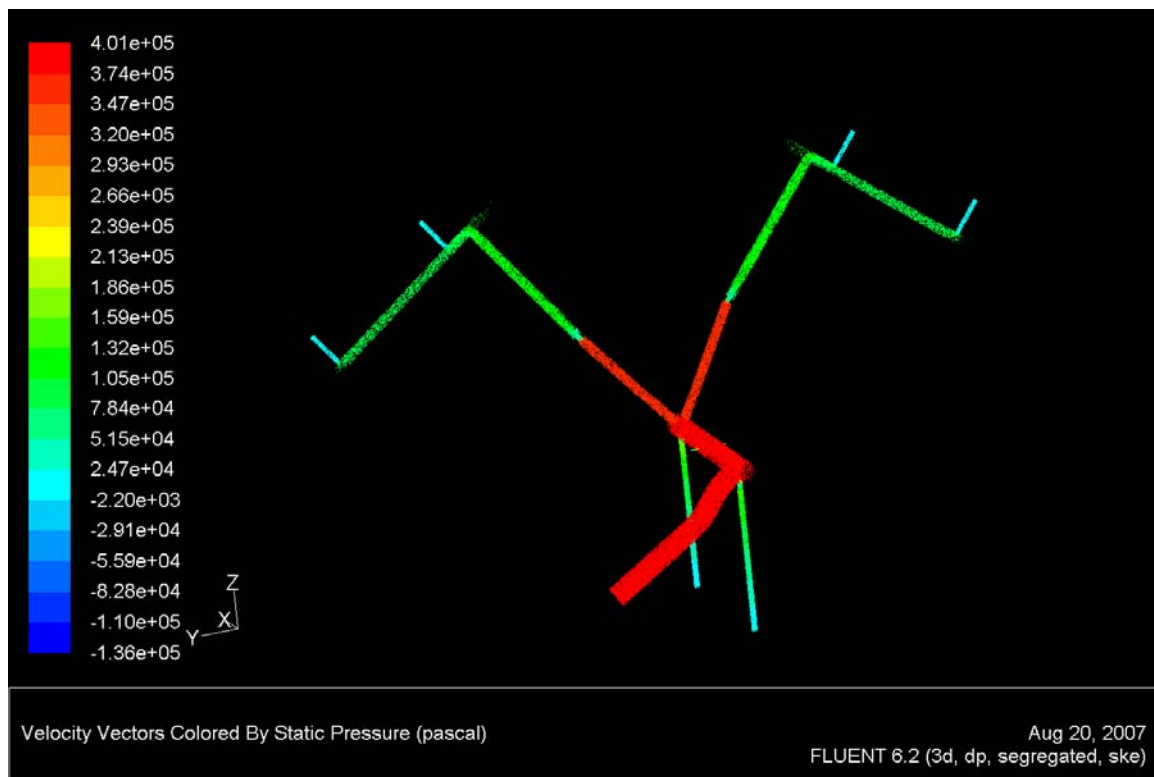


Figure 60 Pressure vectors of oil flow through the engine (3mm orifices)

The main bearings need to be fed at 4bar pressure in order to overcome the crankshaft centrifugal head. The Fluent model in figure 60 shows 0.2-1.8bar pressure in the main bearing feeds. The results in that area seem spurious as two different pressures are seen in a constant cross-sectional area tube with no restrictions on the outlet. Gravitational effects could be considered however, over a length of 100mm it is negligible. The reason for the change in pressure is because of an unrestrained discharge. It is essentially an open ended hose where the velocity is high in the hose but as the fluid exits into an atmosphere with zero restriction a pressure differential occurs as shown in the model.

6.2.1 Recommendations to improve CFD Model of oil flow through engine

In order to model the system more accurately a downstream resistance is needed to simulate the main bearing resistances. In the physical process resistance is created from the oil being forced into a bearing crevice of 5-10microns. By adding a resistance into the model a higher pressure would be created in the main bearing feed lines, possibly bringing it up to 4bar as required. This resistance is the difficult bit to determine. A separate model is needed to simulate bearing resistances.

In order to increase the flow rate into the main bearings the orifice diameters could be changed from 3mm to 1.5mm. This would cause the mass flow rates to shift in the system. The system is a mass balance system with no downstream resistances from the bearings. The only restrictions in the system are the pipe bends, diameter changes, and internal roughness of the pipes. Therefore, the Fluent model is showing the mass balance for an unrestricted system. If restrictions from the cam bearings and main bearings were added then the mass balance would shift around. Ideally, it would shift so that the main bearings are fed at the right pressure and flow rate.

In order to determine the bearing resistance a model such as the one shown in figure 61 needs to be created. Fluent users have created such systems using a sliding mesh model to capture shaft rotation and downstream flow exits. Furthermore,

downstream resistance is modeled through a user defined function (UDF) of a customized porous media model. Time did not permit this study to take place.

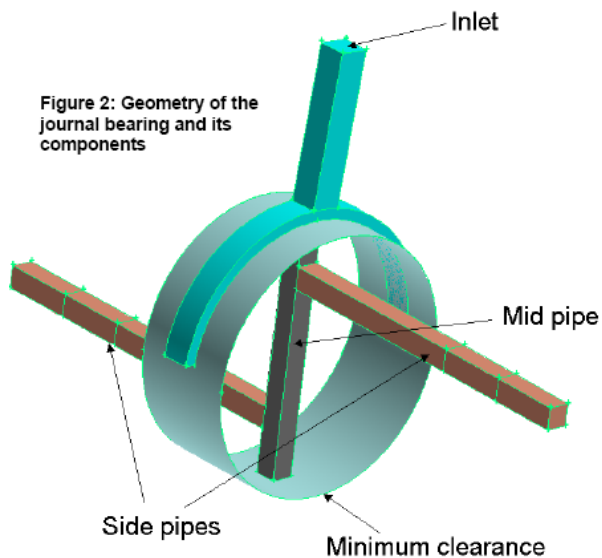


Figure 61 Fluent model of journal bearing [Fluent 2007]

A second Fluent model (shown in figure 62) of the oil system was created with 1.25mm orifice pressure droppers at the block to cylinder head interface.

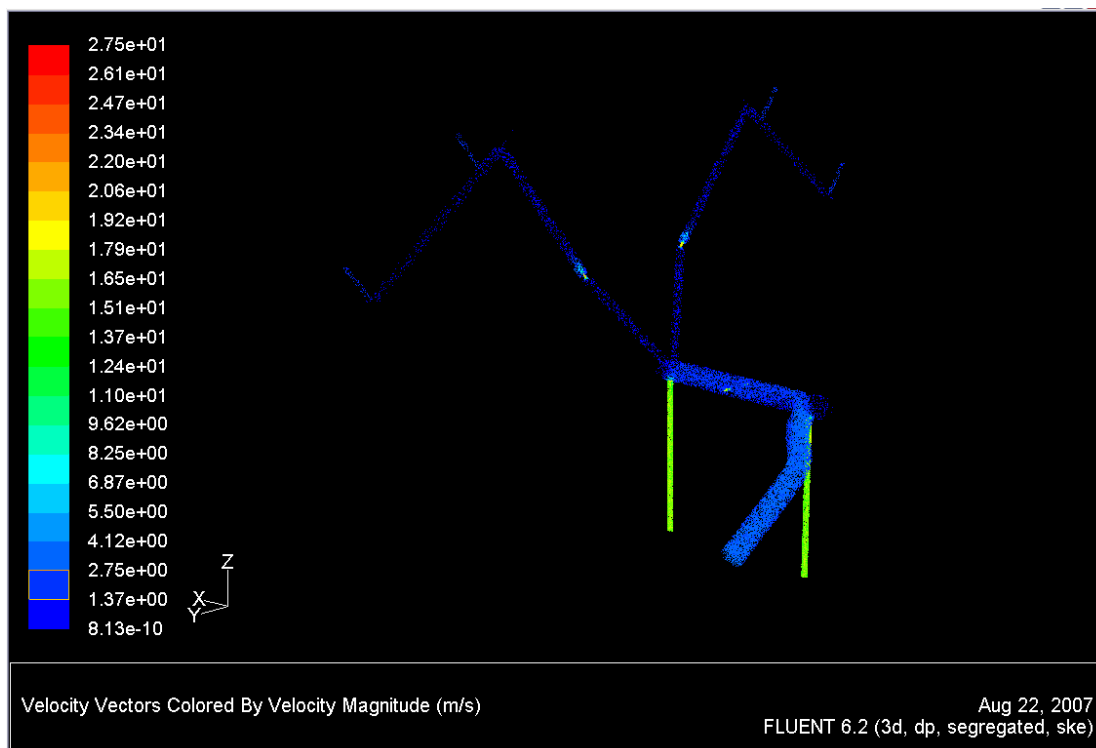


Figure 62 Velocity vectors of oil flow through engine (1.25mm orifices)

By changing the restrictor sizes from 3mm to 1.25mm a change in flow rates occurred. The results from figure 62 are summed up in table 12. The main bearing flow rates increased approximately 1.5liter/min more than the flow rate of 6liter/min from table 11. The flow rates are better distributed however are still lacking in balance. This imbalance indicates the Fluent model needs to be modeled more accurately.

Component	Diameter (mm)	Velocity (m/s)	Flow rate (liter/min)
Main oil gallery	12.4	2.75	19.9
Main bearings	3	18	7.6
Cyl. Head gallery	6	1.37	2.3
#1 Cam bearings	3	2.75	1.2

Table 12 Fluent Model 2 Flow Rates

7 V-TWIN PISTON ASSEMBLY LUBRICATION

Lubrication (Note: lubrication regime = mixed lubrication i.e. boundary + hydrodynamic)

Geoff Goddard Engines Ltd. has determined through experimental testing that race engine pistons can be lubricated with 0.7mm squirt jets within the crankcase and from the oil being flung off of the crankshaft. 0.7mm squirt jets will flow approximately 0.8-1.0 litre/min of hot oil [Goddard 2007]. The squirt jets are fed directly from the main gallery and ensure cooling of the exhaust side of the piston [Goddard 2007]. The V-Twin will use 0.7mm squirt jets. The gudgeon pin is also lubricated from the squirt jets. Alternatively, some engines will have an oil feed drilled through the connecting rod from the big end bearing to the gudgeon pin. The main goal is to cool the piston rings because when detonation occurs it starts at the rings first. If the rings are adequately cooled, the engine can run at higher power and leaner conditions. Leaner because the rings are now being cooled and do not need to rely on a rich fuel mixture to provide cooling. The big end connecting rod bearing is lubricated through two drillings through the connecting rod. As the piston assembly goes down these drillings create extreme low pressures which suck any oil fog into the bearings.

The piston rings operate in mixed lubrication i.e. boundary and hydrodynamic lubrication as shown back in figure 9. The cylinder liners are to be plateau honed to reduce friction and maintain good oil retention in the valleys. See figure 63 which compares conventional single stage honing to plateau honing. Plateau honing is achieved in two stages; stage 1 rough stones and stage 2 fine stones. As oil gets trapped into these valleys the rings will glide over them pushing the oil into the valleys. This causes the oil to hydrostatically lock which creates an oil film thickness for the rings to glide on.

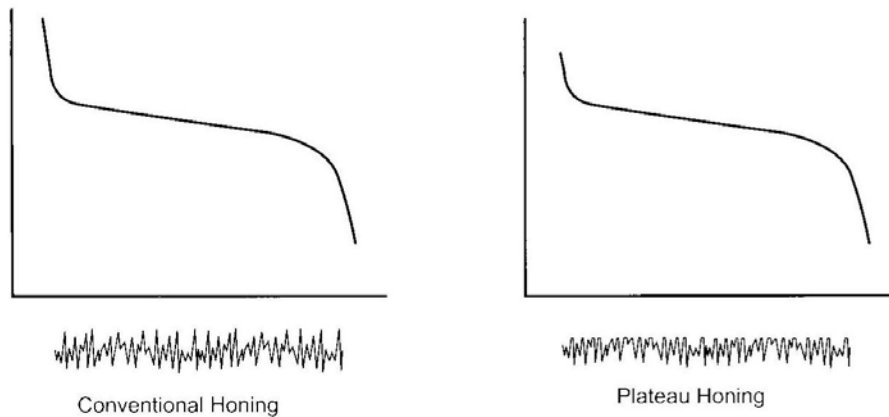


Fig. 15.19. Effects of conventional and plateau honing on cylinder wall surface characteristics

Figure 63 Cylinder wall surface honing [Hoag 2006]

Table 13 lists the piston assembly materials being used for the V-Twin. Materials were selected by other student engineers designing the components based on static, dynamic, and thermal stresses. These materials are important for lubrication because each material comes with a certain surface finish. These surface finishes have to be tailored to the lubrication regime they are operating in. This section is incomplete as time did not permit further discussion to take place.

Part	Material	Material Code	Surface Coating/Finish	Ra (microns)
Piston	Aluminum alloy	RR58	Zylan coated skirts	NA
Rings	Steel	Stainless with molybdenum infill	NA	NA
Gudgeon pin	Steel	EN40C	Nitrided	NA
Small end bearing	Metal Alloy	Bronze Hidural	NA	NA
Circlip	Steel	EN39C	NA	NA
Cylinder liner	Metal Alloy	LM25TF	Nikasil	0.05-1
Connecting Rod	Steel	EN24V	NA	NA
Rod bolts	Steel	SPS H11	NA	NA
Big end bearing	Bi-metal	Steel/bronze + lead indium flash	None (bronze)	

Table 13 V-Twin Piston Assembly Materials

8 V-TWIN VALVE TRAIN LUBRICATION

Lubrication (Note: lubrication regime = boundary lubrication)

From the main oil gallery oil is fed to the cylinder heads via 6mm diameter holes. At the cylinder head an orifice is inserted to drop the pressure from 4bar to 1bar. 1bar pressure has been experimentally determined by Geoff Goddard Engines Ltd. for race engines. The oil from here goes straight to intake and exhaust camshaft bearings number 1. The camshaft bearing is fed at low pressure from the bottom because the tappets are pushing the cam lobes into the top half of the bearing shell and therefore there is no pressure on the bottom half. The second camshaft bearing is fed through the camshaft (hollow). Oil enters the cam through bearing 1 and is then centrifuged inside the cam, because the cam is closed on both ends the oil creeps along the inner walls until it reaches bearing No. 2. In the event oil starvation is occurring on bearing No. 2, an axial keyway or groove could be machined into the cam. This would insure the oil makes it to the other bearing.

The valve train components are lubricated with the oil bleeding from the cam bearings. This oil is slung off of the camshaft onto all of the valve train. If additional lubrication is needed, squirt jets will be placed accordingly. Geoff Goddard Engines Ltd. suggests after running the engine, parts are to be inspected and if color bands made by extreme heat are showing on the metals, then more lubrication will be needed. Because most valvetrain components operate in boundary lubrication, the lubrication is there only to remove heat. The advanced surface finishes have made it possible for components to run dry.

Table 14 lists the materials for the components of the V-Twin valvetrain. Materials were selected by other student engineers designing the components based on static, dynamic, and thermal stresses. These materials are important for lubrication because each material comes with a certain surface finish. These surface finishes have to

be tailored to the lubrication regime they are operating in. This section is incomplete as time did not permit further discussion to take place.

Part	Material	Material Code	Surface Coating	Ra
Camshaft	Metal Alloy	Clean EN16T	Tufftride or Plasma Nitride	NA
Cam bearings	Metal Alloy	LM25TF(direct in housing) or HE15TF (caps)	NA	NA
Intake valve	Metal Alloy	214NS+2% Vanadium	NA	NA
Exhaust valve	Metal Alloy	214NS+2% Vanadium	NA	NA
Int. valve guide	Metal Alloy	Hidural 5 bronze-Langley alloys	NA	NA
Exh. valve guide	Metal Alloy	Hidural 5 bronze-Langley alloys	NA	NA
Int. Valve seats	Metal Alloy	Hidural 5	NA	NA
Exh. Valve seats	Metal Alloy	Hidural 1-10A or Brico Irons or Pluel Irons	NA	NA
Valve springs	Metal Alloy	Chrome Silicon	NA	NA
Tappets	Metal Alloy	EN40B or Tool Steel	Nitrided	NA
Shims	Metal Alloy	EN24V or X Condition	NA	NA

Table 14 Valvetrain Materials

9 CONCLUSION

This report has discussed wet sump and dry sump lubrication systems in general discussing their benefits for the V-Twin engine. Background theory on pump types showed many different pumps are available for oil systems. The V-Twin oil pumps were selected based on pulsed flow effects, power required to drive the pumps, and maintaining constant flow rate with oil viscosity constantly changing.

Background theory of lubricants and bearings was discussed. Lubricant theory suggested synthetic oils (opposed to mineral oils) were best for the V-Twin as the molecular structure of the Hydrogen and Carbon atoms could be specifically tailored to increase lubricant performance. A multitude of additives was available to add or subtract oil properties to further increase the lubricant performance. Additives such as detergents, extreme pressure additives, corrosion inhibitors, and viscosity modifiers were discussed identifying their importance to successful engine lubrication. Journal bearing materials were soft materials while the journal was a hard material. This was important so that the bearing would conform to the journal, reduce friction because of metallurgical compatibility, reduce chances of welding or seizing, and provide embed-ability if foreign particles were to enter the oil film. The V-Twin crankshaft journal was selected to be hardened steel. The main bearings were selected to be a bronze alloy with a steel backing.

V-Twin oil system components were covered along with the determination of oil system pressure and flow requirements. Pressure requirements were determined from the crankshaft centrifugal head. Oil gallery sizes which dictated the flow rates were determined by using an area balance approach. This theory suggested the oil bearing leaks and feeds were the restrictions in the system and not the gallery itself.

Crankshaft balancing was performed in an un-traditional way to determine main bearing loads. Traditionally 50% of the reciprocating mass is added to the balanced rotating mass. At high speeds this method overloaded the V-Twin main bearings. Instead, 3% of the reciprocating mass was subtracted from the rotating mass to give a more uniform bearing load. A mathematical model for journal bearings was created.

This model helped to determine power losses, surface finishes needed to eliminate asperity contact, what type of oil is needed (SAE 30), the redline of the engine, safety factor at redline, and other bearing geometry parameters.

Computational fluid dynamics was used to verify system pressure drops and flow rates. The model was the exact oil system extracted from the main 3D engine model. The model was good for identifying trends but needed more development. Downstream resistances mimicking bearings would need to be modeled to create a more realistic system.

Much work still needs to be done, however, the upside looks positive with the group of motivated student engineers currently developing the V-Twin Engine. Oil system is ready for a trial fit into the engine. Inspection of components would need to be performed after the first initial break-in of the motor. The inspection will validate the theoretical work carried out in this dissertation on the *Formula Student V-Twin Race Engine Lubrication System*.

REFERENCES

1. Balzers Oerlikon Coating Ltd. Internet Site. <http://www.oerlikon.com/balzers/uk/>
Accessed: August 2007.
2. Basshuysen, Richard. Schafer, Fred. *Internal Combustion Engine Handbook*. SAE International ©2004.
3. Booser, E Richard. Khonsari M Michael. *Applied Tribology-Bearing Design and Lubrication*. John Wiley & Sons Inc. ©2001.
4. Barwell, F.T. *Bearing Systems-Principles and Practice*. Oxford University Press. ©1979
5. Controlled Thermal Processing Inc. Internet Site. <http://www.metal-wear.com/>
Accessed: August 2007.
6. ENCYCLOPEDIA BRITANNICA. <http://www.britannica.com/eb/article-47234/gasoline-engine> Accessed: June 2007.
7. Ferguson R. Colin, Kirkpatrick T. Allan. *Internal Combustion Engines*. 2nd ed. John Wiley & Sons, Inc. © 2001.
8. FLUENT. www.fluent.com Accessed: June 2007
9. Goddard, Geoff. Geoff Goddard Engines Ltd. Lecturer at Oxford Brookes University. 2007.
10. Hillier, V.A.W. *Fundamentals of Motor Vehicle Technology*. Stanley Thornes Ltd. Cheltenham. © 1991.
11. Hoag, L. Kevin. *Vehicular Engine Design*. Springer-Verlag, Wien. ©2006
12. Keronite International Ltd. Internet Site. <http://www.keronite.com/> Accessed August 2007.
13. Lansdown, A R. *Lubrication-A Practical Guide to Lubricant Selection*. Pergamon Press Ltd. ©1982.
14. MOROSO. Internet Site.
<http://www.moroso.com/articles/articledisplay3.asp?article=AboutOilPans.html>
Accessed: June 2007.
15. Norton, L. Robert. *Machine Design an Integrated Approach*. 2nd ed. Pearson Education, Inc. © 2000.

16. Pulkrabek, W. Willard. *Engineering Fundamentals of the Internal Combustion Engine*. 2nd Ed. Pearson Prentice-Hall ©2004.
17. Stokes, Alec. *High Performance Gear Design*. Machinery Publishing Co., Ltd. © 1970
18. Stone, Richard. *Introduction to Internal Combustion Engines*. 3rd Ed. Society of Automotive Engineers, Inc. ©1999.
19. Taylor, R.I. “Lubrication, Tribology & Motorsport”. SAE Paper: 2002-01-3355. © 2002.
20. BMW World. Internet Site. <http://www.bmwworld.com/engines/nikasil.htm>
Accessed August 15, 2007
21. White, Frank. *Fluid Mechanics*. 5th ed. McGraw-Hill © 2003

APPENDIX 1 Kinsler Fuel Injection, Inc. Oil Filters

FILTERS



#4156 with #6044 fittings
and #4103 mounting clamp



#4105 stainless steel
element

*Excellent Pump Inlet and/or Outlet Filter
Great for Blown Gas & Alky on Pump Outlet*



MECHANICAL PUMP OUTLET - METHANOL AND NITRO:

- 4156 Filter assembly. For alky, gas, and nitro, stainless steel element. Housing and end caps - hard-anodized, model: Ano-BRL.
- 4105 Element, stainless steel, 22 square inches, 140-micron.
- 4103 Mounting clamp for #4148 and #4156 filter. Stainless steel band with rubber cushion liner and ear to mount.

THE INJECTOR PROTECTOR™ FOR EFI AND LUCAS:

- 8170 Filter assembly, complete, Gasoline ONLY, with #9031 10-micron 35 sq. inch paper element. Housing and end caps - black anodized, model: BRL-paper.
- 4157 Filter assembly, complete, Alcohol, with #9031 10-micron 35 sq. inch paper element. Housing and end caps - hard-anodized, model: Ano-BRL-paper.

NOTE - METHANOL AFFECTS THE ELEMENT, IT MUST BE REPLACED FREQUENTLY.

- 9023 Element, paper, 10-micron, 22 sq. inches. Installed in early filter housing #9020. Can be installed in filters #8170 and #4157.
- 9031 Element, paper, 10-micron, 35 sq. inches 60% more surface area than #9023.



Adapter
Fittings,
Page 87-M

FOR EFI:

Disposable filter, stainless steel, laser welded, 66 sq. in. pleated 10-micron paper.

- 8194 Filter, 3/8" male barbs
- 8197 Filter, 16mm x 1.5 female + o-ring ports
- 6185 Fitting, 6AN male flare
- 6186 Fitting, 8AN male flare

© 2002

All paper element filters are really just porous paper, which is made by laying down a layer of wood fibers mixed with glue. While these filters have a nominal micron rating, they always let through some larger particles...it only takes a couple of these to wipe out the rod or main bearings in your engine.

The only way to obtain absolute control over the filter openings is to go to precisely woven screen. We use a very premium screen in our filters. These can be ultrasonically cleaned for reuse.

Monster Mesh Pump Protector™

Our all new filter is called the MONSTER MESH™ because it has a monstrous amount of screen compared to any other race filter with a similar body length. Light weight billet aluminum housing with o-ring sealed threaded end caps. Anodized blue for gasoline, hard anodized olive-black and sealed for alcohol and nitro. The element has 36 deep pleats of stainless steel screen, with stainless end caps.

Available in four micron ratings: 25, 45, 70, 100 (2.54 microns = .001").

Use 25 for inlet filter for Bosch, Walbro, Airtex pumps.

Use 45 for inlet of all Weldon and Aeromotive pumps.

Use 70 on outlet of mechanical pump for blown gas; 100 on outlet for blown alky.

Available in three housing lengths, all 2.46" outside diameter.

Specify the micron rating you want, and either blue or hard anodized body.

MONSTER MESH™ 73 square inches of pleated screen!

- 8308 Assy, 8AN female ports without fittings 4.77" overall
With 6AN fittings 6.30" overall With 8AN 6.70" overall
- 8310 Assy, 10AN male flare ends 6.89" overall
- 8312 Assy, 12AN male flare ends 7.25" overall

ELEMENTS:

- 8325 25-micron, 8345 45-mic, 8370 70-mic, 83100 100-mic
- 8320 10-micron pleated paper; EFI, carbs, Lucas

MEGA MONSTER MESH™ 110 square inches of pleated screen!!

- 8408 Assy, 8AN female ports without fittings 5.98" overall
With 6AN fittings 7.71" overall With 8AN 7.91" overall
- 8410 Assy, 10AN male flare ends 8.10" overall
- 8412 Assy, 12AN male flare ends 8.46" overall

ELEMENTS:

- 8425 25-micron, 8445 45-mic, 8470 70-mic, 84100 100-mic
- 8420 10-micron pleated paper; EFI, carbs, Lucas

ULTRA MONSTER MESH™ 146 square inches of pleated screen!!!

- 8508 Assy, 8AN female ports without fittings 7.19" overall
With 6AN fittings 8.92" overall With 8AN 9.12" overall
- 8510 Assy, 10AN male flare ends 9.31" overall
- 8512 Assy, 12AN male flare ends 9.67" overall

ELEMENTS:

- 8525 25-micron, 8545 45-mic, 8570 70-mic, 85100 100-mic
- 8520 10-micron pleated paper; EFI, carbs, Lucas

ULTIMATE OIL FILTER -- MONSTER MESH™

In 1996 we were contracted by General Motors to develop an oil filter for their new Indy engine. It had to be fine enough to protect the bearings but coarse enough to flow the oil. 25 micron turned out to be just right, on the pressure side of the pump. Our 8325 element has been on every Indianapolis 500 winning car for the last seven years. For 2003 there will be more room available, so we will go to the 8525 element to get three times the dirt holding capacity.

Use the ULTRA MONSTER MESH™ 25 micron when there is room. Only use our smaller filters if there is no room for the "ULTRA". The "ULTRA" must be cleaned every 1,500 miles, the "MEGA" at 1,000 mi, the "MONSTER" at 500 mi, so you must have spare elements. These mileages are conservative; they cover an engine making a lot of dirt.

Kinsler Fuel Injection, Inc. 1834 THUNDERBIRD TROY, MICHIGAN 48064 U.S.A. Phone (248) 362-1145 Fax (248) 362-1032

49-M

APPENDIX 2 Oil & Scavenge Pump Calculations

Pump Requirements:

Oil Pump

- Needs to supply a minimum of $P = 4\text{bar}$ pressure through a $d := 12\text{mm}$ diameter main oil gallery size which was determined from crankshaft centrifugal head (section 2.4 Pressure Requirements) and flow requirements (section 2.5.1 Main Gallery).
- Flow rate needs to be in a minimum range of 7 to 10 liters/min.

Scavenge Pump

- A high volume low pressure pump with a capacity of 3 to 5 times the oil pressure pump capacity for gasoline fuelled systems and 7 to 10 times for alcohol fuelled systems [Goddard]. The pressure required only needs to be 1bar.

Oil Properties

- Shell Helix Ultra recommended by Ferrari F1. Oil performance data supplied by Mike Evans of Shell Global Solutions (UK). The strategy recommended by Shell is to design for 0W-40 oil and if problems are encountered in the future, 5W-40 will hopefully cure the issue.

Shell Helix Diesel Ultra	0W-40	5W-30	5W-40
SAE Viscosity Grade	0W-40	5W-30	5W-40
Kinematic viscosity (IP 71) @ 40°C cSt @ 100°C cSt	75.2 13.6	68.2 12.2	74.4 13.1
Density @ 15°C (IP 365) kg/l	0.84	0.84	0.84
Flash Point (IP 34) °C	215	215	215
Pour Point (IP 15) °C	-42	-39	-39
HTHS Viscosity @ 150°C PaS	3.68	3.50	3.68

Table 15 Shell Helix Ultra Oil Properties

The first equations are based on the Merritt formulae for spur gear pumps and will determine flow rate, maximum pitch line velocity of gears, power loss in the gears, and horsepower required to drive the pump. The second set of equations is from Tuplin which are used to calculate backlash and capacity in gear pump rotors. The third set of equations are empirical relationships derived by Stokes for determining pump discharge capacity.

Note: All units are in inch-lb-sec as Stokes developed the empirical relationships for inch-lb-sec units.

Nomenclature

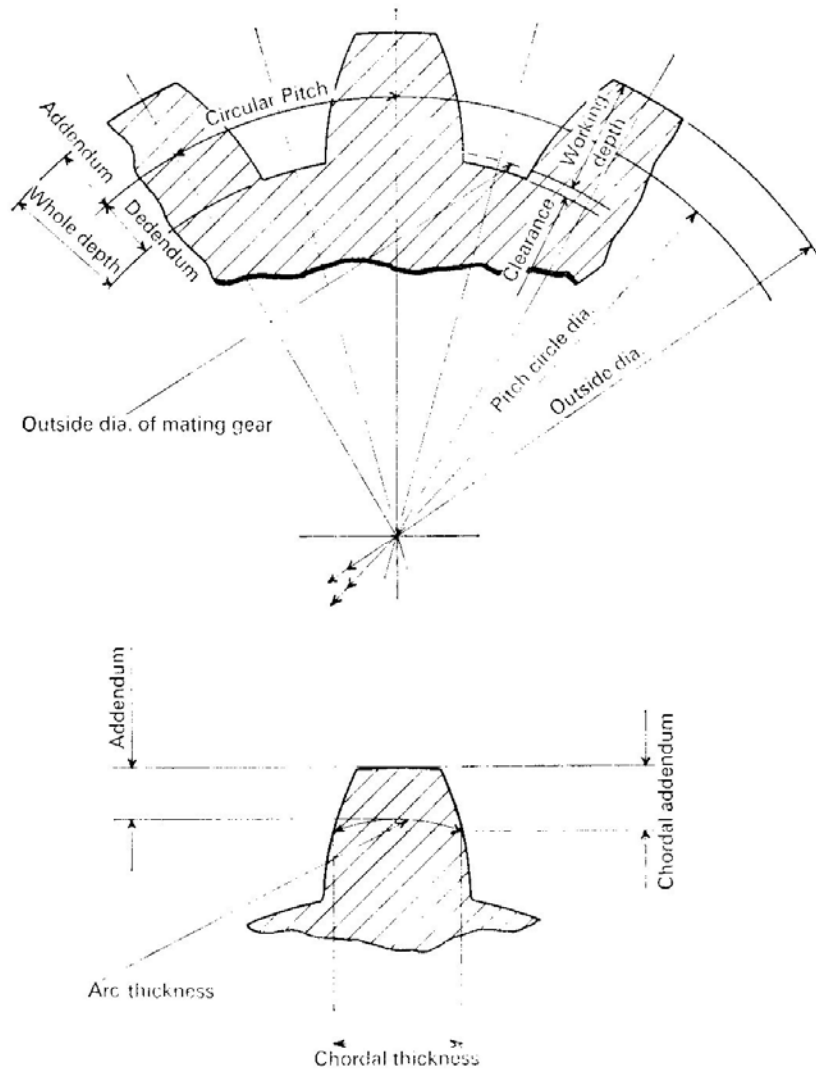
P	Minimum pump pressure required
d	Main oil gallery diameter
N _{eng}	Engine speed
N _p	Pump speed
Q _{nom}	Nominal discharge
Q _{slip}	Loss in nominal discharge
P	Pressure(lb/in ²) difference between suction and discharge
R	viscosity in seconds Redwood 1
Q _{actual}	Actual discharge
P _c	Power loss in pump gears
bhp	Horsepower required to drive pump

Gear tooth Nomenclature

Given: Diametral pitch and number of teeth

DP	Diametral pitch or number of teeth per inch (25.4mm). 6 teeth per inch is per AGMA Standard. Diametral pitch can also be described as normal pitch of rack.
$T := 6$	Number of teeth
P _n	Normal pitch of rack
CP	Circular Pitch
PCD	Pitch circle diameter or mean diameter
D _o	Base circle diameter
W _r	Whole depth
a	Addendum. The tooth height referenced from the pitch circle.
b	Dedendum.
φ	Pressure angle
OD	Root diameter or outside diameter. It is d _p + 2addenda
L	Face width or width of the gear tooth
C	Gear centers distance.
V _{max}	Maximum pitch circle velocity for pump gears
V _{act}	Actual pitch circle velocity for pump gears

A_t	Arc thickness
C_{hs}	Caliper height setting
B	Backlash



Pump Capacity Nomenclature

$Rotor_{cap}$	Capacity per rev for a pair of rotors
$Pump_{cap}$	Pump capacity
V_s	Total swept volume of idler gear
$Scavenge_{pump.cap}(N_p)$	Scavenge pump capacity (flow rate)
$Oil_{pump.cap}(N_p)$	Oil pump capacity (flow rate)

Standard Spur Gear Definitions (from chapter 2 Spur Gears [Stokes])

$$DP := 6 \cdot \frac{1}{\text{in}} \quad p_n := \frac{1}{DP} \quad p_n = 0.167 \text{ in} \quad \phi := 20 \text{ deg}$$

$$CP := \frac{\pi}{DP} \quad CP = 0.524 \text{ in}$$

$$PCD := \frac{T}{DP} \quad PCD = 1 \text{ in}$$

$$D_o := PCD \cdot \cos(\phi) \quad D_o = 0.94 \text{ in}$$

$$W_{r.basic} := \frac{2.157}{DP} \quad W_{r.basic} = 0.36 \text{ in}$$

$$W_{r.british.std} := \frac{2.35}{DP} \quad W_{r.british.std} = 0.392 \text{ in}$$

$$a := \frac{1}{DP} \quad a = 0.167 \text{ in} \quad \text{Addendum and dedendum values valid for 20 or 25 degree pressure angles as defined by the AGMA Full-Depth Gear Tooth Specifications.}$$

$$b := \frac{1.25}{DP} \quad b = 0.208 \text{ in}$$

The center distance is the pitch radii of both gears. Both gears are the same size therefore the center distance is equal to the pitch circle diameter.

$$C := PCD$$

$$OD := PCD + 2 \cdot a \quad OD = 1.333 \text{ in}$$

1. Merritt Formulae for Gear Pumps (Nominal, Slip, and Actual Flow Rates)

$$\text{rpm} := \frac{1}{\text{min}} \quad N_{\text{eng}} := 14000 \text{ rpm} \quad N_p := 0.4 \cdot N_{\text{eng}} \quad N_p = 5600 \text{ rpm} \quad L := .197 \text{ in} \quad a = 0.167 \text{ in}$$

$$C = 1 \text{ in} \quad P = 58.015 \text{ psi} \quad R := 24.75 \quad (\text{Viscosity in seconds Redwood 1 @100C})$$

This below formulas are based on empirical relationships therefore numbers must be entered without their units since Mathcad will convert them and give spurious answers.

$$Q_{\text{nom}} := C \cdot a \cdot L \cdot N_p^2 \quad Q_{\text{nom}} := \frac{1 \cdot 0.167 \cdot 0.197 \cdot 5600}{44} \cdot 1 \cdot \frac{\text{gal}}{\text{min}} \quad Q_{\text{nom}} = 4.187 \frac{\text{gal}}{\text{min}}$$

$$Q_{\text{slip}} := \frac{C + L}{2} \cdot \left(\frac{P}{100 + R} \right)^{\frac{2}{3}} \quad Q_{\text{slip}} := \frac{1 + 0.197}{2} \cdot \left(\frac{43.511}{100 + 24.75} \right)^{\frac{2}{3}} \cdot 1 \cdot \frac{\text{gal}}{\text{min}} \quad Q_{\text{slip}} = 0.297 \frac{\text{gal}}{\text{min}}$$

$$Q_{\text{act}} := Q_{\text{nom}} - Q_{\text{slip}} \quad Q_{\text{act}} = 14.727 \frac{\text{liter}}{\text{min}}$$

Maximum and actual pitch line velocity in gears

$$V_{\text{max}} := \frac{40000}{(R + 100)^{\frac{2}{3}}} \quad V_{\text{max}} = 1602.137 \quad (\text{ft/min})$$

$$\omega := N_p \cdot 2\pi \quad \omega = 586.431 \frac{1}{s} \quad r := \frac{\text{PCD}}{2}$$

$$V_{\text{act}} := r \cdot \omega \quad V_{\text{act}} = 1466.077 \frac{\text{ft}}{\text{min}}$$

The actual velocity is below the max permitted velocity. This verifies good pump design. This is the reason why pump speed needed to be reduced to 0.4 times the engine speed.

Power loss in the gears

$$P_c := \frac{R + 100}{100000} \cdot V_{\max}^{\frac{3}{2}} \quad + \quad P_c = 80$$

Horsepower required to drive pump

$$bhp := \frac{Q_{\text{nom}} \cdot (P + P_c)}{1430} \quad bhp = \frac{4.187 \cdot (58.015 + 80)}{1430} \cdot 1 \text{ hp} \quad bhp = 0.404 \text{ hp}$$

$$bhp_{\text{scavenge}} := \frac{8 \cdot 4.187 \cdot (15 + 80)}{1430} \cdot 1 \text{ hp} \quad bhp_{\text{scavenge}} = 2.225 \text{ hp}$$

2. Tuplin Formulae for Gear Pumps

The Tuplin formulae for gear pump rotor capacity and backlash:

$$C_1 := \frac{p_n}{\pi} \cdot (T + 1) \quad C_1 = 0.371 \text{ in}$$

$$A_t := 1.708 \cdot \frac{p_n}{\pi} \quad A_t = 0.091 \text{ in}$$

$$C_{hs} := 1.189 \cdot \frac{p_n}{\pi} \quad C_{hs} = 0.063 \text{ in}$$

Rotor capacity (gal/rev) and backlash (inch)

$$B := \frac{C_1}{6.2 \cdot T^2 \cdot \left(0.125 + \frac{1}{T}\right) \left(0.5 - \frac{1}{T}\right)} \quad B = 0.017 \text{ in}$$

$$\text{Rotor}_{\text{cap}} := \frac{C_1^2 \cdot L}{600}$$

$$\text{Rotor}_{\text{cap}} := \frac{0.371^2 \cdot 0.197}{600} \quad \text{Rotor}_{\text{cap}} = 4.519 \times 10^{-5}$$

The estimation is based on 85% volumetric efficiency at low speed against moderate pressure.

3. Stokes Formulae for Gear Pump Capacity: Oil & Scavenge Pump

Pump capacity (gal/min)

$$\rho_{15C} := 0.84 \frac{\text{kg}}{\text{liter}}$$

$$g = 32.174 \frac{\text{ft}}{\text{s}^2}$$

$$A_s := \frac{\pi d^2}{4}$$

$$ID := OD - 2 \cdot (a + b)$$

$$ID = 0.583 \text{ in}$$

$$V_s := 0.7854 (OD^2 - ID^2)$$

$$V_s = 1.129 \text{ in}^2$$

$$\text{Pump}_{\text{cap}} := \frac{V_s \cdot L \cdot N_p}{277.42}$$

$$\text{Pump}_{\text{cap}} := \frac{1.129 \cdot 0.197 \cdot 5600}{277.42} \cdot 1 \frac{\text{gal}}{\text{min}}$$

$$\text{Pump}_{\text{cap}} = 16.995 \frac{\text{liter}}{\text{min}}$$

$$\text{Pump}_{\text{cap}} = 4.49 \frac{\text{gal}}{\text{min}}$$

$$N_{\text{eng}} := 1000, 2000 \dots 14000$$

$$N_p := 0.4 \cdot 1000, 0.4 \cdot 2000 \dots 0.4 \cdot 14000$$

$$\text{Oil}_{\text{pump.cap}}(N_p) := \frac{1.129 \cdot 0.197 \cdot N_p}{277.42} \cdot 1 \frac{\text{gal}}{\text{min}}$$

$$\text{Scavenge}_{\text{pump.cap.gas}}(N_p) := \frac{1.129 \cdot 0.7878 \cdot N_p}{277.42} \cdot 1 \frac{\text{gal}}{\text{min}}$$

A face width of 0.7878 is based on a scavenge pump capacity of 4 times the oil pump capacity. Calculation not shown.

$$\text{Scavenge}_{\text{pump.cap.E85}}(N_p) := \frac{1.129 \cdot 1.576 \cdot N_p}{277.42} \cdot 1 \frac{\text{gal}}{\text{min}}$$

A face width of 1.576 is based on a scavenge pump capacity of 8 times the oil pump capacity. Calculation not shown.

$N_{eng} =$	$N_p =$	Oil _{pump.cap} (N_p) $\frac{\text{liter}}{\text{min}}$	Scavenge _{pump.cap.gas} (N_p) $\frac{\text{liter}}{\text{min}}$	Scavenge _{pump.cap.E85} (N_p) $\frac{\text{liter}}{\text{min}}$
1000	400	1.214	4.855	9.711
2000	800	2.428	9.709	19.423
3000	1200	3.642	14.564	29.134
4000	1600	4.856	19.418	38.846
5000	2000	6.07	24.273	48.557
6000	2400	7.284	29.127	58.269
7000	2800	8.498	33.982	67.98
8000	3200	9.711	38.836	77.692
9000	3600	10.925	43.691	87.403
10000	4000	12.139	48.545	97.115
11000	4400	13.353	53.4	106.826
12000	4800	14.567	58.254	116.538
13000	5200	15.781	63.109	126.249
14000	5600	16.995	67.963	135.961

APPENDIX 3 Mathematical Bearing Model Calculations

Declare units for Mathcad: $\text{rev} := 2 \cdot \pi \cdot \text{rad}$ $\text{rpm} := \text{rev} \cdot \text{min}^{-1}$ $\mu\text{reyn} := 10^{-6} \cdot \text{lb} \cdot \text{sec} \cdot \text{in}^{-2}$

Notes: Mathcad converts units automatically, therefore care must be taken to avoid formulae containing unit conversions.

Journal Bearing Design (performed in MathCad)

Objective: Design main bearings of crankshaft and establish; bearing eccentricity ratio, maximum pressure and its location, minimum film thickness, coefficient of friction, torque, power lost in bearing, lubricant required to operate at 190F, flow rate, and temperature rise in bearing.

Known: The bearing loads were computed from the crankshaft balance section. Therefore, $F_{\text{bearing}} := 22500\text{N}$. Note, this force has been previously divided by 2 because of two main bearings.
Crankshaft journal diameter or inner bearing diameter is $d := 49.2\text{mm}$
Bearing axial length is 20mm.
Crankshaft speed is $n := 12000\text{rpm}$

Assumptions: Use a clearance ratio of $\text{CR} := 0.0017$ and an l/d ratio of 0.406.

1. Finding tangential velocity U from rpm.

$$n = 200 \frac{\text{rev}}{\text{sec}}$$

$$U := \frac{d}{2} \cdot n \quad U = 1.21706 \times 10^3 \frac{\text{in}}{\text{sec}} \quad (a)$$

2. The diametral and radial clearances are found from the given diameter and the assumed clearance ratio:

$$\begin{aligned} c_d &:= \text{CR} \cdot d & c_d &= 0.0033\text{in} & c_d &= 83.64\mu\text{m} \\ c_r &:= 0.5 \cdot c_d & c_r &= 0.00165\text{in} & c_r &= 41.82\mu\text{m} \end{aligned} \quad (b)$$

Diametral clearance is extremely important. If the clearance is too big then the following factors could happen; reduced load carrying capacity, oil whirl (a vibration that occurs in high speed journal bearings), cavitation erosion, etc... On the other hand, a too little clearance leads to oil flow restriction; this increases the temperature which changes the viscosity which reduces the film thickness. Hirani et al noted two authors "Stolarksi" and "Constantinescu" which developed empirical relationships for suggested minimum diametral clearance. Stolarski's equation suggested to keep the bearing from overheating use $C_d = 0.00075D$ and Constantinescu suggested $C_d = 1.4 \times N \times (1000D)^{1.5} \times 10^{-8}$ mm as a function of diameter and speed. Note that in both equations (D) is in meter and (N) in rpm.

$$c_{d.stolarski} := 0.00075 \cdot 0.042 \text{ m} \quad c_{d.stolarski} = 31.5 \mu\text{m}$$

$$c_{d.constantinescu} := \left(1.4 \cdot 125000 \cdot 0.042^{1.5} \cdot 10^{-8} \text{ m} \right) \quad c_{d.constantinescu} = 1.5063 \mu\text{m}$$

3. The bearing length is given from $L_{overd} := 0.40 \epsilon$

$$\begin{aligned} L &:= L_{overd} \cdot d & L &= 0.78643 \text{ in} & (c) \\ & & L &= 19.9752 \text{ mm} \end{aligned}$$

4. Find the experimental eccentricity ratio from equation (d) or from Figure 1 below using the suggested value of $O_N := 90$.

$$\varepsilon_x(O_N) := 0.21394 + 0.38517 \log(O_N) - 0.0008(O_N - 60) \quad (d)$$

$$\varepsilon_x(90) = 0.94266$$

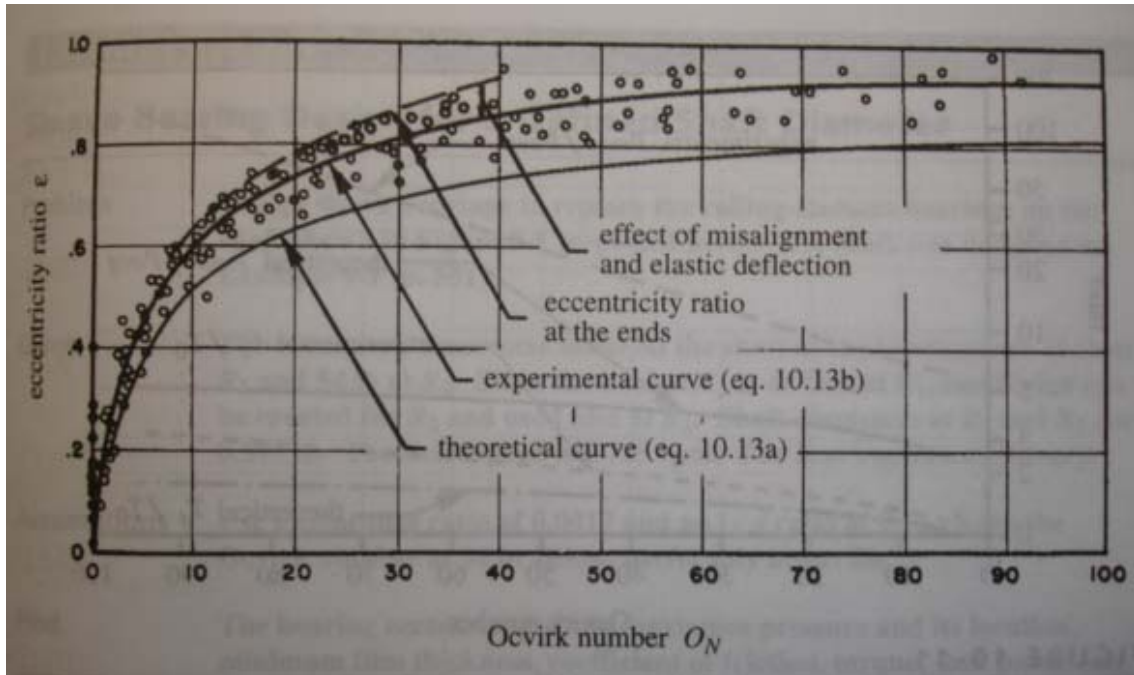


Figure 1[Norton 2000]

5. Dimensionless parameter K_ε that is a function of the eccentricity ratio ε .

$$K_\varepsilon(O_N) := \frac{O_N}{4\pi} \quad K_\varepsilon(90) = 7.16197 \quad (e)$$

6. The viscosity η of lubricant required to support the design load

F_{bearing} .

$$\eta(O_N) := \frac{F_{\text{bearing}} \cdot c_r^2}{K_\varepsilon(O_N) \cdot U \cdot L^3} \quad \eta(90) = 3.2343 \mu\text{reyn} \quad (f)$$

$$\eta(90) = 0.0223 \frac{\text{kg}}{\text{m}\cdot\text{s}}$$

Use this viscosity value to determine the oil needed for a desired temperature. Refer to figure 2 below.

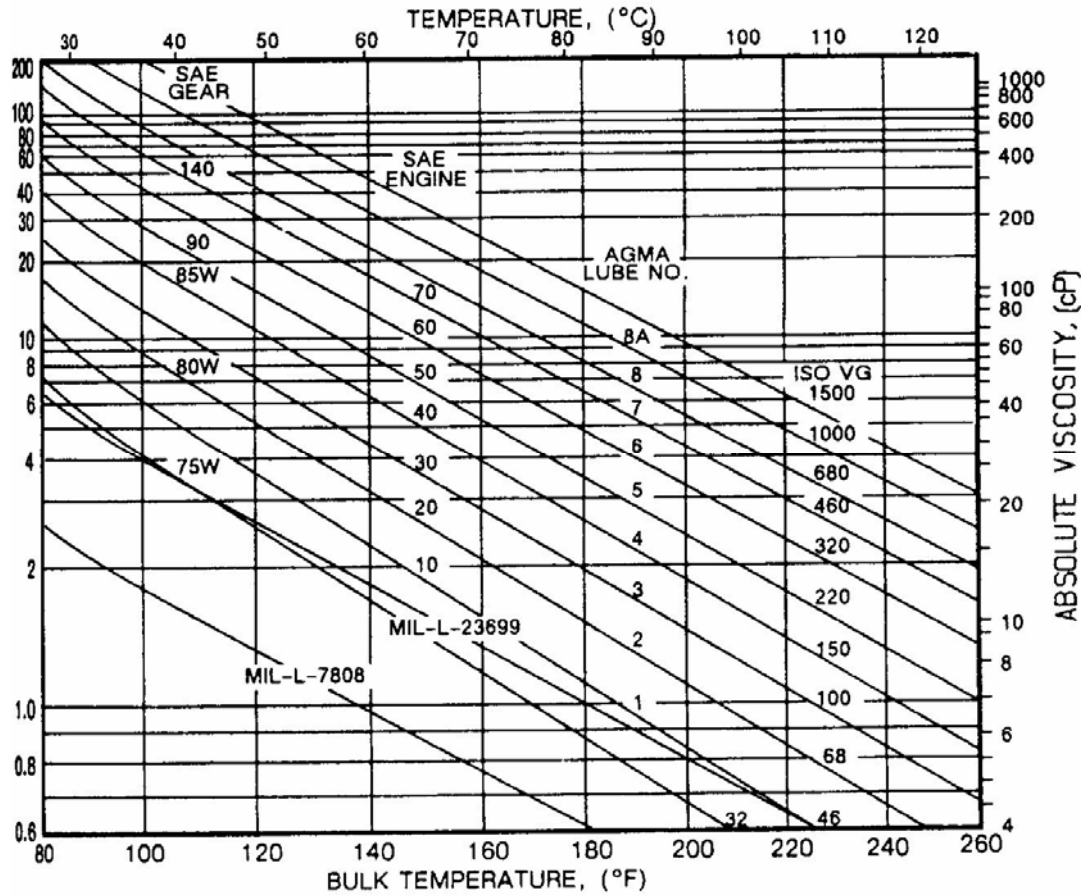


Figure 2 [Norton 2000]

7. The average pressure in the oil film is:

$$p_{avg} := \frac{F_{bearing}}{L \cdot d} \quad p_{avg} = 3320.53 \text{ psi} \quad (g)$$

8. Angle θ_{max} at which max pressure occurs is found using the experimental value of $\epsilon_x = \text{function}$,

$$\theta_{max}(O_N) := \arccos \left(\frac{1 - \sqrt{1 + 24 \epsilon_x(O_N)^2}}{4 \epsilon_x(O_N)} \right) \quad (h)$$

$$\theta_{max}(90) = 171.1 \text{ deg}$$

Angle θ_{max} can also be found from figure 3 below for $O_N = 90$ using the experimental curve.

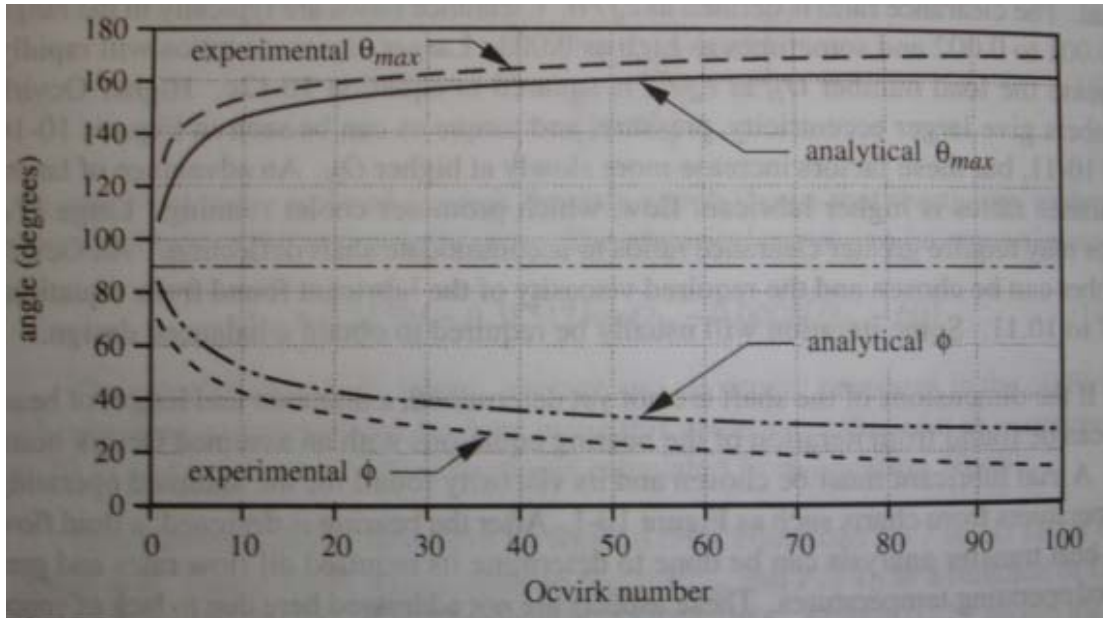


Figure 3 [Norton 2000]

9. Maximum pressure is found by substituting θ_{max} into equation (i) known as the Ocvirk solution or the short-bearing solution. $z := 0$ in since it is maximum at the center of the bearing length l .

$$p_{max}(O_N) := \frac{\eta(O_N) \cdot U}{0.5 \cdot d \cdot c_r^2} \cdot \left(\frac{L^2}{4} - z^2 \right) \cdot \frac{3 \cdot \varepsilon_x(O_N) \cdot \sin(\theta_{max}(O_N))}{(1 + \varepsilon_x(O_N) \cdot \cos(\theta_{max}(O_N)))^3} \quad (i)$$

$$p_{max}(90) = 3 \times 10^5 \text{ psi}$$

The max pressure can also be found and checked by reading the ratio of p_{max}/p_{avg} from the experimental curve in Figure 4 below. For $O_N = 20$, $p_{max}/p_{avg} = 9.1$. This can be multiplied by p_{avg} from step 7 above to get the same result.

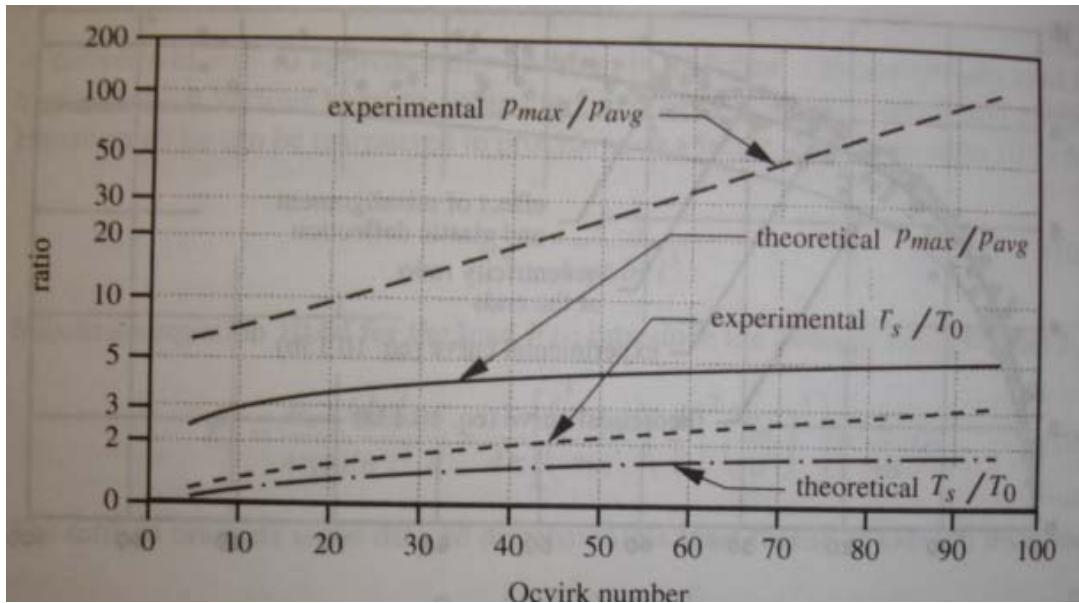


Figure 4 [Norton 2000]

10. Find the angle ϕ , which locates the $\theta = 0$ to π axis with respect to the applied load F_{conrod} from equation (j)

$$\phi(O_N) := \text{atan} \left(\frac{\pi \cdot \sqrt{1 - \epsilon_x(O_N)^2}}{4 \cdot \epsilon_x(O_N)} \right) \quad \phi(90) = 15.54 \text{deg} \quad (j)$$

11. The stationary and rotating torques can now be found from equations (k) (substituting 0 for U_1) and (l) using the angle ϕ .

$$T_s(O_N) := \eta(O_N) \cdot \frac{d^2 \cdot L \cdot U}{c_d} \cdot \frac{\pi}{\sqrt{1 - \epsilon_x(O_N)^2}} \quad (k)$$

$$T_s(90) = 2.7667 \text{ lbf} \cdot \text{ft}$$

$$T_s(90) = 3.7511 \text{ N} \cdot \text{m}$$

$$T_r(O_N) := T_s(O_N) + F_{\text{bearing}} \cdot c_r \cdot \varepsilon_x(O_N) \cdot \sin(\phi(O_N)) \quad (l)$$

$$T_r(90) = 2.9419 \text{ lbf} \cdot \text{ft}$$

$$T_r(90) = 3.98874 \text{ N} \cdot \text{m}$$

12. Finding power loss in the bearing.

$$\Phi(O_N) := T_r(O_N) \cdot n \quad \Phi(90) = 6.7217 \text{ hp} \quad (m)$$

$$\Phi(90) = 5012.3981 \text{ watt}$$

12.1 Finding flow rate

$$n = 1.25664 \times 10^3 \frac{1}{s} \quad \omega := n \cdot 2\pi \quad R := \frac{d}{2}$$

$$Q := \omega \cdot R \cdot L \cdot c_r \cdot \varepsilon_x(90)$$

The Short Bearing Approximation for the lubricant flow rate required to avoid lubricant starvation.

$$Q = 9.17708 \frac{\text{liter}}{\text{min}}$$

$$Q = 2.42433 \frac{\text{gal}}{\text{min}}$$

$$Q = 9.33366 \frac{\text{in}^3}{s}$$

12.2 Alternative equation for power loss in bearing

NOTE: For this equation, values must be input manually because formula is an empirical relationship with unit conversion factors.

$$P_{\text{bearing}} := P_{\text{max}}(90) \quad P_{\text{bearing}} = 3.12882 \times 10^5 \text{ psi} \quad Q = 2.42433 \frac{\text{gal}}{\text{min}} \quad \eta_{\text{pump}} := 0.5$$

$$\text{bhp} := 0.000007 P_{\text{bearing}} \cdot Q \cdot 2 \cdot \eta_{\text{pump}}^2$$

$$\text{bhp}_m := 0.0000073 \cdot 1.2882 \cdot 10^5 \cdot 2.42433 \cdot 0.5 \cdot 1 \text{ hp} \quad \text{bhp}_m = 5.3097 \text{ hp}$$

13. Finding coefficient of friction in the bearing from the ratio of the shear force to the normal force.

$$\mu(O_N) := \frac{2 \cdot T_r(O_N)}{F_{\text{bearing}} \cdot d} \quad \mu(90) = 0.0072 \quad (n)$$

14. Finding minimum oil film thickness. The film thickness h is maximum at $\theta=0$ and minimum at $\theta=\pi$.

$$\mu_{\text{in}} := 10^{-6} \cdot \text{in} \quad h_{\text{min}}(O_N) := c_r \cdot (1 - \varepsilon_x(O_N)) \quad h_{\text{min}}(90) = 94 \mu\text{in} \quad (o)$$

$$h_{\text{min}}(90) = 2.40 \mu\text{m}$$

$$h_{\text{max}}(O_N) := c_r \cdot (1 + \varepsilon_x(O_N)) \quad h_{\text{max}}(90) = 81.24186 \mu\text{m}$$

15. Specific film thickness, Λ . Where h_c is the film thickness of the lubricant at the center of the contact patch and R_{a1} and R_{a2} are the rms average roughnesses of the two contacting surfaces.

$$R_{a1} := 0.0408 \mu\text{m}$$

Average surface roughness of crankpin or journal. Values taken from Evans&Price Ltd. supplied by Geoff Goddard.

$$R_{a2} := 0.3 \mu\text{m}$$

Average surface roughness of bearing

$$h_c := \frac{4}{3} \cdot h_{\text{min}}(90)$$

$$\Lambda := \frac{h_c}{\sqrt{R_{a1}^2 + R_{a2}^2}}$$

$$\Lambda = 10.56119$$

$$h_c = 3.19752 \mu\text{m}$$

This is the minimum surface rms value needed to eliminate asperity contact.

16. Varying the Ocvirk number. Let O_N vary over the range

$O_N := 10, 15 \dots 95$, then we have

$O_N =$	$\varepsilon_x(O_N) =$	$\frac{\eta(O_N)}{\mu\text{reyn}} =$	$\frac{p_{\max}(O_N)}{\text{psi}} =$	$\frac{\Phi(O_N)}{\text{hp}} =$	$\frac{h_{\min}(O_N)}{\mu\text{m}} =$	$T_r(O_N) =$	N·m
10	0.639	29.109	22760	25.3848	15.09	15.1	
15	0.703	19.406	26068	18.4916	12.42	11.0	
20	0.747	14.554	30253	14.9608	10.58	8.9	
25	0.78	11.643	35315	12.8059	9.18	7.6	
30	0.807	9.703	41356	11.3528	8.08	6.7	
35	0.829	8.317	48534	10.3083	7.17	6.1	
40	0.847	7.277	57052	9.5239	6.40	5.7	
45	0.863	6.469	67166	8.9162	5.74	5.3	
50	0.876	5.822	79188	8.4346	5.17	5.0	
55	0.888	5.292	93499	8.0466	4.67	4.8	
60	0.899	4.851	110565	7.7303	4.23	4.6	
65	0.908	4.478	130952	7.4706	3.84	4.4	
70	0.917	4.158	155352	7.2565	3.49	4.3	
75	0.924	3.881	184604	7.0800	3.17	4.2	
80	0.931	3.639	219735	6.9350	2.89	4.1	
85	0.937	3.425	261990	6.8168	2.63	4.0	
90	0.943	3.234	312882	6.7217	2.40	4.0	
95	0.948	3.064	374240	6.6469	2.19	3.9	

17. Determining safety factor against asperity contact. By using the above worst case conditions the load factor can be worked out and then compared to the current F_{bearing} load.

From the table above for $h_{\min} := 2.4 \mu\text{m}$ $O_N := 90$ $\varepsilon_x(90) = 0.94266$

and at $O_N := 95$ $\eta := 3.064 \mu\text{reyn}$

therefore from equation (f)

$$F_{\text{bearing},95} := \frac{\eta \cdot K_e(95) \cdot U \cdot L^3}{c_r^2} \quad F_{\text{bearing},95} = 5 \times 10^3 \text{ lbf}$$

$$F_{\text{bearing},95} = 22.49945 \text{ kN}$$

The safety factor is $N := \frac{F_{\text{bearing},95}}{F_{\text{bearing}}}$, $N = 1.0$

18. Temperature rise in bearing (equations from [Booser 2001] pg 231)

$$c_p := 1670 \frac{\text{J}}{\text{kg} \cdot \text{K}} \quad JJ := 4.15 \frac{\text{J}}{\text{cal}} \quad \rho := 885 \frac{\text{kg}}{\text{m}^3}$$

$$TT := \frac{\text{bhp}_m}{JJ \cdot \rho \cdot c_p \cdot Q} \quad TT = 17.67078\text{K}$$

This implies a temperature rise of 18 deg C (66.2 deg F). Therefore, if inlet temp. is 65C then resulting temp is 65C + 18 C = 83C.

NOTES: Norton[Norton 2007] states "If this safety factor had indicated that a small overload could put the bearing in trouble, redesigning the bearing for a lower Ocvirk number would give more margin against failure under overloads. Equation 10.11c, repeated here as p shows what could be changed to reduce O_N ."

$$O_N = \left(\frac{p_{\text{avg}}}{\eta \cdot n} \right) \cdot \left(\frac{d}{l} \right)^2 \cdot \left(\frac{c_d}{d} \right)^2 \quad (p)$$

Norton[] states "It would require some combination of: decreasing the clearance ratio, decreasing the d/l ratio, or using a higher viscosity oil. Assuming the rotational speed, load, and shaft diameter remain unchanged, the bearing length could be increased or the diametral clearance reduced as well as η increased to improve the design."

APPENDIX 4 Files on accompanying CD

4.1 Microsoft Excel Spreadsheet on Oil System Pressure & Flow Requirements

4.2 Microsoft Excel Spreadsheet on Crankshaft Balancing

4.3 Mathcad file on Oil Pressure & Scavenge Pump Design

4.4 Mathcad file on Mathematical Journal Bearing Model

4.5 PDF file of MSc Dissertation

APPENDIX 5 Main Bearings & Big End Con-Rod Bearings

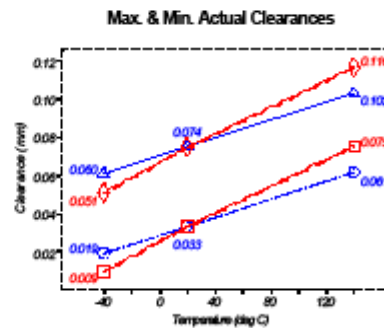
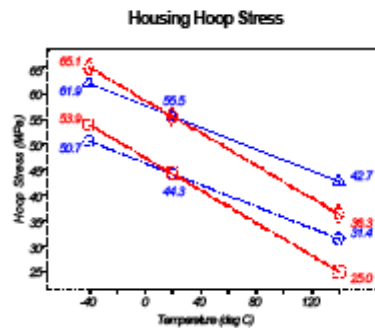
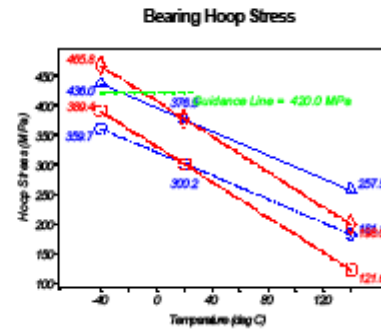
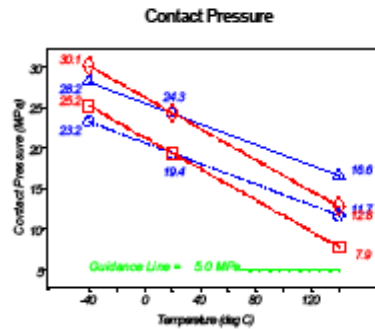
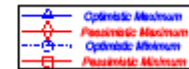
5.1 Main Bearings



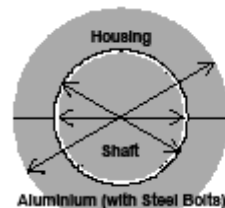
GLACIER VANDERVELL BEARINGS

SABRE-Fit
v2.0.11

Customer: **Nicholson McLaren Engines**
Part no.: **NME421**



Bearing Housing and Shaft



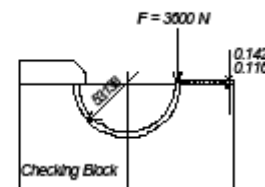
Outside Housing Diameter = 1.6 x ID
Shaft Diameter = 40.213 / 40.200 mm
Housing Diameter = 53.138 / 53.130 mm

Bearing Dimensions



Overall Axial Length: 20.000 mm
Wall Thickness: 1.955 / 1.947 mm
Steel Thickness: 1.000 mm

Centreline Checking Details



Results

Bearing material: Steel/Bronze
Effective Wall Thickness: Steel + Half of Lining
Effective Wall Thickness: 1.776 mm
Effective Cross Sectional Area: 35.515 mm²
Compression under Checking Load: 0.036 mm
Interference: 0.121 / 0.005 mm
Housing Swell: 0.032 / 0.025 mm
Swell @ Max/Min Clearance: 0.030 / 0.028 mm

U:\My Documents\Sabre-fit\NME 421.brg - 08/02/2005

SABRE-Fit © 2002 by Glacier Vandervell Bearings, a Division of the Dana Corporation

5.2 Big End Connecting Rod Bearings

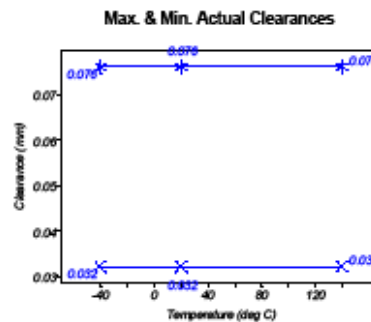
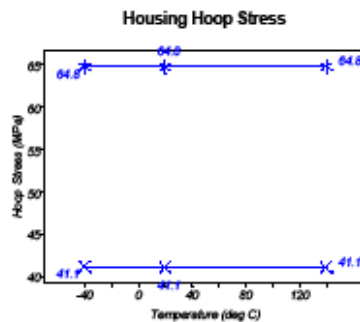
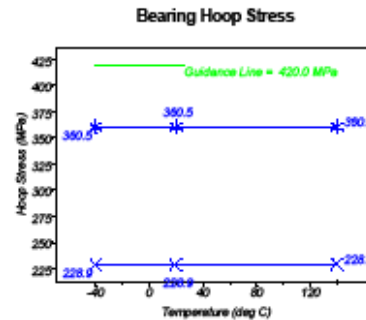
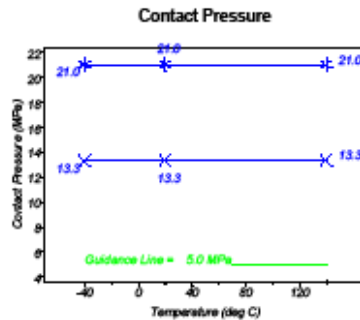


GLACIER VANDERVELL BEARINGS

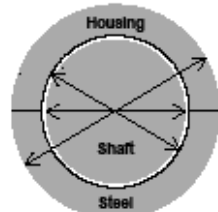
SABRE-Fit
v2.0.11

Customer: **Nicholson McLaren**
Part no.: **NME 410**

—*— Maximum
—x— Minimum

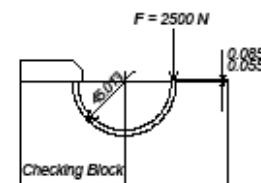


Bearing Housing and Shaft



Outside Housing Diameter = 1.4 x ID
Shaft Diameter = 42.000/ 41.088 mm
Housing Diameter = 45.013/ 45.000 mm

Centreline Checking Details



Bearing Dimensions

Overall Axial Length: 16.870 mm
Wall Thickness: 1.400 / 1.481 mm
Steel Thickness: 1.220 mm

Results

Bearing material: Steel/Bronze
Effective Wall Thickness: Steel + Half of Lining
Effective Wall Thickness: 1.353 mm
Effective Cross Sectional Area: 22.821 mm²
Compression under Checking Load: 0.033 mm
Interference: 0.088 / 0.050 mm
Housing Swell: 0.015 / 0.010 mm
Swell @ Max/Min Clearance: 0.013 / 0.012 mm

U:\My Documents\Sabre-fit\NME410.brg - 14/01/2003

SABRE-Fit © 2002 by Glacier Vandervell Bearings, a Division of the Dana Corporation